Angelika Maria Schlick

Antibiofilm and Antimicrobial Activities of Cellobiose Dehydrogenase

MASTERARBEIT

zur Erlangung des akademischen Grades einer

Diplom-Ingenieurin

des Masterstudiums Biotechnologie

erreicht an der

TECHNISCHEN UNIVERSITÄT GRAZ

Betreuer: Univ. - Prof. Dr. Georg Gübitz

Institut für Umweltbiotechnologie

2013

Declaration

EIDESSTATTLICHE ERKLÄRUNG

Ich erkläre an Eides statt, dass ich die vorliegende Arbeit selbstständig verfasst, andere als die angegebenen Quellen/Hilfsmittel nicht benutzt, und die den benutzten Quellen wörtlich und inhaltlich entnommene Stellen als solche kenntlich gemacht habe.

Graz, am …… ……..

(Unterschrift)

STATUTORY DECLARATION

I declare that I have authored this thesis independently, that I have not used other than the declared sources / resources, and that I have explicitly marked all material which has been quoted either literally or by content from the used sources.

…… ……..

Date (signature)

Acknowledgements

First of all, I would like to thank Professor **Georg Gübitz** for giving me the great opportunity to do my master thesis and the whole Institute of Environmental Biotechnology. Furthermore, I would like to thank **Gibson Nyanhongo** for always having time for meetings and being a great supporter during the process of writing my thesis. Special thanks go to **Endry Nugroho Prasetyo** for your help, advice and assistance of performing the HPLC and TLC. I want to thank as well my supervisor **Barbara Thallinger,** who always offered me advice and support!

Thanks to the whole members of the **Gübitz group** for the pleasing working atmosphere and especially my colleagues **Daniel, Vanessa, Claudio, Massimiliano, Annemarie, Tamara** and **Stefan** for finding a sympathetic ear and for the nice conversations in the coffee breaks.
I would like to express special thanks to **Sonja, Sarah, Markus, Chris, Claudia** and **Aylin** for their friendship and support.
Finally, I would like to express my gratitude to **my parents** and my boyfriend **Philipp** for their understanding and support.

Thank you!

Abstract

This work was part of the collaborative project NOVO financed by the European commission with the major aim of developing novel strategies for preventing the colonization of biofilms formed on indwelling medical devices such as urinary catheter. The main focus of this thesis was the investigation whether the enzyme cellobiose dehydrogenase (CDH) possesses the ability to use extracellular polymeric substances (EPS) or enzymatically co-hydrolyzed EPS polymers as a substrate for the production of hydrogen peroxide. Therefore, this study involved the production, extraction and characterization of extracellular polymeric substances (EPS) produced by *Escherichia coli* and *Staphylococcus aureus* as model microorganisms colonizing catheters. The incubation of EPS with CDH resulted indeed in the production of hydrogen peroxide at a concentration of 0.16 µM. To enhance the production, the EPS were hydrolyzed using different enzymes. Consequently, the best hydrolytic enzyme was an alpha amylase, which boosted the production of hydrogen peroxide by CDH up to 20 µM hydrogen peroxide for *S. aureus* and 13 µM for *E. coli* EPS. Furthermore, two cellulases from *Aspergillus niger* were as well very effective in the hydrolysis and interestingly, in the production of hydrogen peroxide, one was more effective in the hydrolysis of *E. coli* EPS and the other one of *S. aureus* EPS. The enzyme combinations reached concentrations up to 13 µM for *E. coli* and 9 µM for *S. aureus* EPS. Subsequently, the pre-testing for development of an antimicrobial and antibiofilm system was performed to determine the minimal inhibitory concentration (MIC) for both organisms using hydrogen peroxide as well as newly formed one by combining CDH with the substrate cellobiose. The MIC_{50} of hydrogen peroxide was for both model microorganisms in the range of 200 to 500. A complete inhibition was detected for both at concentrations between 1000 to 1500 µM and higher for the newly formed one. It can be concluded that CDH, in combination with one or more hydrolytic enzymes, is needed to reach such high concentrations.

Kurzfassung

Diese Masterarbeit wurde im Rahmen des EU-Projektes NOVO durchgeführt und hatte das Hauptziel verschiedene Strategien zu entwickeln um die Besiedlung von Biofilmen auf medizinischen Geräten wie Blasenkatheter zu verhindern. Der Schwerpunkt dieser Arbeit lag auf der Untersuchung ob das Enzym Cellobiose Dehydrogenase (CDH) extrazelluläre polymere Substanzen (EPS) oder enzymatisch co-hydrolysierte EPS Polymere als Substrat für die Herstellung von Wasserstoffperoxid verwenden kann. Die Arbeit konzentriert sich dabei auf die Herstellung, Gewinnung und Charakterisierung von extrazellulären polymeren Substanzen (EPS) von *Escherichia coli* und *Staphylococcus aureus* als Katheter kolonisierende Modelorganismen. Die Inkubation von EPS mit CDH resultierte in Wasserstoffperoxid Konzentrationen von bis zu 0,16 µM. Um die Produktion zu erhöhen, wurde das EPS zuvor mit verschiedenen Enzymen hydrolysiert. Von den getesteten Enzymen war eine Alpha-Amylase am Besten, sie erhöhte die Wasserstoffperoxid Produktion unter Zugabe von CDH auf bis zu 20 µM für *S. aureus* und 13 µM für *E. coli* EPS. Des Weiteren waren zwei unterschiedliche Cellulasen von *Aspergillus niger* bei der Hydrolyse, und auch bei der Herstellung von Wasserstoffperoxid mithilfe von CDH sehr effektiv. Interessanterweise war eine wirksamer bei der Hydrolyse von *E. coli,* die andere von *S. aureus* EPS. Die Enzymkombinationen erreichten Wasserstoffperoxid Konzentrationen von bis zu 13 µM für *E. coli* und 9 µM für *S. aureus* EPS. Daraufhin wurde die Vortestung für die Entwicklung eines Antimikrobiellen/Antibiofilm Systems durchgeführt, um die minimale Hemmkonzentration (MIK) für beide Organismen unter Verwendung von sowohl Wasserstoffperoxid als auch neu gebildetem Wasserstoffperoxid durch das Kombinieren von CDH mit Cellobiose zu bestimmen. Die MIK_{50} von Wasserstoffperoxid war für beide Modelmikroorganismen im Bereich von 200 bis 500 µM. Eine totale Inhibition wurde bei einer Konzentration von 1000 bis 1500 µM festgestellt und diese war allerdings für das neu gebildete Wasserstoffperoxid deutlich höher. Daraus lässt sich schlussfolgern, dass CDH, in Kombination mit einem oder mehreren hydrolytischen Enzymen, notwendig ist, um so hohe Konzentrationen zu erreichen.

Table of Contents

List of Figures

List of Tables

1 Introduction

Biofilms

Biofilms can be composed of single or multiple species accumulation, containing algae, bacteria, fungi as well as protozoa [1,2]. It is believed that they exist for over 3.8 billion years [3] and according to Watnick et al. [4] biofilms are the main microbial life form. Moreover, they are irreversibly attached to biotic or abiotic surfaces and seem to prefer rough surfaces due to lower shear forces [5,6]. The microbial community needs for perfect growth conditions aside a surface for attachment, additionally, a moist environment with the presence of nutrient flow [1,6]. In the environment, single species biofilms are uncommon; most of them comprise mixtures of various microorganisms and this results in particular interspecific and intraspecific interactions [7].

They can be defined as well organized assemblage of cells, which collaborate and form single layers or even more complex constructions such as 3-D structures [2].

Structure and composition of biofilms

Generally, the structure of a biofilm can be visually subdivided into mushroom, column or pillar [8] (rodlike) shaped microcolonies, which are connected by channels [9,10]. The connections ensure the water flow for circulation on the one hand, to distribute nutrients and on the other, to remove detrimental metabolites [9]. It is likely that hydrodynamics are influencing the biofilm structure; in case of laminar flow the microcolonies are round shaped and when turbulent flow is present, they broaden in downstream direction [9]. According to Donlan [6] this suggests, the higher the velocity is the thinner the produced biofilm. The cells are enclosed in a complex polymeric matrix of extracellular polymeric substances (EPS), which mainly consists of polysaccharides [6]. Besides, EPS the biofilm also contains high amounts of water (up to 95 %) [3]. Furthermore, non cellular constituents can be present in the biofilm depending on their surroundings such as blood components, mineral crystals, clay, corrosion and split particles [2,6]. Besides, polysaccharides they contain proteins, nucleic acids, lipids and humic substances [1].

Biofilm-associated microorganisms have differences in their structure, composition and transcribed genes in comparison to their planktonic, freely suspended relatives [1,4]. They show reduced growth rate and have the ability of generating extracellular polymeric matrices, which are important for biofilm formation [2].

Biofilm formation

The biofilm formation can be summarized in the following five steps. First, the adsorption of free suspended bacteria happens [11]. Second, the cells attach irreversibly to a surface [9,11], which is composed of either biotic material such as wood, tissue or abiotic one like soil particle, plastic, glass, medical implant materials as silicone [2]. Third, the growth of the bacteria proceeds; fourth, the EPS is produced and biofilm formation takes place [4,11]. Finally, the layered biofilm is formed. The whole process can be seen in Figure 1.

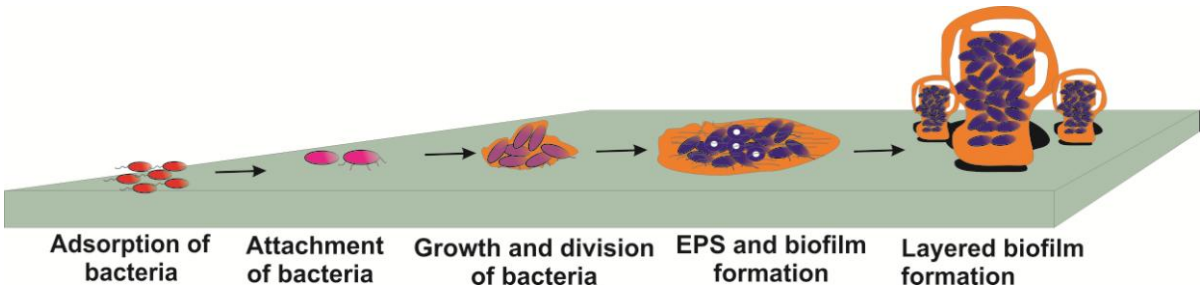

Figure 1: Stages of biofilm formation [12]

When the environmental conditions are changing and are becoming subsequently unsuitable for the biofilm, a detachment of bacterial cells may occur to find a more favorable surrounding [11]. Principally, the attachment itself is conducted by fimbriae, flagella, pilli and EPS [2,4]. Specific membrane proteins, called adhesins, are essential for connecting the surface with the cells [9]; additionally, the type IV pilus and flagella are organelles, which are described to be important for the initial interaction between cell and surface. Furthermore, type VI pili mediate the gliding motility for moving along surfaces [4,11]. For connections of cells among themselves or with a surface the F pilus is described to be important as adhesion factor, too [6].

Based on the paper of Marić and Vraneš [9], the formation of the biofilm is regulated on the one hand by environmental factors (pH, temperature, nutrient supply, oxygen availability, etc.) and on the other hand by genetic factors like bacterial motility (such as flagella and fimbriae), membrane proteins (e.g. adhesins), extracellular polysaccharides and signal molecules. They described signal molecules (e.g. RpoS) as general stress responses caused by negative environmental conditions or high cell densities that are important as regulatory mechanism. RpoS is an RNA polymerase sigma factor subunit; it controls several genes, which are related to passing cells into stationary phase and the quorum sensing. According to Marić and Vraneš [9] the biofilm formation of different organisms is generally the same, but has slight differences; in case of *Escherichia coli* it was observed that oxygen must be available and additionally the RpoS plays a major role.

The biofilm formation of *L. monocytogenes* is temperature sensitive and of *Vibrio cholerae* it is dependent on the pH value [9].

It is a fact that the merge of organism forming a biofilm has some outstanding advantages such as the protection from environmental stress and therefore they possess the ability to develop resistance to amoebae, antibiotics, bacteriophages, some chemically biocides and even in case of an host infection to immune response [1]. In the environment they have the ability to survive various extreme conditions for instance temperatures from -5 to 120 °C, pH values from 0 to 13 and additionally, pressures up to100 MPa [3]. Due to the great potential of biofilms to survive different environmental conditions and to develop resistances, they are a great danger.

The importance of biofilms to microbial communities

Biofilm forming is important for microbial communities and the organisms are living in an ideal ecological niche [12]. According to Kokare et al. [2], they can even have a kind of symbiotic relationship and the biofilm is effective in protecting the cells against environmental stress (dehydration, pH shifts, UV radiation or osmotic shock), antibiotics and antimicrobial agents. Marić and Vraneš [9] described that bacteria of the biofilm community are physiologically dissimilar and that this characteristic is essential for possessing antibiotic resistance. Additionally, they showed that biofilms own a high resistance against antimicrobial agents, host immune response and mechanical attacks or impacts.

The biofilm possess the ability to perform gene transfer by exchanging of plasmids, which may encode for resistance to antimicrobial agents and antibiotics by conjugation with the F (conjugative) pilus and the transfer is more likely to occur in biofilms than in planktonic cells due to their immediate proximity [6]. Besides, that the horizontal gene transfer (HGT) by virus mediated gene transduction, transposons and bacteriophages can result in the exchange of certain genes.

According to Kokare et al. [2] some of the antibiotics and antimicrobial agents are ineffective, based on the structure of the EPS matrix; it can act as a diffusion barrier or even function as an anion exchanger to avoid penetration of antimicrobial agents and antibiotics, especially positively charged and hydrophilic ones, for instance aminoglycosides. The authors described that some antibiotics have the mechanism to affect the growth phase of bacteria, but therefore the biofilm can remain in a dormant phase. It can be concluded that the form of living as a biofilm, including their special structure, composition, physiological symbiosis, is a great advantage for the microorganisms [2].

The most common resistance mechanisms for drug inactivation in the microbial community are using endogenous enzymes, efflux pumps, acquisition of genes, modifying target protein with different strategies such as varying binding sites or preventing the access of the drug [12,13].

According to Nikaido [14] some endogenous enzymes could be observed to be responsible for antibiotic resistances, for instance the beta lactams such as penicillins, cephalosporins and carbapenems can be inactivated by enzymes called beta-lactamases. As another example, the author described aminoglycosides such as kanamycin, amikacin and tobramycin, which can be inactivated by several enzymatic reactions like phosphorylation, acetylation and adenylation.

Moreover, the danger of biofilms can be explained by their antibiotics resistance, caused by persisters. After antibiotics treatment the planktonic cells which survive are destructed by the immune response of the host; in case of biofilm associated cells, they are assumed to survive. Their persisters survive due to the polysaccharide matrix and it can be supposed that they have damage in their apoptosis system [9].

The mechanisms of resistance in detail are still unexplained, but several theories are known and the most common ones are: first, slow or incomplete diffusion of antibiotics, second, bacteria can live in a dormant stage and third, the presence of high differentiated cells with a highly resistant phenotype [2,9]. The resistances of biofilms are causing serious problems in different areas and they pose a threat to public health.

Problems associated with biofilm

The biofilm has a great danger for public health, as well as in medicine, the food industry and in water distribution systems [2] such as industrial and portable ones [6]. Especially, the microorganism *Listeria monocytogens* can be present in diary plants, *Bacillus* spp in pipelines, *Salmonella* spp. in poultry processing environments and moreover, *Pseudomonas* spp. is connected with the food industry and water systems [2]. Biofilms are even a problem in piping systems. They can attach and produce a slime layer within a few seconds.

Moreover, they exist on all medical devices and implants as central venous catheter, needleless connectors, mechanical heart valves, pacemakers, endotracheal tubes, tympanostomy tubes, prosthesis, prosthetic joints, voice prostheses, artificial hips, urinary catheters, peritoneal dialysis catheters, contact lenses and intrauterine devices [2,15,16]. Additionally, fracture fixation devices, vesicular shunts and even mammary implants are affected [17]. Kokare et al. [2] wrote that biofilm develops around the tissue, which surrounds the valve or prosthesis.

Moreover, they are associated with several chronic infections for examples native valve endocarditis, otis media, chronic bacteria prostitis, cystic fibrosis or periodontitis [2,16]. Beyond this chronic osteomyelitis, chronic cystitis, chronic pneumonia are associated with biofilms [9]. Affected by colonization are especially indwelling medical devices such as catheters.

Biofilms on catheters

Microorganism can attach to medical indwelling devices such as central venous or urinary catheters [2]. Central venous catheters are primarily colonized by *S. epidermidis* [18], *S. aureus*, *P. aeruginosa*, *C. albicans* and *K. pneumonia* and the colonization takes place within three days [15]. An infection caused by microorganism is named CRBSI, catheter-related bloodstream infection [19]. Several methods are tested to avoid the colonization either by impregnating with cationic surfactants for bonding of cephalosporin or treating the material with combinations of minocycline, rifampicin or chlorhexidine and silver sulfadiazine [2].

A great danger is caused by biofilm colonization of urinary catheters on the inner and outer surface [15]. According to Kokare et al. [2] the catheters are composed of tubular latex or silicone, their surface is likely to be colonized by microorganism and it causes urinary tract infections (UTI). The longer the catheter remains in the body, the more likely is an infection. According to the authors just 10 to 20 % of the patients have the catheter for a short time up to seven days, but the majority has the indwelling medical device for longer over 30 days and consequently, all of them show UTIs, generally caused by microorganisms like *S. epidermidis*, *Enterococcus faecalis*, *E. coli*, *Proteus mirabilis*, *P. aeruginosa*, *K. pneumoniae* and other gram-negative bacteria.

Moreover, they describe that the main problem of the biofilm relating to urinary catheters besides, causing infection is that gram-negative bacteria interact with divalent cations such as calcium and magnesium; this causes an increase of pH and ionic strength of the urine and results in a higher level of bacterial attachment. Some of the biofilm associated organism posses the ability to produce an enzyme, named urease [2,15]. The enzyme can hydrolyze urea to ammonium hydroxide, this pH shift causes a precipitation of minerals like struvite and hydroxyapatit, these can blockade the inner lumen of the urinary catheter [2,15].

To solve the problems of microbial growth on catheters the biofilm has to be destroyed before formation. The production of EPS is an important step in the formation of biofilms and due to its chemical composition it can function as a potential target.

Chemical composition of EPS and its potential as target

The EPS composition is very complex and consists mainly of polysaccharides. The attachment is irreversible and the EPS production is involved in this process. Based on Eboigbodin and Biggs [20], two types of EPS exist, the cell-bound (capsular) EPS and the slimy free one. The EPS is linked by London forces, electrostatic interactions and hydrogen bonds [21]. Basically, it can be concluded that the complex matrices of EPS keep the cells together.

According to Vu et al. [1] the composition depends on the one hand, on the environmental surrounding like pH, temperature, nutrient supply including oxygen and nitrogen and on the other hand, on the biofilm-forming microorganism like type (gram-negative or gram-positive), nature and age. Moreover, the authors describe that the composition of EPS of gram-positive, such as *Staphylococcus aureus*, and gram-negative bacteria, such as *Escherichia coli,* are different due to the polyanionic or neutral and cationic nature of their cell walls. It can be assumed that the EPS can have an amount of 50 to 90 % organic matter within a biofilm [1]. By using several staining methods, such as osmium tetroxide, it was proven that the main components of the EPS are polysaccharides [2], also called exopolysaccharide, and due to the results of the staining with ruthenium red, it was confirmed that the biofilm comprise not so many cells as EPS [15].

The exopolysaccharides of different organisms are varying and can contain homopolymers such as cellulose, curdlan, dextran and sialic acid or heteropolymers, which are comprised of some alginate, gellan or xanthan units [7]. Moreover, they can contain monosaccharides such as D-glucose, D-galactose, D-mannose, D-ribose, D-xylose, L-fucose, L-rhamnose, L-arabinose, N-acetyl-D-glucosamine and N-acetyl-D-galactosamine as well as uronic acids (D-glucuronic acid, D-galacturonic acid, D-mannuronic acid and L-guluronic acid) [22,23]. Cerca et al. [24] showed that *S. aureus* biofilms contain poly-N-acetyl-glucosamine (PNAG) as a huge exopolysaccharide and *E. coli* polyglucosamine. Some *E. coli* strains are able to produce colanic acid as EPS. Colanic acid is a complex sugar polymer, which contains galactose, fucose, glucose and glucuronic acid [25]. Based on the results of the glycosyl composition analysis of Bales et al. [26] the EPS of *E. coli* consists mainly of glucose, N-acetyl-galactosamine and fucose. Moreover, the authors detected that the *E. coli* EPS contains small amounts of galactose, mannose and N-acetyl-glucosamine.

In addition, they tested the microorganism *Staphylococcus epidermidis* and showed that in comparison to *E. coli* that there is a difference in the composition and the amounts of the respective sugars. Their glycosyl composition analysis of *S. epidermidis* indicated that the EPS contained no fucose, but high amounts of mannose, moreover, galactose, glucose, N-acetyl-galactosamine, N-acetyl-glucosamine were detected. Arvaniti et al. [27] showed the presence of hexosamines, neutral sugars, phosphates, proteins, sulfates and uronic acids in the EPS of *S. epidermidis* biofilms; subsequent analysis by HPLC detected high amounts of glucosamine, neutral sugars such as glucose, fucose and xylose. Additionally, the authors identified low concentrations of sulfate and glucuronic acids by HPLC.

According to Sutherland [7] polysaccharide degrading enzymes, also known as polysaccharases, as well as polysaccharide lyases seem to be more effective than proteases due to their wide range and high specificity. Craigen et al. [28] already demonstrated already the great potential of hydrolytic enzymes to prevent the formation of biofilms or destroy already formed ones. As mentioned above the EPS consist of less cells and mainly polysaccharide [6], therefore they can be used as target.

Antimicrobial and antibiofilm approaches

The problem caused by multi resistant biofilms, which are not susceptible to antibiotics or common antimicrobial treatments, lead according to Thallinger et al. [12] to the development of bio-based antimicrobial agents. The authors described that some green strategies for biofilm controlling are enzyme based systems, relying on bacteriophages or on influencing microbial interactions by affecting metabolite molecules [12,13]. Chemicals like chlorite, hydrogen peroxide, iodophors, or quaternary ammonium compounds are already used for disinfection of surfaces [29]. The disadvantage of hydrogen peroxide is that catalase could possibly avoid the penetration in the biofilm [30].

Nevertheless, the antimicrobial agent hydrogen peroxide is, according to Alt et al. [31], already used as a disinfectant of wound, it has some advantages like little costs and additionally, it is non harming human tissue. Furthermore, they described that the antimicrobial agent possesses the ability to destroy gram-negative and gram-positive bacteria, fungi and yeasts. The authors demonstrated with the study that 3 % hydrogen peroxide resulted in a noticeable reduction concerning microbial growth.

According to Thallinger et al. [12] several approaches were tested for their antimicrobial and antibiofilm potential and they summarized three major enzyme systems: proteolytic, polysaccharide degrading and oxidative enzymes. They described that the most common proteolytic enzymes used, are subtilisin, lysostaphin and bacteriophages lysine. The polysaccharide degrading enzymes such as amylases, alginate lyases and oxidative enzymes like myeloperoxidase, cellobiose dehydrogenase, lactoperoxide, glucose oxidase and horseradish peroxidase were tested for antimicrobial and antibiofilm systems [12].

New biofilm control strategies seem to be important [13] due to the fact that biofilms are a great danger for public health and are causing problems in medicine, food industry, water systems. Especially, in hospitals biofilms are dangerous for patients, who need indwelling medical devices, and can cause serious health problems [15].

NOVO Project

According to Curtis et al. [32] more than 40 % of all nosocominal infections are affecting the urinary tract, and nearly all of them are directly related to catheterization. Biofilms grow on all medical devices and form often a pathogenic biofilm on them. As a result of the impact on public health, the project NOVO was initiated. The project NOVO is a collaborative project by the European commission with the aim of developing strategies for preventing the colonization of biofilms on medical devices such as urinary catheters. The focus was on three strategies: sonochemical coating with nanoparticles, coating of antimicrobial phenolics and immobilization of enzymes, which possess the ability to produce antimicrobial molecules [33]. In this study, the focus is on the development of an enzyme based system, which uses hydrogen peroxide as antimicrobial and antibiofilm agent for the destruction of biofilms. Due to its ability to use components of the EPS as electron donors for the production of hydrogen peroxide, the focus was on the enzyme cellobiose dehydrogenase.

Cellobiose dehydrogenase

Cellobiose dehydrogenase (CDH), formerly known as cellobiose oxidase, is an extracellular enzyme, which is produced by numerous wood degrading fungi and belongs to the flavocytochromes [34].

The following studies were performed by using the cellobiose dehydrogenase from *Myriococcum thermophilum*. This CDH has a molecular mass of 94 kDa and consists of about 828 amino acids, but the mass is depending on the degree of glycolysation and thus, it can vary about 20 percent [35,36]. The cellobiose dehydrogenase (CDH) is a protein, which is produced by various organisms, such as white rot fungi, brown rot fungus, some soft rot fungi and molds [37]. Henriksson et al. [38] described that the CDH is as a monomeric enzyme, it is comprised of two major domains: the catalytic domain with FAD as cofactor and a second one, which consists of cytochrome b-type heme. According to the authors the catalytic domain with FAD as cofactor has the key role in electron transfer and takes the electrons from the electron donor and transfers them to the electron acceptor. They pointed out that the function of the heme is still unexplained, but that it has been proven to be responsible for the increasing activity towards one electron acceptors. Additionally, they described that the dehydrogenase has a specific site for binding the standard substrate cellulose. Both domains are adjunct to a linker region, which can be cleaved by proteases and it contains about 20 to 30 amino acids [39,40].

Based on Pricelius et al. [39] the CDH seems to have a broad spectrum of electron acceptors, such as cellobiose, lactose, higher cellodextrins, cellulose and other sugars. One electron acceptor such as cytochrome c, semi-quinones and ferric complexes and two electron acceptors like 2,6-dichloroindophenol sodium salt hydrate (DCIP), methylene blue, molecular oxygen and benzoquinone can be used by the enzyme [39].

The dehydrogenase can act as a cellobiose oxidase; hence, it has the ability to reduce molecular oxygen and produce hydrogen peroxide and also act as Fe (III) reductase due to its ability as elector acceptor [41]. Reactions catalyzed by CDH are shown in Figure 2.

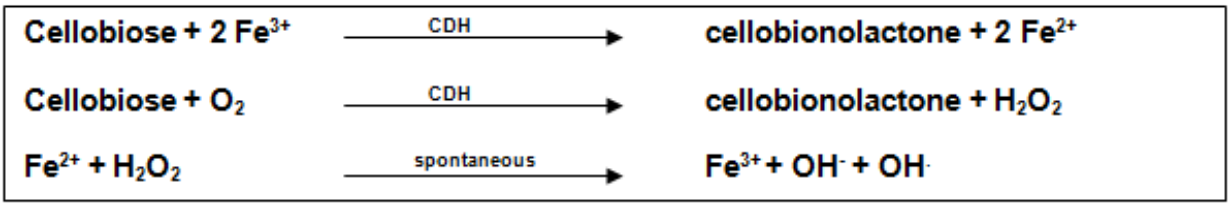

Figure 2: Reactions catalyzed by CDH according to Henriksson et al. [42]

The physiological role of the CDH in the organism is still unknown, but one of the biological functions is the inhibition of cellulases by cellobiono-δ-lactone [43,44]. Generally, it can be said that the enzyme oxidizes the reducing groups of the sugar such as cellobiose, cellodextrine etc. to generate the respective lactone and it is involved in lignin decomposition [43]. According to Hallberg et al. [45], the enzyme has the ability to oxidize cellobiose by removing two electrons of the sugar, which can be utilized in different ways; on the one hand it can be used to produce hydrogen peroxide from oxygen or on the other it can oxidize Fe(III) to Fe(II). During this reaction the electrons are transferred from the flavin to the heme.

Moreover, the enzyme prevents the re-polymerization of phenoxy radicals, which were previously formed by lignin peroxidases or laccases and this results in an influence of the celluloytic process [38,46]. However, with a complex process, which involves hydroxyl radicals by a Fenton type reaction, the CDH can degrade carboxylmethyl cellulose soluble xylan and synthetic lignin, on the condition that cellobiose, hydrogen peroxide and Fe^{3+} are present [38]. According to Hallberg et al. [45] the ferrous iron reacts with the hydrogen peroxide and as a result, reactive hydroxyl radicals are produced.

Henriksson et al. [38] tested several sugars as electron donor and they have identified that thiocellobiose is even a better substrate in comparison to cellobiose, because it achieved a higher Kcat value. Moreover, their substrate specificity testing indicates that galactose cannot be used as substrate by the CDH, isolated of *P. chrysosporium* and this suggests that it only interacts with the B-site and not to the C-site, because it seems to inhibit the binding of the standard substrate cellobiose.

The authors described that a competitive inhibition occurred in case of the presence of the two sugars cellobiose and galactose. They came to the conclusion that for the enzyme β-1,4 dihexosides with the sugar residues glucose/mannose as reducing end are likely to be favorable substrates. Typical sugar substrates are: cellobiose, cellotriose, cellotetraose, lactose, mannobiose, thiocellobiose, galactosyl-mannose.

The production of hydrogen peroxide is shown in Figure 3. Basically, two different classes of CDH could be identified; for the class I CDH monosaccharides are bad substrates and for the class II they were good ones even glucose [47]. Pricelius et al. [39] reported that the CDH from *M. thermophilum* (ascomycete) was able in contrast to other CDHs such as *Phanerochaete chrysosporium* (basidiomycete) to oxidize glucose or other monosaccharides. Furthermore, they tested that CDH oxidizes glucose with a very high efficiency. This also applies to other monosaccharides, disaccharides and oligosaccharides, but unfortunately with a lower effectiveness [35].

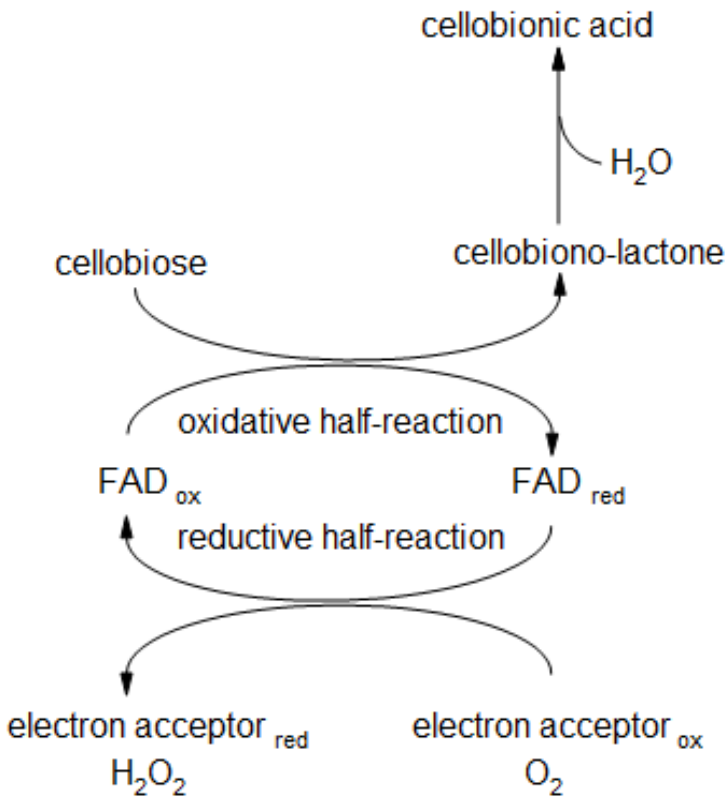

Figure 3: Half reactions of the FAD containing domain catalyzed by CDH based on Sygmund et al. [35] (drawn by Accelrys Draw 4.1)

Many applications of the enzyme were described for monitoring the degradation of cellulose, production of prebiotics, as detergent for bleaching cotton [46,47].

Furthermore, the CDH can be used in paper and pulp industry, biofuel cell anodes, medicaments and bioelectrosynthesis [36,39].

Even applications in biosensors for detecting cellodextrins, maltose, lactose, diphenolic compounds, catecholamines like dopamine, adrenaline, noradrenaline are described [48]. Moreover, the hydrogen peroxide production of the CDH can be used besides, the already described applications also for aseptic packaging of nourishments, detoxification of cyanide in mines and degradation of cyanides, sulfides and phenols [46]. Additionally, it can be used in medical applications like catheters [35] and for treatment of chronical wounds. In these wounds the dehydrogenase can be used for quenching free radical species, which are oxidizing newly formed biomolecules in the wounds and act as promoter of pro-inflammatory responses [48].

Aim of the thesis

The main focus of this master thesis is on using EPS as a substrate for the production of hydrogen peroxide, which in turn kills the microorganisms forming the biofilms on catheter. First, this study aimed on gaining insight into the chemical composition of EPS using *S. aureus* and *E. coli* as model microorganisms. This is followed by the investigation of many hydrolytic enzymes to hydrolyze EPS in smaller oligosaccharides, which can be used by the cellobiose dehydrogenase as substrates to produce the antimicrobial agent hydrogen peroxide.

2 Material and Methods

2.1 Materials

The lists of the used chemicals and equipment are shown in the Section 8 and 9. The used enzymes are shown in Table 1.

Table 1: Enzyme list

Enzyme	Company
Alpha Amylase	Novozyme
Alpha Amylase from Bacillus amyloliquefaciens	Sigma
Alpha Amylase	*
Alpha Amylase from *Aspergillus oryzae*	Sigma
Beta Glucanase	*
Cellulase from Aspergillus niger	Fluka
Cellulase from Aspergillus niger	Sigma
Cellulase	*
Enzyme Mixture	*
Lysozym from chicken egg white	Sigma Aldrich
Mannanase	Novozyme
Pectinase from Aspergillus aculeatus	Sigma
Pulpzyme	Novozyme
Horseradish Peroxide (HPO)	Fluka
Lignin Peroxide (LIP)	*
Cellobiose Dehydrogenase from *Myriococcum thermophilum*	x
Catalase from bovine liver	Sigma Aldrich

* unknown origin; x produced

The modified cellobiose dehydrogenase (CDH) of *Myriococcum thermophilum* was kindly provided and produced in several batches by the group of Roland Ludwig from the institute of food biotechnology at the University of Natural Resources and Life Sciences. The different batches were genetically modified variants of the *Mt*CDH. Batch I and II were recombinant oxy plus *Mt*CDH with an improved hydrogen peroxide production and III, IV, V, VI, VII, VIII, IX, X were other variants, which produced more hydrogen peroxide than the wild type enzyme, but less than the oxy plus variants.

2.2 Methods

First, biofilms of *Escherichia coli* and *Staphylococcus aureus* were produced. Then the extracellular polymeric substances (EPS) of both organisms were harvested, extracted, enzymatically hydrolyzed and characterized using several colorimetric assays and analytical methods. In the rest of this section each of the performed methods will be described in more detail.

2.2.1 Biofilm formation and production of extracellular polymeric substances (EPS)

For the biofilm production *Escherichia coli* and *Staphylococcus aureus* were grown in tryptic soy broth overnight at 37 °C and 125 rpm. The compositions of the tryptic soy broth (TSB) and the tryptic soy agar are shown in Table 2.

Table 2: Composition for one liter media of the overnight culture and agar plates

ONC		Agar plates	
Amount [g]	**Chemicals**	**Amount [g]**	**Chemicals**
30	TSB = Caso-Bouillon	30	TSB = Caso-Bouillon
5	Glucose	5	Glucose
30	Sodium chloride (NaCl)	30	NaCl
0	Agar Agar	15	Agar Agar

Both media were autoclaved to ensure sterility and then overnight cultures were inoculated with the respective microorganism. The next day 1000 µl of the ONC of both organisms were distributed equally on agar plates and were incubated in the brood chamber at 37 °C for 24 hours facing upwards to guarantee a moist environment for perfect biofilm growth conditions. Subsequently, was the harvesting of the biofilm forming bacteria by scratching them carefully off the agar plates with a spatula. Biofilms were collected in sarstedt tubes and stored in the fridge at 4 °C. The EPS extraction was carried out as described by Pan et al. [49], they added the equal volume of 2 % (w/v) ethylenedinitrilo-tetra acetic acid tetrasodium salt tetrahydrate (EDTA) to the harvested samples, followed by three hours of incubation on ice. Afterwards the samples were centrifuged for 20 minutes with 5,600 rpm. The extraction was repeated twice to receive higher amounts of EPS. Additionally, an overnight extraction was performed as third step. The supernatant was filtrated with PET-filters Acrodisc® and purified with a dialysis membrane (3,500 Da) for 24 hours. Dialysis was carried out to remove EDTA, a metal chelating agent, which might have negative effects on the CDH activity, as well as of glucose, which was supplemented in the media.

To determine the dry weight of the extracted EPS, the samples were placed in a drying oven at 75 °C for several hours, weighted and then re-suspended in buffer that was used for enzymatic hydrolysis (20 mM sodium phosphate buffer, pH 6.9; 6.7 mM NaCl).

The amount of EPS in the samples was calculated based on the prior determined dry weight. The previously extracted and purified EPS samples were stored in the fridge until subsequent use.

2.2.2 Pretesting of CDH incubated with EPS and enzymatic hydrolysis

The first experiment was the incubation of cellobiose dehydrogenase with the biofilm directly. Because this attempt did not produce significant amounts of hydrogen peroxide, it was decided to investigate whether the hydrolytic enzymes could be used to produce substrates for CDH. The enzymatic hydrolysis of EPS was performed with different enzymes. The extracellular polymeric substances (EPS) extracted of *Escherichia coli* and *Staphylococcus aureus* biofilms were hydrolyzed using various enzymes, which are listed in Table 3. For the hydrolysis the enzyme (3 U/ml) was mixed with an equal volume of EPS and incubated at 50 °C and 400 rpm for 24 hours. The hydrolysates were stored in the freezer at -20 °C until subsequent use. The enzyme activity in the samples was 1.5 U/ml.

Table 3: List of the tested enzymes for the enzymatic EPS hydrolysis and their abbreviations

No.	Enzyme	Company	Abbreviation
1	Alpha Amylase	Novozyme	A-amyla-Nov
2	Alpha Amylase from Bacillus amyloliquefaciens	Sigma	A-amyla-Sig
3	Alpha Amylase	*	A-amyla-U
4	Cellulase from Aspergillus niger	Sigma	Cellu-Sig
5	Cellulase from Aspergillus niger	Fluka	Cellu-Flk
6	Cellulase	*	Cellu-U
7	Enzyme Mixture	*	Enz-mix-U
8	Beta Glucanase	*	B-Gluc-U
9	Mannanase	Novozyme	Mann-Nov
10	Pulpzyme	Novozyme	Pulp-Nov
11	Pectinase from Aspergillus aculeatus	Sigma Aldrich	Pect-Sig
12	Lysozym from chicken egg white	Sigma Aldrich	Lyso-Sig

*unknown origin

For simplification and easy distinction between the various samples each batch was named with a code. The first two letters of the code determines the microorganism, either *S. aureus* (Sa) or *E. coli* (Ec) and the following number indicates the number of the batch. This is adjoined by the letter “D” or “U”, which declares whether the sample was dialyzed or not. The subsequent number followed by the letter "e" specifies how often the EDTA extraction step had to be conducted to gain the sample. After evaluating the results of the first batch, selected enzyme combinations were tested for both organisms. The tested enzyme combinations for *E. coli* are listed in Table 4 and for *S. aureus* in Table 5. The hydrolysis of combining two or three hydrolytic enzymes with an activity of 3 U/ml was performed by mixing the enzymes with an equal volume of EPS. Then it was incubated at 50 °C and 400 rpm for 24 hours. For comparison of the enzyme combinations with the single hydrolytic enzymes the total activity of the combinations was 1.5 U/ml per sample.

Table 4: List of tested enzyme combinations for *E. coli*

No.	Enzyme 1	Enzyme 2	Enzyme 3
Ec1_D_1e-Ek1	A-amyla-Nov	Cellu-Flk	-
Ec1_D_1e-Ek2	A-amyla-Nov	Cellu-Flk	Mann-Nov
Ec1_D_1e-Ek3	A-amyla-Nov	Enz-mix-U	-
Ec1_D_1e-Ek4	A-amyla-Nov	Mann-Nov	-
Ec1_D_1e-Ek5	A-amyla-Nov	Pulp-Nov	-
Ec1_D_1e-Ek6	Cellu-Flk	Cellu-Sig	-
Ec1_D_1e-Ek7	Cellu-Flk	Mann-Nov	-
Ec1_D_1e-Ek8	Cellu-Flk	Pulp-Nov	-
Ec1_D_1e-Ek9	Mann-Nov	Pulp-Nov	-
Ec1_D_1e-Ek10	Mann-Nov	A-amyla-Sig	-

Table 5: List of tested enzyme combinations for *S. aureus*

No.	Enzyme 1	Enzyme 2	Enzyme 3
Sa1_D_1e-Ek1	A-amyla-Nov	A-amyla-Sig	-
Sa1_D_1e-Ek2	A-amyla-Nov	Cellu-Sig	Enz-mix-U
Sa1_D_1e-Ek3	A-amyla-Nov	Cellu-Flk	-
Sa1_D_1e-Ek4	A-amyla-Nov	Enz-mix-U	-
Sa1_D_1e-Ek5	A-amyla-Nov	B-Gluc-U	-
Sa1_D_1e-Ek6	A-amyla-Nov	Pulp-Nov	-
Sa1_D_1e-Ek7	A-amyla-Nov	Lyso-Sig	-
Sa1_D_1e-Ek8	A-amyla-Sig	Cellu-Sig	-
Sa1_D_1e-Ek9	A-amyla-Sig	Enz-mix-U	-
Sa1_D_1e-Ek10	A-amyla-Sig	B-Gluc-U	-

2.2.3 Characterization of EPS and its hydrolysates

The extracellular polymeric substances (EPS) and hydrolysates of *E. coli* and *S. aureus* were analyzed regarding sugar and protein content using colorimetric assays as well as analytical methods.

2.2.3.1 Dubois assay

According to Dubois et al. [50] the phenol-sulfuric acid method was implemented to estimate the amount of uronic acids in the EPS samples and hydrolysates. The assay was modified to be performed in 96-well plates and 5 % (w/v) phenol was used. Furthermore, galacturonic acid was used as standard substrate to obtain the calibration curve. An amount of 60 µl of the sample was transferred into a 96-well plate. Subsequently, 30 µl phenol solution and 150 µl concentrated sulfuric acid (H_2SO_4) were added. The plate was incubated at room temperature for ten minutes uncovered under the hood, followed by a 20 minute incubation step in the thermomixer at 25 °C and 400 rpm.

For the measurement 140 µl of the reaction mixture were transferred into a new well and the absorbance of the characteristic yellow-orange color was detected at 480 nm.

2.2.3.2 Anthrone assay

The anthrone assay is a colorimetric method introduced by Dreywood et al. [51], which was used for the quantitative determination of total sugar content in the EPS samples and hydrolysates. The principle of the method relies on the fact that carbohydrates possess the ability to form furfural derivates in hot acidic systems. These compounds form a green colored product with anthrone, a tricyclic aromatic ketone, which can be measured at a wavelength of 630 nm. The assay was modified according to Foster et al. [52] for the analysis of EPS in 96-well plates. Therefore, 100 µl of sulfuric acid containing 123.5 mM anthrone were added to 40 µl sample. The reaction mixture was incubated in the drying oven at 92 °C for 3 minutes and measured in the plate reader at 630 nm. The calibration curve was obtained by using glucose as standard.

2.2.3.3 DNS assay

Although the DNS reagent itself is nonspecific, it is used for the quantification of the reducing sugars in the EPS samples and hydrolysates according to King et al. [53]. The dinitrosalicylic acid method of Bernfeld relies on the principle that 3,5-dinitrosalicylic acid (DNS) interacts with free carbonyl groups of reducing sugars. While the aldehyde or ketone groups of reducing sugars are oxidized to carboxyl groups, 3,5-dinitrosalicylic acid is reduced to 3-amino-5-nitrosalicylic acid, which absorbs strongly at a wavelength of 540 nm. The assay was carried out to quantify the amount of five and six carbon reducing sugars (aldoses and ketoses) in the enzyme solution [54]. The calibration curve was obtained with the standard cellobiose. Moreover, the protocol was modified in order to carry out the assay in 96-well plates. The conducted steps are shown in the flow chart in Figure 4. All samples were measured in triplicates.

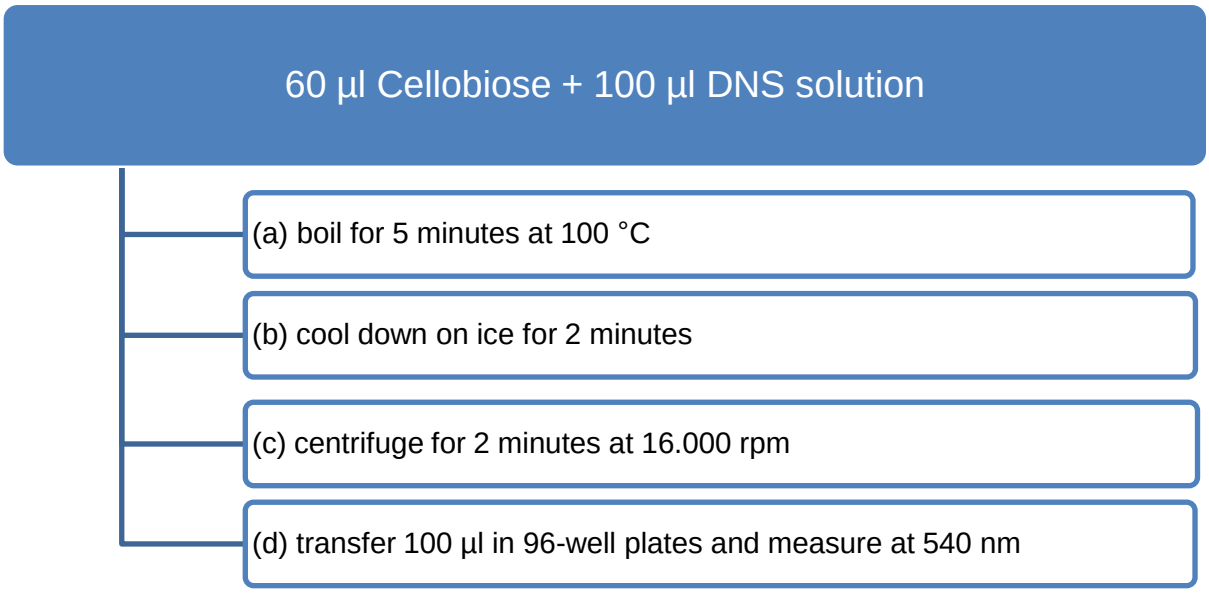

Figure 4: Flow chart of the modified DNS assay for 96-well plates

2.2.3.4 HPLC-RI

The HPLC, high performance liquid chromatography, was performed with a sugar column called “Luna NH_2 (Amino)”. According to the Phenomenex protocol the column was especially developed for separations of polar compounds like simple and complex sugars, sugar alcohols and hydrogen bonding compounds [55]. In the case of EPS and hydrolyzed samples, the normal phase was chosen as a separation mode. Mobile phase for analysis of simple sugars was a mixture of acetonitrile (ACN) and ddH_2O in the ratio of 80:20, as recommended in the Phenomenex protocol.

Many different standards with a concentration of 1 % (w/v) were analyzed by the HPLC to identify the hydrolyzed carbohydrates in the EPS and hydrolysates of *E. coli* and *S. aureus*. The list of the tested standards is shown in Table 6.

Table 6: Carbohydrate standards for the HPLC analysis

No.	Carbohydrate Standard
1	Cellobiose
2	Cellohexaose
3	Cellotetraose
4	D (+)-Galactose
5	D(-)-Fructose
6	D(+)-Mannose
7	D(+)-Saccarose
8	D(+)-Trehalose dihydrate
9	D(+)-Xylose
10	D-Ribose
11	Galacturonic acid
12	Glucosamine
13	Glucuronic acid
14	L (+)-Arabinose
15	Lactose monohydrate
16	L-Rhamnose monohydrate
17	Maltose (monohydrate)
18	N-Acetyl-Galactosamine
19	α-D (+)-Glucose monohydrate

The Refraction index (RI) detector was used to detect the carbohydrates; further settings are listed in Table 7. Whereas flow rates as high as 3 ml/min cannot be handled by the mass spectrometer, it was necessary to collect the peaks of each sample manually to have the possibility for further analysis by mass spectrometry.

Table 7: HPLC settings for analyzing EPS, hydrolysates and carbohydrate standards

Parameter	
Column	Luna 5µm NH_2 Amino
Mobile Phase	ACN:ddH_2O (80:20)
Gradient	No
Duration of run	15 min
Flow rate	3 ml/min
Temperature	40 °C
Detector	Refraction Index
Injection volume	10 µl

All samples acquired through enzymatic hydrolysis, including EPS blanks, were measured and used with the described settings above.

2.2.3.5 HPLC/MS

The HPLC was coupled with the mass spectrometer (MS) to determine mono-, di-, or oligosaccharide by mass in the EPS hydrolysates without any column, because the machine is not able to handle such high flow rates as 3 ml/min. Moreover, it's a frequently used method to confirm the results generated by HPLC-RI.

The manually collected samples were dried to remove the buffer and re-suspended in 300 µl ddH_2O. A mobile phase, containing 400 ml acetonitrile, 100 ml ddH_2O and 0.5 ml formic acid (HCOOH) was used for the analysis. The samples were analyzed in positive mode and further parameters for the conducted measurement are shown in Table 8.

Table 8: HPLC and MS settings

Parameters	
Column	No
Mobile Phase	80:20 acetonitrile: ddH_2O + 0.1 % formic acid
Mode	Positive mode
Duration of run	20 min
Flow rate	1 ml/min
Injection volume	100 µl
Sample holder temperature	15 °C
Column oven temperature	25 °C

2.2.3.6 Thin layer chromatography (TLC)

Thin layer chromatography (TLC) is a chromatographic technique. For the stationary phase pre-coated aluminum foils (0.2 mm layer) were used, which were coated with silica gel 60 Å mean pore size with fluorescent indicator. The following parameters were tested throughout the optimization process to enhance the separation and detection of carbohydrates:

a)TLC plates preparation

Some different preparations were tested like:

(1)no previously preparations

(2)acidified ethanol (99 ml ethanol + 1 ml o-phosphoric acid)

(3)soaking of the plates in 0.5 M sodium phosphate buffer (pH 7), followed by drying for 30 minutes in the drying oven

b)Distance between spots

0.5 to 1 cm

c)Spotting volume

1 to 2 µl

d)Composition of mobile phase

(1)	2-Propanol: Acetone: Lactic Acid (0.1 M)	3:4:3
(2)	2-Propanol: Acetone: ddH_2O: o-Phosphoric acid	20:30:10:2
(3)	2-Propanol: Acetone: ddH_2O: o-Phosphoric acid	20:30:5:2
(4)	2-Propanol: Acetone: ddH_2O: o-Phosphoric acid	20:30:2.5:1
(5)	2-Propanol: Acetone: ddH_2O: o-Phosphoric acid	20:30:5:1

The content of the mobile phase with the best separation characteristics was (5); hence it was used for the further analysis. After optimization process the following parameters, shown in Table 9, were chosen for the analysis of the EPS, hydrolysates and sugar standards.

Table 9: TLC parameters

Parameter	
Spotting volume	1 µl
Spotting distance	1 cm
TLC sheet preparations	no
Mobile phase	(5)

According to Bailey et al. [56] the TLC plates were sprayed with two different solutions for the visualization of carbohydrates. The color reaction relies on the conversion of pentose/hexose in the presence of o-phosphoric acid to furfural/5-hydroxymethylfurfural respectively. Hence, the products react with the sprayed reagent to give a colored compound. The composition of the sprays as described by Buchan et al. [57] and is shown in Table 10. The TLC plates were sprayed with the first spray, incubated for 5 minutes at 80 °C on a hot plate and then immediately with the second one and treated with the same conditions.

Table 10: Composition of the sprays for visualization of carbohydrates

Spray 1		**Spray 2**	
Chemicals	**Amount**	**Chemicals**	**Amount**
diphenylamine	2 g	aniline	2 ml
ortho-phosphoric acid	10 ml	ortho-phosphoric acid	10 ml
acetone	100 ml	acetone	100 ml

All EPS samples and hydrolysates were tested by TLC as described above, therefore two standard mixes were prepared. The first standard (I) comprised four different sugars rhamnose, glucose, galacturonic acid and maltose and for the second one (II) fructose, arabinose, ribose were mixed together. Additionally, a fructose standard was prepared.

2.2.3.7 BCA assay of residual protein in the EPS

Protein concentrations were determined by the bicinchoninic acid (BCA) assay kit and are based on the biuret reaction. The kit contains the BCA solution and 4 % (w/v) cupric sulfate solution. BCA is a chromogenic reagent; in alkaline solution Cu^{2+} of the cupric sulfate solution is reduced to Cu^{1+} and forms a Cu^{1+}-protein complex. BCA chelates with the Cu^{1+} and produces a purple complex which strongly absorbs at 562 nm. As protein standard, bovine serum albumin (BSA) was used in different concentrations to obtain the calibration curve. The assay was performed in 96-well plates according to the protocol.

2.2.4 Monitoring production of hydrogen peroxide using cellobiose dehydrogenase

EPS samples were first hydrolyzed with several hydrolytic enzymes to generate simple sugars, which can be used by cellobiose dehydrogenase (CDH) for the production of hydrogen peroxide. Several methods are known to determine hydrogen peroxide, based on the reaction mechanism, they can be summarized according to Mottola et al. [58] in following categories: oxidation of metal ions or metal chelates, iodide ion or organic compounds and the production of fluorescence or luminescence.

2.2.4.1 Determination of the CDH activity and substrate specificity using DCIP

The 2,6-dichloroindophenol (DCIP) assay was carried out according to Ludwig et al. [39] and is a standard method to determine the activity of cellobiose dehydrogenase (CDH) in crude extracts as well as purified preparations. Lactose was chosen over cellobiose as electron donor due to lower costs and less problems with substrate inhibition [59]. This assay is based on the ability of CDH to transfer the electrons of the substrate to the redox-dye 2,6-dichloroindophenol (DCIP). The reduction of DCIP, which is blue in its oxidized state, leads to a decolorization. The scheme is shown in Figure 5 and the pipetting protocol listed in Table 11. The CDH was added after 20 minutes at 30 °C in the thermomixer. The reduction of absorbance is measured with the spectrophotometer at 520 nm.

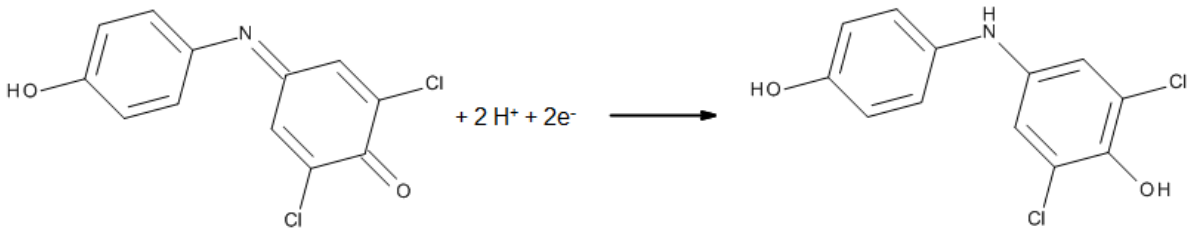

Figure 5: DCIP reaction: Reduction of the electron acceptor DCIP (drawn by Accelrys Draw 4.1)

Table 11: Protocol of the DCIP assay

Reagent	Concentration [mM]	Amount [µl]
DCIP solution (10 % Ethanol)	3	100
Lactose solution	300	100
Sodium acetate buffer (pH 4)	200	780
CDH		20

Furthermore, the substrate specificity of CDH was analyzed, therefore the DCIP assay was done as described above. Alternative electron donors were tested in two different concentrations:

a) 300 mM: lactose, N-acetyl-glucosamine, glucosamine and cellotetraose
b) 55.8 mM: galactosamine HCl and lactose

2.2.4.2 Activity staining of catalase and CDH after electrophoresis

Gel electrophoresis was conducted using native polyacrylamide gels (8 % or 6 % separation gel and 4 % stacking gel) to test the catalase and CDH activity. The electrophoresis was carried out at 50 Volt for around 300 minutes at 4 °C, based on the method of Kandukuri et al. [60]. The composition of the separating gel is illustrated in Table 12, the stacking gel in Table 13; the loading and running buffer are shown in the Table 14 and Table 15 below.

Table 12: Composition of separating gel (8 % and 6 %)

Chemical compound	Amount [ml] (8%)	Amount [ml] (6%)
40 % Acrylamide Bis	2	1.5
Tris HCL 1.5 M/ 8.8 pH	2.5	2.5
ddH2O	5.4	5.9
10 % APS	0.05	0.05
TEMED	0.012	0.012

Table 13: Composition of stacking gel (4 %)

Chemical compound	Amount [ml]
40 % Acrylamide Bis	1
Tris HCL 0.5M/ 6.8 pH	2.5
ddH2O	6.5
10 % Ammonium persulfate (APS)	0.05
TEMED	0.012

Table 14: Composition of running buffer

Chemical compound	Amount [g]
Tris	15
Glycin	72

Table 15: Composition of loading buffer

Chemical compound	Amount [ml]
Tris HCl/ 6.8 pH	1.55
1 % Bromphenol blue (0.5 g in 50 ml)	0.25
ddH_2O	0.70
Glycerol	2.50

After the electrophoresis was performed, the gel was washed three times with 60 ml ddH_2O for 15 minutes at 4 rpm on the shaking platform.

Staining for the detection of catalase activity was performed according to the protocol of Woodbury et al. [61]. The method relies on the fact that hydrogen peroxide reacts with potassium ferricyanide (III), consequently the compound is reduced to potassium ferricyanide (II) and peroxide is oxidized to molecular oxygen. Ferric chloride interacts with the reduced ferricyanide (II) and forms a stable blue pigment. Hence, the gel is colorized dark green and the catalase bands are light yellow and stable for several hours. It is worth mentioning that the band intensity is not strictly proportional to the detected catalase activity in the samples [61].

Several solutions were prepared based on the protocol:

I: 2 % potassium ferricyanide $K_3[Fe(CN)_6]$

II: 2 % ferric chloride (FeCl)

III: 10 mM H_2O_2-solution (in 50 mM sodium phosphate buffer with pH 7)

After the washing step the gel was placed in 50 ml of the hydrogen peroxide solution for 10 minutes and was rinsed shortly before incubating it in a freshly prepared 1 % $K_3[Fe(CN)_6]$/FeCl solution. To ensure stability of the stained gels, they should be stored in the dark.

The activity staining of CDH is based on the enzymatic activity assay using DCIP and cellobiose. After the washing step the gel was incubated in the DCIP solution for ten minutes. The gel was rinsed to remove any traces of the color solution followed by a 10 minute incubation step in 50 mM lactose.

Moreover, a sodium dodecyl sulfate (SDS) gel electrophoresis (6 % separation gel and 4 % stacking gel) was performed to check the purity of the CDH. It was prepared by adding 10 % SDS in the stacking and separation gel, 4 % SDS in the loading buffer and 1 g to the running buffer. The rest was done as described above, except that a different staining method was conducted. For the SDS gel the Kang staining was performed, the content of the staining and destaining solution are shown in Table 16. First the gel was washed, followed by an overnight staining for approximately 12 hours to visualize the protein bands. Hence, washing steps were done with distilled water to remove the staining solution; afterwards the gel was incubated for 3 hours in the destaining solution to increase the contrast between the visualized bands and the gel.

Table 16: Composition of Kang staining and destaining solution

KANG staining Compound	Amount	KANG destaining Compound	Amount
0.02 % (w/v) Coomassie Blue CBB G-250	0.2 g	10 % ethanol (96%)	100 ml
5 % aluminum sulfate 18 hydrate	50 g	2 % o-H_3PO_4 (100 %)	20 g
10 % ethanol (96%)	100 ml	90 % dH_2O	900 ml
2 % o-H_3PO_4 (100 %)	20 g		
90 % dH_2O	900 ml		

Moreover, a size exclusion chromatography was conducted with CDH batch VI to analyze if contamination of the batch with catalase could be observed. Therefore 100 mM sodium acetate buffer (pH 4) was prepared and filtrated. For the chromatography the column Superdex 200 was used with a flow rate of 0.2 ml/min.

2.2.4.3 Leuco crystal violet (LCV) assay and its optimization

The leuco crystal violet (LCV) assay was published 1970 by Mottola et al. [58] and is a very sensitive method for determining the hydrogen peroxide concentration. The principle of the assay relies on the ability of horse radish peroxidase to oxidize leuco crystal violet to a violet cation that can be measured at 590 nm. The measured absorbance is linearly correlated to the concentration of hydrogen peroxide in the sample. The assay, which was used for the determination of hydrogen peroxide in the samples, was carried out according to the protocol of Pricelius et al. [39]. The reaction mixture was prepared as illustrated in Table 17 and incubated for 30 minutes at 40 °C and 1050 rpm in the thermomixer.

Table 17: Composition of reaction mixture used for LCV assay

Chemical compound	Amount [µl]
Sodium phosphate buffer (55 mM; pH 6.5)	555
Substrate (EPS/hydrolysates)	100
Desferrioxaminemesylate (DM)	100
CDH III (0.5 U/ml)	100

Afterwards, the previously prepared reaction mixture was boiled for 2 minutes at 99 °C in the thermomixer, due to the fact that the activity of the CDH interferes with the peroxidase activity [39]. The boiling step was prolonged to 20 minutes, because the CDH is extracted from the thermophilic organism *Myriococcum thermophilum*. Then the color initiation is started by adding LCV, peroxidase and sodium acetate buffer as shown in Table 18.

Table 18: Initiation of the color reaction

Chemical compound	Amount [µl]
LCV (1 mM dissolved in 0.06 M HCl)	25
Sodium acetate buffer (200 mM, pH 4)	550
Peroxidase (1 mg/ml)	50

Blank includes the enzyme catalase (30 U/ml) to decompose hydrogen peroxide and avoid the production of the positive leuco crystal violet cation CV^+. Furthermore, according to Cohn et al. [62] catalase was necessary for correct measurements. The calibration curve was obtained using hydrogen peroxide in the range of 0 to 200 µM. Several optimization experiments had to be conducted to improve the output of the assay:

a)Variation of the pH value by using different buffers

b)Initiation of the colorimetric reaction with 2,2'-azino-bis(3-ethylbenzthiazoline-6-sulphonic acid) (ABTS) or leuco crystal violet (LCV)

c)Peroxidases such as horseradish peroxide (HPO) and Lignin Peroxide (LIP)

d)Metal chelator such as desferrioxaminemesylate (DM) and EDTA

2.2.4.4 Amplex Red Assay

The Amplex® Red Assay was performed for the determination of hydrogen peroxide concentration in the hydrolyzed and untreated EPS samples. Amplex Red (10-acetyl-3,7-dihydroxyphenoxazine) is a colorless substrate that reacts with hydrogen peroxide in the ratio 1:1 to produce highly fluorescent resorufin. The reaction scheme is shown in Figure 6. The CDH and peroxidase are coupled in the enzyme assay. The CDH oxidizes the cellobiose to cellobionolactone and reduces at the same time the oxygen to hydrogen peroxide, which is used by the peroxidase to reduce the Amplex Red dye to resorufin.

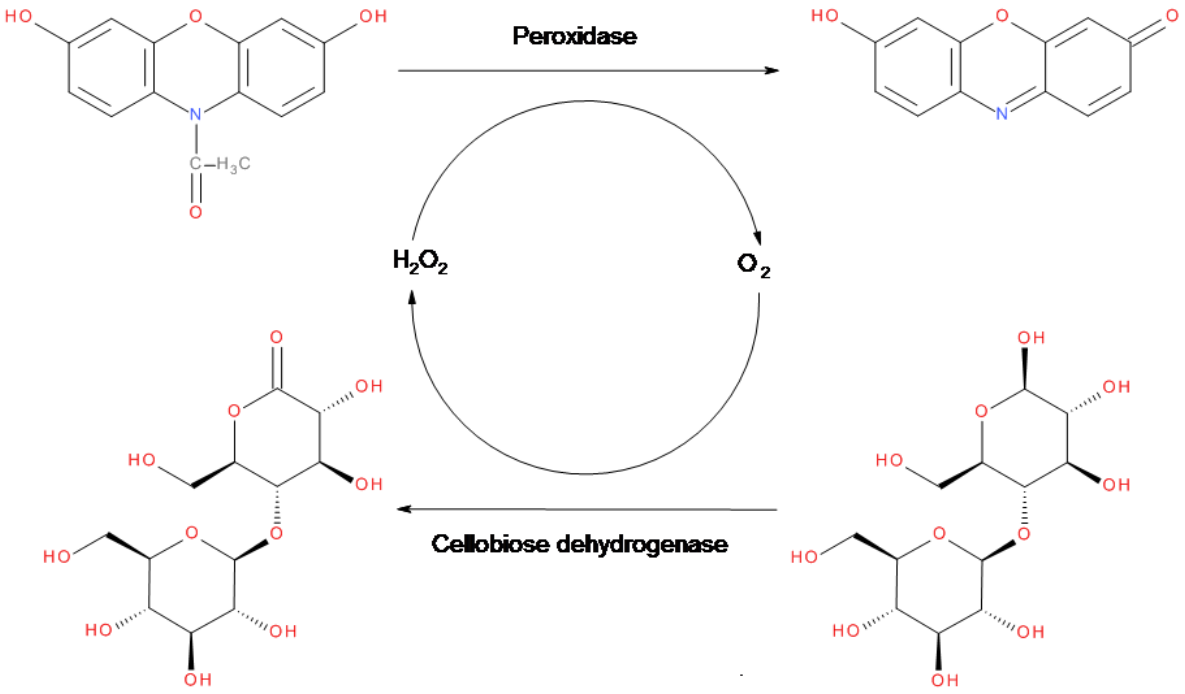

Figure 6: Amplex Red reaction scheme (drawn by Accelrys Draw 4.1)

The assay was performed according to the protocol. Hence, the EPS samples and hydrolysates were boiled at 99 °C and 300 rpm for ten minutes to denature the hydrolyzing enzyme. Afterwards 157.5 µl sodium phosphate (0.25 M pH 7.4), 30 µl sample and 10 µl CDH were transferred in a black plate, covered with parafilm and placed in a thermomixer for three hours at 40 °C and 600 rpm to produce hydrogen peroxide. After that 0.5 µl Amplex Red and 2 µl HPO were added and measured at an excitation of 550 nm, at an emission wavelength of 587 nm with a gain of 73. The calibration curve was obtained using hydrogen peroxide in the concentration of 0.25 to 25 µM. In this case the three hour incubation step was not necessary since hydrogen peroxide was already present in solution. The concentrations used in the assay are shown in Table 19.

Table 19: Protocol of the Amplex Red assay

Reagent	Stock solution	Concentration in assay	Amount in assay [µl]*
Amplex Red	10 mM	25 µM	0.5
Cellobiose	200 mM	30 mM	30

* Total volume of 200 µl

2.2.4.5 H_2O_2 sensor

The H_2O_2 sensor of the Joanneum Research was tested as an additional method to determine the hydrogen peroxide concentration amperometric. The principle of the reaction relies on the oxidation of hydrogen peroxide to oxygen after applying a voltage (polarization voltage) on the working electrode in the three electrode system, which contains the working, reference and counter electrode. The reaction is shown in Figure 7.

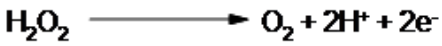

Figure 7: Reaction scheme of the sensor (drawn by Accelrys Draw 4.1)

In the reaction two electrons are released by one molecule of hydrogen peroxide, thereby it can be concluded that the measured voltage is proportional to the hydrogen peroxide concentration [63].

CDH was tested with several lactose concentrations in the range of 3.9 - 1000 µM to obtain the calibration curve. The electrode was washed between the measurements with 50 mM sodium phosphate buffer. For obtaining the calibration curve the current is plotted against the concentration of lactose to determine the linear equation for calculation of the hydrogen peroxide concentration in the tested samples.

Additionally, CDH was tested with lactose as electron donor. Therefore, 700 µl were prepared in total containing: 100 µl lactose, 100 µl CDH and 500 µl of a 50 mM sodium phosphate buffer. After 300 seconds the enzyme was added.

2.2.5 Antibiofilm and antimicrobial activity assay

The assay was performed according to Craigen et al. [28]. For *S. aureus* and *E. coli* an overnight culture was prepared. The OD_{600} value was determined followed by the dilution to a value of 0.01 with tryptic soy broth (TSB). Two different media compositions, which are listed in Table 20, were used for *E. coli* and *S. aureus* to meet the requirements of the respective microorganism.

Table 20: Composition for one liter media of the overnight culture (without agar) and plates

TSB-media *E. coli*		**TSB-media *S. aureus***	
Amount [g]	**Chemicals**	**Amount [g]**	**Chemicals**
30	TSB = Caso-Bouillon	30	TSB = Caso-Bouillon
8	Glucose	8	Glucose
15	Agar Agar	6	Yeast extract
		2	Sodium citrate
		15	Agar Agar

The aim of the antibiofilm assay is to determine the total biomass of the biofilm formed on the silicone plates using crystal violet staining and the viability of cells after the treatment with growth inhibiting substances. Hydrogen peroxide was used in different concentrations to analyze, which one is necessary to completely inhibit the growth of the respective organism. Moreover, that effect on cell growth of newly formed H_2O_2 should be examined by combining CDH with various cellobiose concentrations.

The assay was performed in 96-well culture plates. One autoclaved silicone plate was placed in each well. To each well media, bacteria, cellobiose (0.5 to 6 mM) and cellobiose dehydrogenase or hydrogen peroxide (125 to 2000 µM) were added. Subsequently, the culture plate was incubated for 18 hours at 37 °C. For the viability testing the silicone plates were transferred to eppendorf tubes and 500 µl of 0.9 % NaCl solution were added. The samples were treated with ultrasonic (parameters: 120 %, 26 °C with the degas program) and 100 µl of different dilutions were streaked out on agar plates and incubated at 37 °C. The other half of the samples, which were used for the determination of the total biomass, was stained with 100 µl crystal violet for ten minutes after one hour of drying in the drying oven. After the staining the silicone plates were washed several times with distilled water to remove any traces of unbound crystal violet. Then 100 µl of 30 % acetic acid were transferred on the stained silicone plates for 10 minutes to solubilize the crystal violet. Only 50 µl were transferred in a new 96-well plate to measure the absorbance at 595 nm in the plate reader.

3 Results and Discussion

3.1 Biofilm formation and production of extracellular polymeric substances (EPS)

The biofilm formation and the extraction of extracellular polymeric substances (EPS) were successfully performed for both microorganisms. The formation and composition of the biofilms varied despite following the same protocol. For comparing of the produced EPS batches, they were characterized and the dry weight was determined by drying the samples in a drying oven; the amount of the respective batches is shown in Table 21.

Table 21: Dry weight determination of the first and second EPS batch

No.	Sample name	Dry weight [mg/ml]
1	Sa1_U_1e	21.54
2	Sa1_D_1e	3.08
3	Ec1_U_1e	29.85
4	Ec1_D_1e	0.46
5	Ec1_D_1e-Ek	12.31
6	Sa1_D_1e-Ek	3.08
7	Ec2_D_1e	2.06
8	Ec2_D_2e	3.05
9	Ec2_D_3e	1.78
10	Sa2_D_1e	3.14
11	Sa2_D_2e	4.50
12	Sa2_D_3e	1.33
13	Sa2_D_1e-b	1.18
14	Sa2_D_2e-b	1.88
15	Sa2_D_3e-b	2.67

The dry weight of the first dialyzed and not dialyzed EPS batch was determined for both organisms; a fascinating observation was that there was a huge difference between the samples. The dialysis seems to get rid of a lot of sugars, it is likely that mainly monosaccharide were removed, especially glucose, which was supplemented in the media. In the first *S. aureus* EPS batch the undialyzed one (Sa1_U_1e) had a dry weight of 21.54 mg/ml and is reduced after dialysis by a factor of 7 to 3.08 mg/ml. The second dialyzed EPS batch (Ec2_D) had after the extraction with EDTA dry weights in the range of 1.18 to 4.50 mg/ml. The Ec1_U_1e compared to Ec1_D_1e was reduced by a factor of about 60. The results of the dry weight determination of the *E. coli* EPS, which was used for the hydrolysis of the enzyme combinations, was very strongly deviating.

3.2 Hydrogen peroxide production using CDH and EPS

The incubation of the dialyzed EPS of both microorganisms with cellobiose dehydrogenase produced very low amounts of hydrogen peroxide, which were in the range of 0 to 0.16 µM and were detected using the LCV assay. It can be assumed that the undialyzed EPS would produce higher values of hydrogen peroxide, but the dialysis was necessary. It had to be performed on the one hand to remove EDTA, a metal chelating agent, which might have a negative effect on the CDH activity and on the other hand to avoid falsification of the results caused by glucose, which was supplemented in the media.

Generally, the cellobiose dehydrogenase from *M. thermophilum* has a broad substrate spectrum and based on the studies of Pricelius et al. [39] it can use carbohydrates such as glucose, galactose, mannose, maltose, lactose, cellobiose, cellotriose, cellopentaose, cellotetraose, 1,4-β-xylo-oligosaccharides (X1 to X6), manno-oligosaccharides (M2 to M6) and substituted galactosyl-mannose-oligosaccharides (G-M3 to G-M5) as substrate, but the enzyme seems not to be able to use fructose for the production of hydrogen peroxide.

The EPS of *E. coli* comprises according to Bales et al. [26] mostly of glucose, N-acetyl-galactosamine, fucose and in low concentrations galactose, mannose and N-acetyl-glucosamine. Some *E. coli* strains have colanic acid as component of the EPS matrix [25]. It is a complex sugar polymer, which contains galactose, fucose, glucose, glucuronic acid. The EPS of *S. epidermidis*, which is an organism of the same genus such as *S. aureus*, contained no fucose, but high amounts of mannose; additionally, galactose, glucose, N-acetyl-galactosamine, N-acetyl-glucosamine were detected by the analysis of Bales et al. [26] .

Based on the knowledge about the composition of the EPS and the CDH substrate spectrum, it is possible to boost the hydrogen peroxide production with a previous hydrolyzing step. Consequently, for enhancement of the hydrogen peroxide production, the EPS was hydrolyzed using several hydrolytic enzymes to produce smaller molecules, which can be used by the cellobiose dehydrogenase as electron donor. This was achieved by incubating different enzymes with EPS.

3.3 Enzymatic hydrolysis of the EPS

To confirm that the enzymatic hydrolysis of extracellular polymeric substances was successful, the untreated EPS samples and hydrolysates were characterized using several methods and the results are described in more detail in the following chapter.

3.4 Characterization of EPS and its hydrolysates

3.4.1 Untreated EPS

3.4.1.1 BCA assay

To determine protein concentrations of the EPS batches, the BCA assay was performed as described; the calibration curve was obtained by using bovine serum albumin (BSA) and is illustrated in Figure 8.

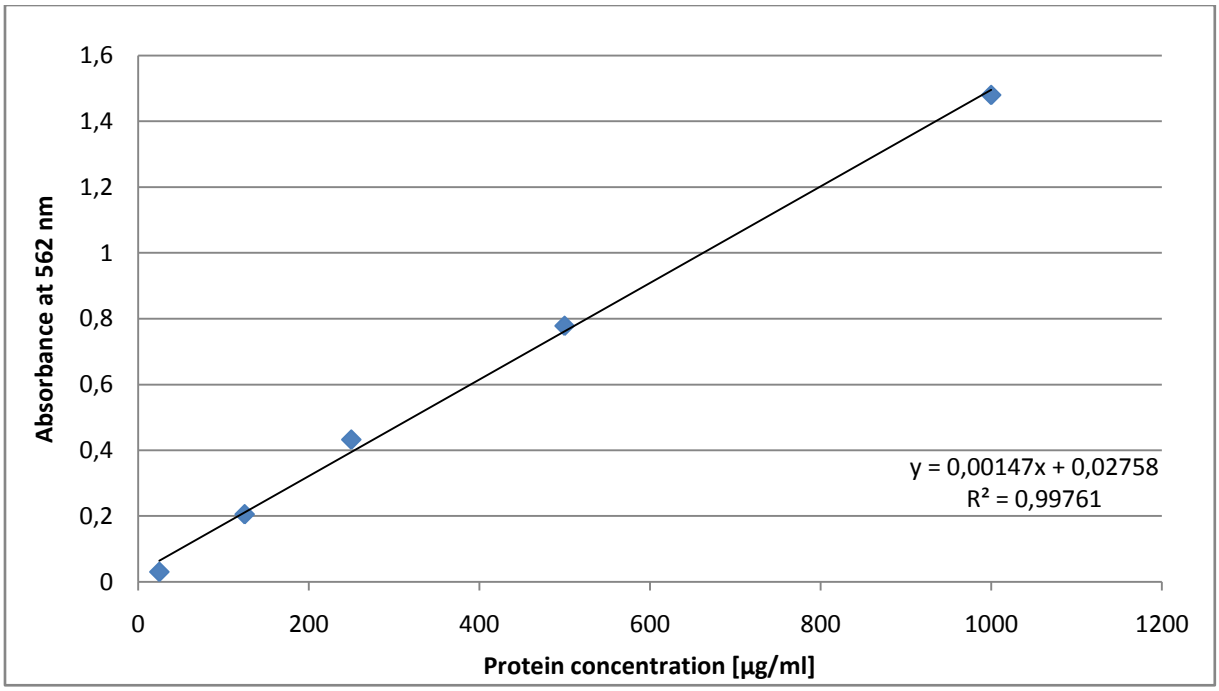

Figure 8: Calibration curve of the BCA assay to determine the protein concentration

The untreated EPS batches were tested in triplicates and were calculated by using the linear equation: y = 0.00147 x + 0.02758; for each batch the average value of the protein concentrations can be seen in Table 22. Even the protein concentrations of the batches were varying.

Table 22: Protein concentration of all untreated *E. coli* and *S. aureus* batches

No.	Sample name	Protein concentration [mg/ml]				
		1.	2.	3.	Standard deviation	Average
1	Sa1_U_1e	1.537	1.625	1.647	0.058	1.603
2	Sa1_D_1e	0.954	0.986	1.004	0.025	0.981
3	Ec1_U_1e	1.911	1.927	2.051	0.076	1.963
4	Ec1_D_1e	1.137	1.811	1.227	0.366	1.392
5	Ec2_D_1e	0.694	0.670	0.695	0.014	0.686
6	Ec2_D_2e	0.618	0.617	0.609	0.005	0.615
7	Ec2_D_3e	0.418	0.408	0.435	0.013	0.420
8	Sa2_D_1e	0.593	0.553	0.567	0.020	0.571
9	Sa2_D_2e	0.335	0.329	0.322	0.007	0.329
10	Sa2_D_3e	0.250	0.247	0.221	0.016	0.239
11	Sa2_D_1e-b	0.495	0.465	0.476	0.015	0.479
12	Sa2_D_2e-b	0.360	0.346	0.342	0.010	0.349
13	Sa2_D_3e-b	0.257	0.253	0.250	0.004	0.253

3.4.1.2 Dubois assay

The calibration curve was performed with galacturonic acid in the range of 0.5 to 3.5 mM and is depicted in Figure 9.

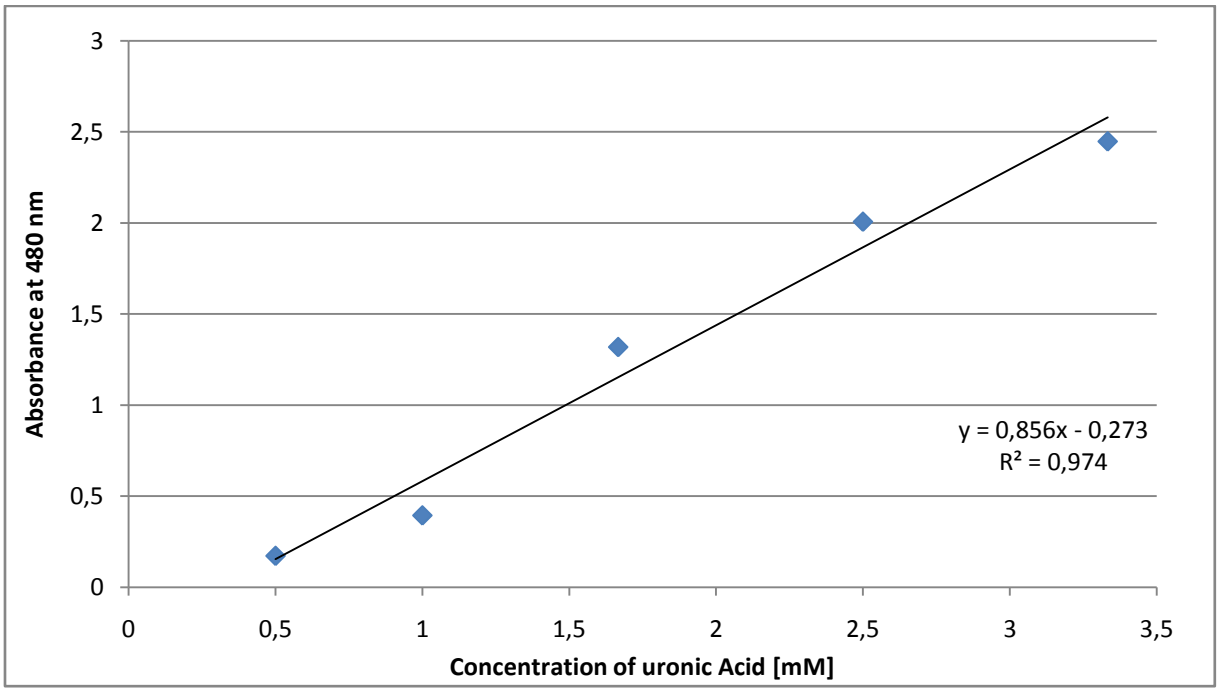

Figure 9: Calibration curve of the dubois assay to determine the uronic acids concentration

The equation y = 0.856 x - 0.273 was used to determine the concentration of uronic acids in the EPS batches of both organisms. The obtained results are shown in Table 23; the whole data set is in the Appendix.

Table 23: Dubois assay of the dialyzed EPS batches to determine the uronic acid concentration

No.	Sample name	Concentration of uronic acid [mM] 1	2	3	Standard deviation	Average
1	Ec1_D_1e	1.0268	1.0861	0.9675	0.32	1.03
2	Sa1_D_1e	0.7032	0.5110	0.6836	0.37	0.63
3	Ec2_D_1e	0.5772	0.6977	0.4814	0.37	0.59
4	Ec2_D_2e	0.4518	0.7004	0.4408	0.41	0.53
5	Ec2_D_3e	0.5279	0.5655	0.5239	0.29	0.54
6	Sa2_D_1e	1.0943	1.1066	0.6901	0.50	0.96
7	Sa2_D_2e	0.6178	0.6594	0.6954	0.30	0.66
8	Sa2_D_3e	0.5320	0.5183	0.5206	0.27	0.52
9	Sa2_D_1e-b	1.3626	1.3629	1.3053	0.30	1.34
10	Sa2_D_2e-b	0.7596	0.7303	0.6943	0.30	0.73
11	Sa2_D_3e-b	0.6025	0.6480	0.5617	0.31	0.60

3.4.1.3 Anthrone assay

The anthrone assay was performed to determine the total sugar content of the EPS batches and the calibration line was obtained by using glucose in the range of 0.16 to 5 mM and is shown in Figure 10.

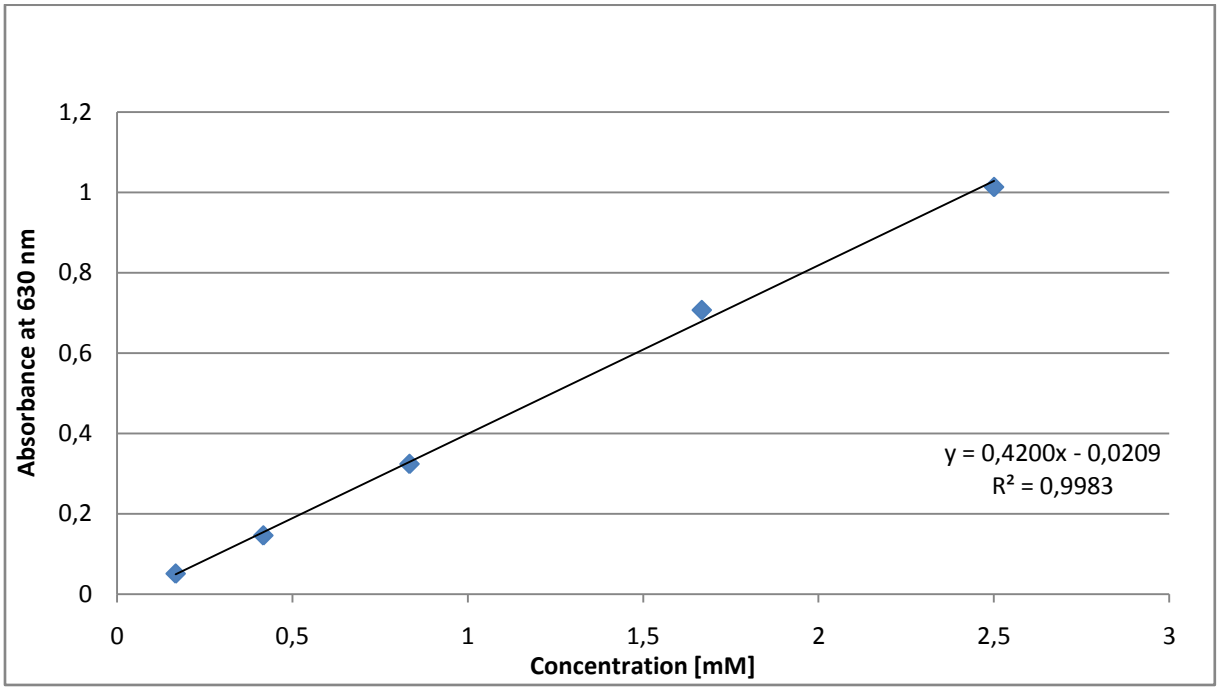

Figure 10: Calibration curve of the anthrone assay for determination of the total sugar content

Using the anthrone assay the untreated EPS samples were measured and are shown in Table 24.

Table 24: Anthrone assay of the untreated first and second EPS batch

No.	Sample name	Sugar concentration [mM] 1	2	3	Average	Standard deviation
1	Sa1_D_1e	0.62	0.66	0.66	0.65	0.02
2	Ec1_D_1e	0.45	0.53	0.43	0.47	0.05
3	Ec2_D_1e	2.03	1.42	1.50	1.65	0.33
4	Ec2_D_2e	0.66	0.66	0.60	0.64	0.03
5	Ec2_D_3e	0.31	0.40	0.38	0.36	0.05
6	Sa2_D_1e	1.65	1.70	1.67	1.67	0.03
7	Sa2_D_2e	0.55	0.69	0.62	0.62	0.07
8	Sa2_D_3e	0.39	0.47	0.38	0.41	0.05
9	Sa2_D_1e-b	2.41	2.00	2.19	2.20	0.20
10	Sa2_D_2e-b	0.84	0.96	0.91	0.90	0.06
11	Sa2_D_3e-b	0.43	0.60	0.58	0.54	0.09

Based on the results of the anthrone assay, it can be assumed that most of the sugars are extracted in the first extraction step. Moreover, it can be seen that the first EPS batch contained less sugars than the second one.

3.4.1.4 Summary of the untreated EPS

For evaluating the untreated EPS batches the results of the dubois, BCA and anthrone assay are shown in Figure 11. According to Pan et al. [49] the extracted amounts of protein and sugar are depending on the extraction method.

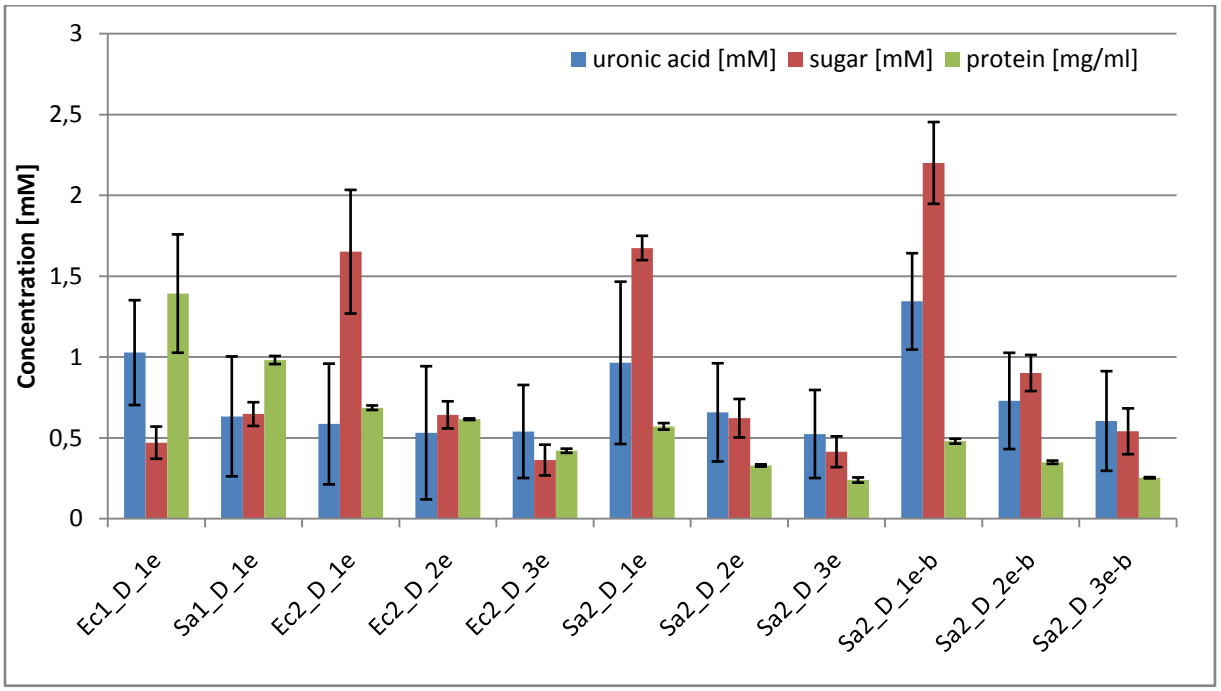

Figure 11: Evaluation of the BCA, dubois and anthrone assay

The dubois assay of the first *E. coli* EPS batch (Ec1_D_1e) compared to the second one (Ec2_D_1e) had 43 % less uronic acids. This difference can only be explained due to the fact that biofilms can grow differently despite using the same conditions. When comparing the uronic acid concentration of the sample Ec2_D_1e after the first EDTA extraction step with the second and third one, there is a reduction of 7 %. In the case of the first (Sa1_D_1e) and the second *S. aureus* EPS batch (Sa2_D_1e), it is the other way around, the second batch showed a higher concentration. In the extraction step two and three of the *S. aureus* EPS batch (Sa2_D_2e and Sa2_D_3e) 44 % and 52 % loss were demonstrated and in the other one (Sa2_D_2e-b and Sa2_D_3e-b) 30 % and 43 %.

The interesting part about the determination of the concentration of uronic acids and sugars was that the results were very varying. Sugar concentrations of both organisms seemed to be significantly lower in the first batch in comparison to the second one. The fascinating thing was the significant decrease after every EDTA extraction step. Maybe the extraction was more efficient for sugars after the first step and less effective for the uronic acids.

The protein concentration was determined with the BCA assay. Measured protein concentration of the first EPS batch (Sa1 and Ec1) was between 1.60 and 1.96 mg/ml before dialysis and afterwards between 0.98 and 1.39 mg/ml. The second EPS batch (Ec2 and Sa2) had in comparison to the first one a significantly lower concentration of proteins. The values of the determined protein concentrations were for Sa2_D_1e in the range of 0.48 - 0.57 mg/ml and for Ec2_D_1e around 0.69 mg/ml. Such variations in protein concentrations are common, despite having the same cultivation, growth and extraction conditions. It was observed that lower protein concentrations were extracted per additionally performed EDTA-extraction step. Important is the fact that the amount of extracted proteins, sugars and nucleic acids is depending on the chosen extraction method based on Comte et al. [64]. Moreover, Pan et al. [49] compared five different extraction methods of EPS: ultrasonic, centrifugation, EDTA, formaldehyde and formaldehyde with the addition of sodium hydroxide (NaOH) and concluded that they work with an different efficiency. This agrees with the achieved results, which were very varying.

3.4.2 Hydrolyzed samples

3.4.2.1 DNS assay

The DNS assay was conducted to determine the amount of five and six carbon reducing sugars in the EPS samples and hydrolysates. The calibration curve was performed with cellobiose and is depicted in Figure 12.

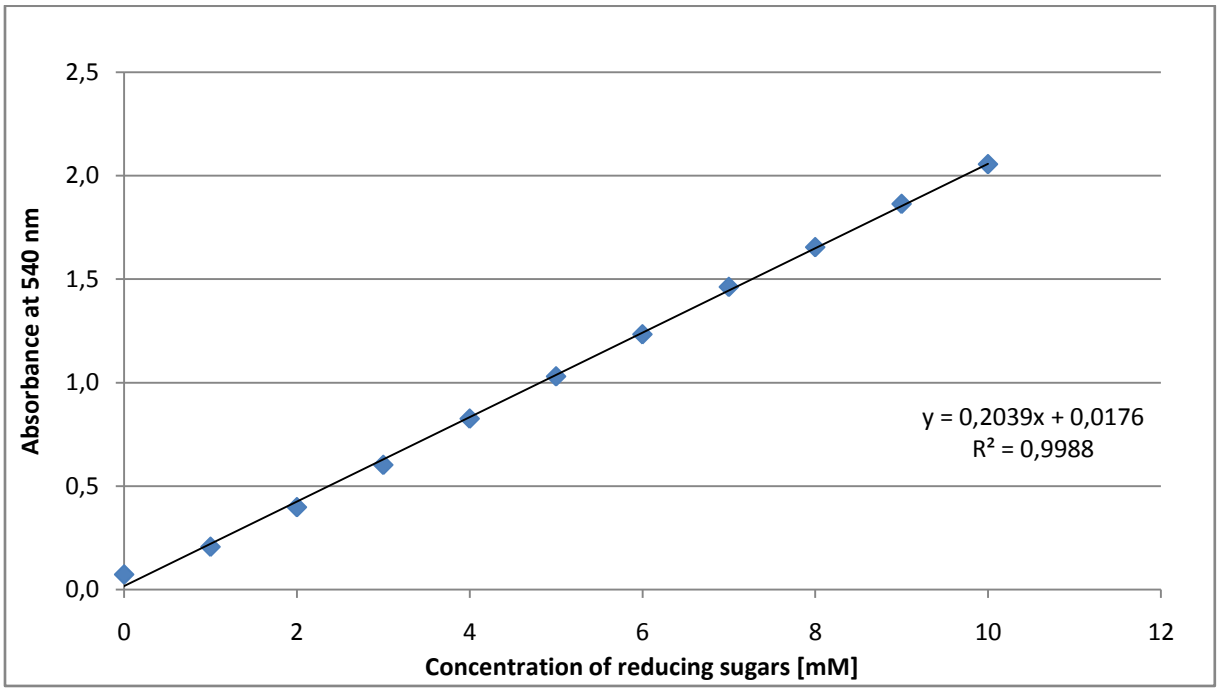

Figure 12: Calibration curve of the DNS assay

The untreated EPS samples of the first (Ec1_D_1e and Sa1_D_1e) and the second batch (Ec2_D_1e and Sa2_D_1e) were tested and the whole data set is illustrated in the Appendix. The amount of reducing sugars of the untreated EPS batches were in the range of 0.25 to 0.32 mM and were determined by using the linear equation: y = 0.2039 x + 0.0176. The hydrolyzed samples reached high values of reducing sugars and some had to be diluted for measurement to remain in the range of the calibration curve. The highest concentration of reducing sugars was always determined in the samples of the following hydrolyzing enzymes: A-amyla-Nov, A-amyla-U, Cellu-Sig, Cellu-Flk. The values of the four best enzymes and corresponding blanks are illustrated in Table 25 and depicted in Figure 13.

Table 25: DNS assay of selected EPS hydrolysates

		Reducing sugars [mM]			
No.	Sample name	A-amyla-Nov	A-amyla-U	Cellu-Sig	Cellu-Flk
1	Sa1_D_1e	45.4	9.6	12.2	19.4
2	Ec1_D_1e	125.2	31.4	30.0	11.3
3	Sa2_D_1e	46.6	12.1	10.9	14.1
4	Ec2_D_1e	48.7	10.7	11.6	15.3
5	Blank Enzyme	8.1	12.9	4.4	4.2

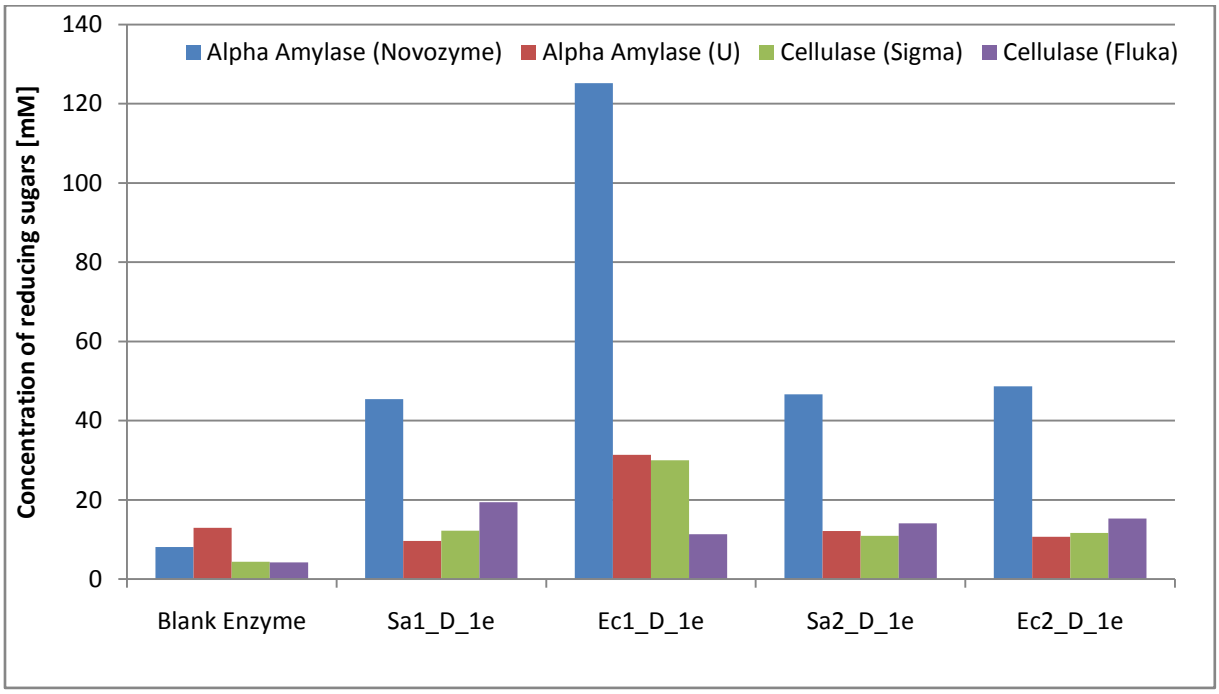

Figure 13: DNS assay of the EPS hydrolysates

The enzyme blank was measured due to the fact that enzyme preparations could possibly contain carbohydrates for stabilizing the biological product. According to the measurements the hydrolysis with cellulase and alpha amylase was very effective, because of the significant increase of the reducing sugar concentration after the 24 hours incubation. The blank of the enzyme A-amyla-U was higher than some of the measurements; explanations could be pipetting mistakes or variations within the measurement. In the Appendix the concentration of reducing sugars of all EPS samples and the used hydrolytic enzymes are shown and approve the fact, that nearly all enzyme preparations contained more or less carbohydrates. In order to increase the reducing sugar content combinations of the best performing enzymes were tested. Especially, the alpha amylase of Novozyme (A-amyla-Nov) was tested for most combinations due to the high yield of reducing sugars. The achieved results of the used enzyme combinations are shown below in Table 26 for Ec1_D_1e-Ek and in the Table 27 for Sa1_D_1e-Ek.

Table 26: DNS assay of *E. coli* enzyme combinations Ec1_D_1e-Ek

Sample name	Concentration of reducing sugar [mM]
Ec1_D_1e-Ek1	238.38
Ec1_D_1e-Ek2	178.04
Ec1_D_1e-Ek3	250.80
Ec1_D_1e-Ek4	130.58
Ec1_D_1e-Ek5	161.49
Ec1_D_1e-Ek6	13.57
Ec1_D_1e-Ek7	12.21
Ec1_D_1e-Ek8	8.42
Ec1_D_1e-Ek9	3.10
Ec1_D_1e-Ek10	2.58

The hydrolysates, which were produced by combining two or three hydrolyzing enzymes reached a higher yield of reducing sugars than the single enzyme hydrolysates. For *E. coli*, the combinations Ec1_D_1e-Ek3 (A-amyla-Nov and Enz-mix-U), Ec1_D_1e-Ek1 (A-amyla-Nov and Cellu-Flk), Ec1_D_1e-Ek2 (A-amyla-Nov + Cellu-Flk + Mann-Nov), Ec1_D_1e-Ek5 (A-amyla-Nov and Pulp-Nov) and Ec1_D_1e-Ek4 (A-amyla-Nov and Mann-Nov) achieved a very high concentration of reducing sugars. The remaining enzyme combinations, which were produced without using A-amyla-Nov, had a significantly lower amount.

Table 27: DNS-Assay of *S. aureus* enzyme combinations Sa1_D_1e-Ek

Sample Name	Concentration of reducing sugar [mM]
Sa1_D_1e-Ek1	103.15
Sa1_D_1e-Ek2	131.21
Sa1_D_1e-Ek3	110.07
Sa1_D_1e-Ek4	98.44
Sa1_D_1e-Ek5	97.15
Sa1_D_1e-Ek6	80.43
Sa1_D_1e-Ek7	59.47
Sa1_D_1e-Ek8	5.34
Sa1_D_1e-Ek9	0.93
Sa1_D_1e-Ek10	2.73

Due to the reason that the samples, which were hydrolyzed using the alpha amylase of Novozyme (A-amyla-Nov), achieved a high yield of reducing sugars, various combinations were performed. All combinations of the hydrolytic enzyme, which contained A-amyla-Nov, reached a higher concentration of reducing sugar than the hydrolysate produced by the single enzyme. The enzyme combination Sa1_D_1e-Ek2 resulted in a nearly three times as high concentration of reducing sugars as the enzyme alpha amylase of Novozyme (A-amyla-Nov), alone. The combinations Sa1_D_1e-Ek3, Sa1_D_1e-Ek1, Sa1_D_1e-Ek4, Sa1_D_1e-Ek5 achieved a concentration twice as high. The reducing sugar concentrations of the enzyme combinations were compared to the single enzymes by addition of the achieved results of the respective single enzymes and their results are shown in Figure 14 and Figure 15.

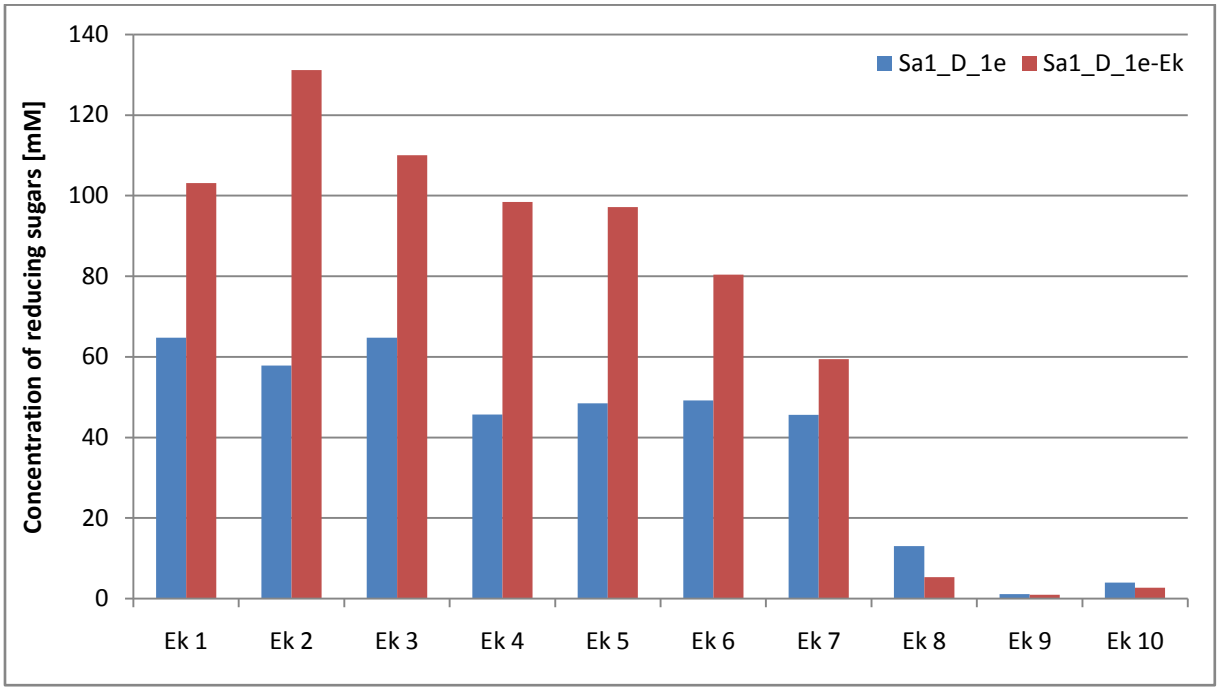

Figure 14: DNS assay of the *S. aureus* enzyme combinations compared to single enzymes

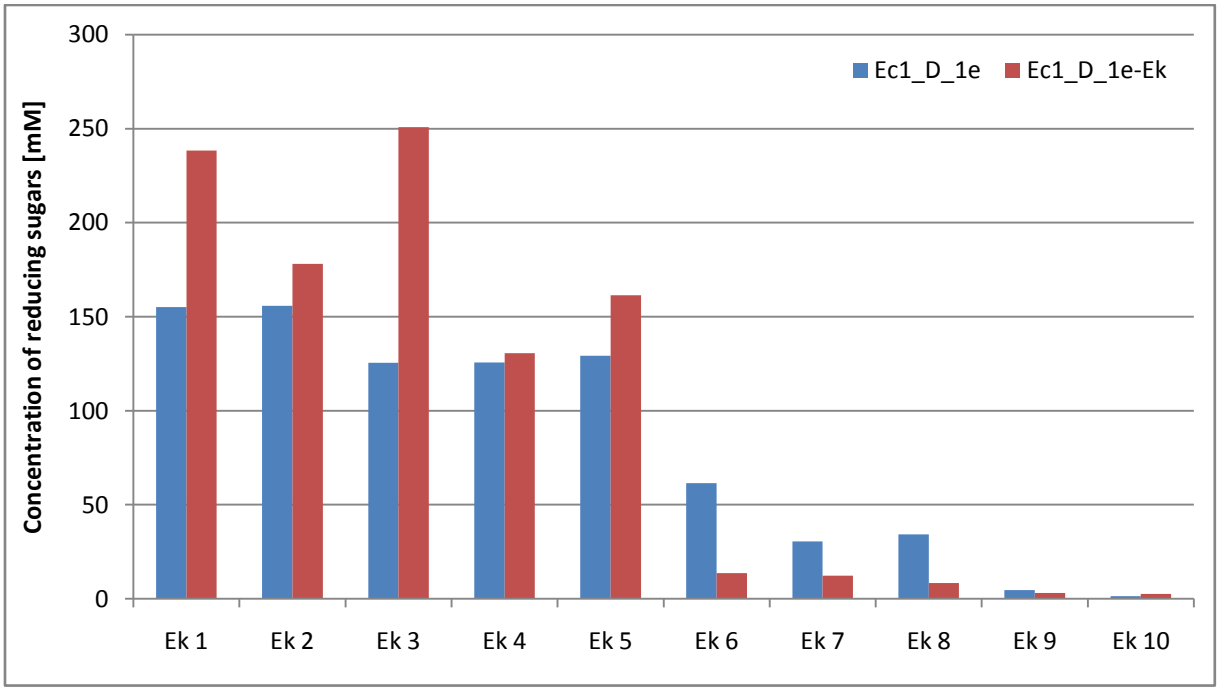

Figure 15: DNS assay of the *E. coli* enzyme combinations compared to single enzymes

3.4.2.2 HPLC-RI

The chromatograms of the measured standards are shown in the Appendix. The used column was very sensitive; the pressure was varying during each measurement. A possible explanation for the unstable pressure would be that the polysaccharides are stuck into the column. Therefore the secure cartridge was exchanged. The retention times of each standard are listed in Table 28.

Table 28: Retention times of the sugar standards at two different pressures

Sugar standard	Retention Time [min] at 130 bar	Retention Time [min] at 124 bar
Arabinose	2.169	2.416
Fructose	2.334	2.666
Galactose	2.755	3.242
Ribose	1.847	1.989
Glucose	2.701	3.193
Mannose	2.551	2.965
Lactose	4.331	5.693
Saccharose	3.614	4.625
Maltose	4.134	5.413
Xylose	2.099	2.335
Trehalose	4.495	6.039
Rhamnose	1.905	1.958
Cellobiose	4.128	5.364
Glucosamine	0.919	1.096
Cellotetraose	x	-
Cellohexaose	x	-
Glucuronic acid	x	-

-no peak x not testedwith this pressure

After analyzing the sugar standards the analysis of the hydrolysates at the beginning of the hydrolysis and after 24 hours was performed to detect the newly cleaved sugars of the respective EPS samples. Then the analysis of the two measured time points t_0 and t_1 of Sa1_D_1e, which was hydrolyzed by the alpha amylase of Novozyme (A-amyla-Nov), was conducted and can be seen in the Appendix as well as the chromatogram of Cellu-Sig and Enz-mix-U. Interestingly, there was an obvious difference between both time points. The figures, which are in the Appendix, showed that peaks were appearing, the retention times of the detected peaks are listed in Table 29.

Table 29: Retention times of the analyzed samples

Sample Name	Peak No.	Retention time [min]
Sa_D_1e+A-amyla-Nov	1	0.980
Sa_D_1e+A-amyla-Nov	2	1.325
Sa_D_1e+A-amyla-Nov	3	1.695
Sa_D_1e+A-amyla-Nov	4	2.724
Sa_D_1e+A-amyla-Nov	5	3.285
Sa_D_1e+Cellu-Sig	6	4.740
Sa_D_1e+Cellu-Sig	1	1.208
Sa_D_1e+Cellu-Sig	2	3.251
Sa_D_1e+Enz-mix-U	1	1.125
Sa_D_1e+Enz-mix-U	2	1.774

The first peak with the retention time of 0.980 of Sa_D_1e hydrolyzed with A-amyla-Nov seems to contain glucosamine based on the comparison with the standards. The second peak is the solvent peak, the third one is part of the solvent peak. The fourth peak can possibly contain glucose; the last two peaks could not be clearly identified based on the tested sugar standards.

The other tested samples of the Sa_D_1e EPS hydrolyzed with Cellu-Sig and Enz-mix-U contained the solvent peak and a not clearly identifiable sugar. Interestingly, based on nearly the same retention time the peak at 3.251 minutes of Sa_D_1e treated with Cellu-Sig and the one at 3.285 minutes (hydrolyzed with A-amyla-Nov) contained the same sugar.

Nevertheless, only some of the HPLC chromatograms showed that new peaks appeared after 24 hours of hydrolysis. Cellu-Flk and B-Gluc-U showed no additional peak. As a result, no enzymatically hydrolyzed sugars were detected, the chromatogram of both are shown in the Appendix. Some possible explanations for the observation of no peaks (except the solvent peak) were that no smaller fragments were hydrolyzed by the hydrolytic enzymes or at least no one, which could be detected by HPLC. The retention time of 3.014 minutes could not be compared with a performed standard.

Moreover, the EPS blank of both organisms of all batches were analyzed by HPLC and there was any visible peak. It was a remarkable result that no monosaccharide such as glucose was detectable by the HPLC due to the fact that it was contained in the used media. It can be concluded that either the concentration was under the detection limit or the performed dialysis step was a highly efficient method to get rid of the monosaccharides. Nevertheless, after comparing the chromatograms of the respective enzymes of both organisms, it was detected that the few samples, which showed a clear peak besides the solvent peak, exhibited always the same. The first assumption was that the enzyme was able to cleave both EPS, which was verified due to the ability to detect higher amounts of reducing sugars after hydrolysis.

That is the reason why regardless the results the enzyme was measured without adding EPS; the chromatogram of Sa1_D_1e EPS hydrolyzed with the enzyme A-amyla-Nov (+CDH) and the enzyme itself (+CDH) is shown in the Appendix.

The HPLC analysis showed good separation characteristics while analyzing the standards, but the result of the hydrolysates was not as expected. The evaluation of the chromatogram revealed that only sugar stabilizers were detected, which are present in the hydrolytic enzyme preparations. To get better results the EPS samples should be concentrated to achieve a higher signal, but pressed for time it was not possible to continue the HPLC analysis. Dogsa et al. [65] performed a gel filtration for concentrating the samples, because of low polysaccharide concentrations after dialysis. Another option would be to exchange the used column or to test the carbohydrates with a second one. However, the HPLC analysis of *Pseudomonas aeruginosa* was performed by Meisen et al. [66] with two different columns and they developed a method for qualitative and quantitative determination of various mono-, oligosaccharides and uronic acids.

3.4.2.3 HPLC/MS

The HPLC coupled with MS without using a column was performed with three standards: fructose, N-acetyl-glucosamine (N-Ac-Glu) and saccharose. The fructose and N-acetyl-glucosamine standards are shown in Figure 16.

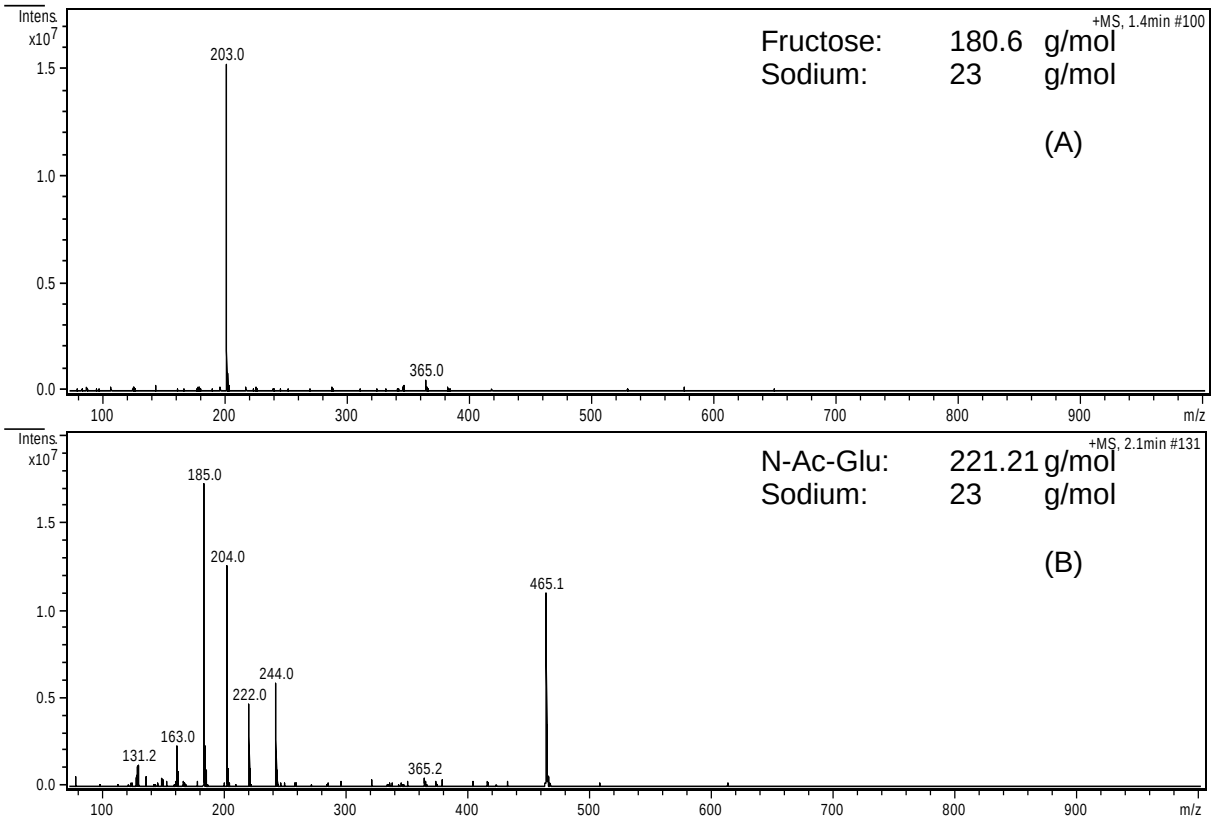

Figure 16: Spectra of two standards: fructose (A) and N-acetyl-glucosamine (B)

The mass spectrometer measured the m/z value of 203 for fructose and 244 for N-acetyl-glucosamine. The carbohydrate fructose has a molar mass of 180.6 g/mol and N-acetyl-glucosamine of 221.21 g/mol, but the samples seemed to be contaminated with sodium. In the case of fructose the molar mass 180.6 g/mol plus 23 g/mol results in the m/z value of 203 and of N-acetyl-glucosamine 221.21 g/mol plus 23 g/mol results in 244.21.

The third standard saccharose showed two peaks of both the mass spectrum is shown in Figure 17.

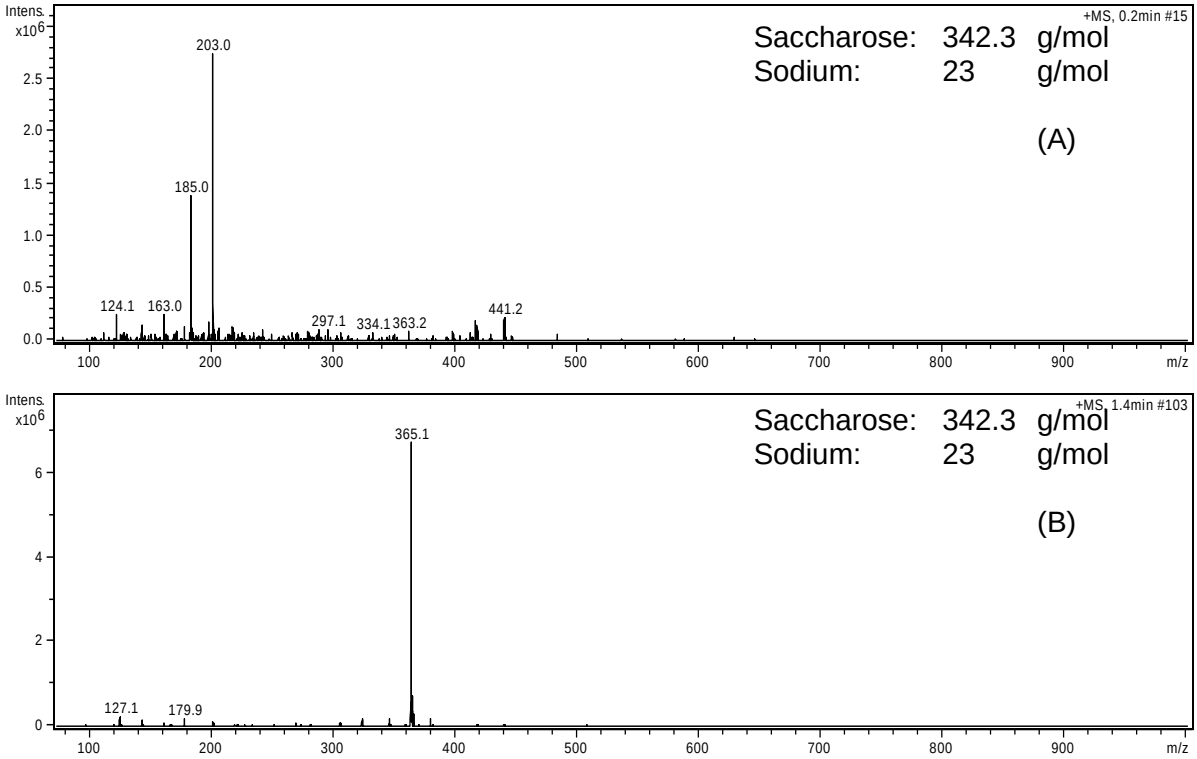

Figure 17: Mass spectrum of the standard saccharose: peak 1 (A) and peak 2 (B)

In this figure the spectrum (A) illustrates the first peak, which implies that the saccharose standard was contaminated or due to degradation the starch was already partially degraded into glucose monomers. This can be concluded from the fact that the molar mass of 203 results in the addition of the molar mass of glucose (180.6 g /mol) to sodium (23 g /mol). As an example, only one of the manually collected peaks of the hydrolysate Sa1_D_1e+Cellu-Sig is shown in Figure 18.

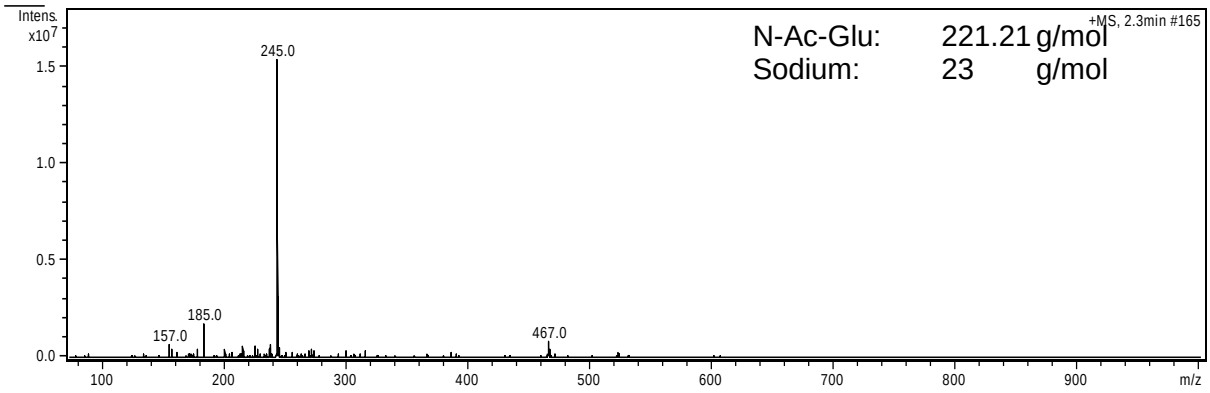

Figure 18: Mass spectrum of the sample Sa1_D_1e+Cellu-Sig

Based on the molar mass (221.21 g/mol plus 23 g/mol due to Sodium), it can be concluded that N-acetyl-glucosamine was present in the sample. It is likely that the *S. aureus* EPS contains N-acetyl-glucosamine, based on the study of Bales et. al. [26], because they showed that *Staphylococcus epidermidis*, a relative of the same genus, contains this monosaccharide derivate of glucose.

Moreover, some few mass spectra more were performed of the Sa1_D_1e+A-amyla-Sig, +A-amyla-U, and +Cellu-Sig, but they are depicted in the Appendix. Due to time limitations, no further measurements could be conducted. However, this method is a very nice and accurate method to detect mono-, oligo- or polysaccharides in the samples.

3.4.2.4 Thin layer chromatography (TLC)

The TLC was used as a chromatographic method to identify carbohydrates in the hydrolysates. Due to the separation by TLC and the sprays each carbohydrate has a different Rf-value and color. Several mobile phases were tested to optimize the separation of the tested carbohydrates. As a negative example the TLC plate with an unsuitable mobile phase (20 ml 2-propanol, 30 ml acetone, 10 ml dH_2O, 2 ml ortho-phosphoric acid), which produced bad and insufficient separation characteristics, is shown in Figure 19 with the standards glucose, fructose, rhamnose and galactose.

Figure 19: TLC of the standards (1) glucose, (2) fructose, (3) rhamnose and (4) galactose

In Figure 20 below, the thin layer chromatogram of the sugar standards is illustrated; it was generated by using the optimized mobile phase (20 ml 2-propanol, 30 ml acetone, 5 ml dH_2O, 1 ml ortho-phosphoric acid).

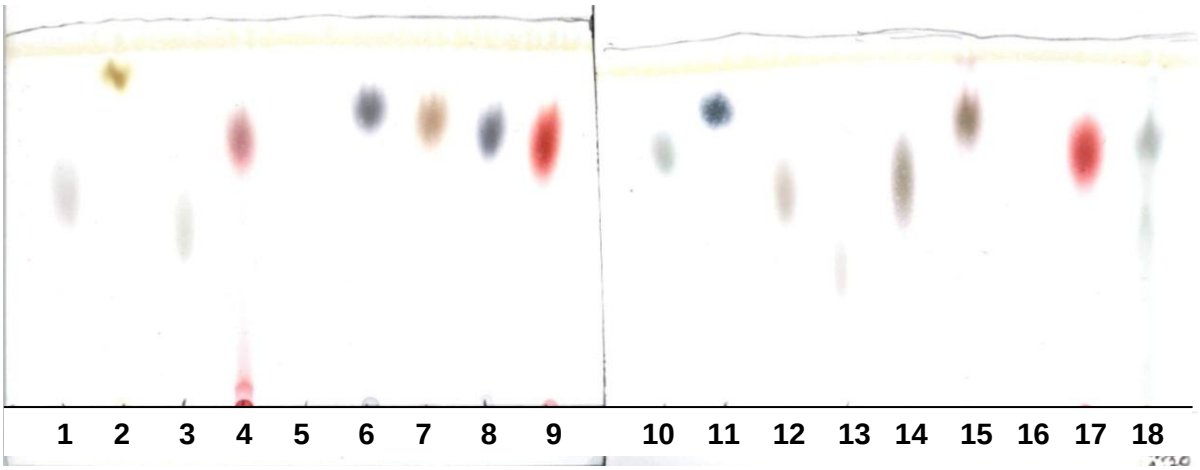

Figure 20: TLC of some sugar standards using for distinguishing due to color and Rf-value

In comparison to the figure above, the improvement of the separation by reducing the amount of distilled water and ortho-phosphoric acid was clearly recognizable. The Rf-values of the sugar standards were calculated and are shown in Table 30. All sugar standards showed a good separation characteristic and were distinguishable due to the color of the spots and the calculation of the Rf-value.

Table 30: Evaluation of the chromatogram of the sugar standards

No.	Standard	Rf-value	Color of the spot
1	Maltose	0.57	light grey
2	Rhamnose	0.87	ochre-green
3	Trehalose	0.49	light grey
4	Saccarose	0.71	red grey
5	Glucosamine	0.33	light ochre
6	Ribose	0.77	dark grey
7	Mannose	0.74	brown
8	Arabinose	0.70	dark grey
9	Fructose	0.68	red
10	Glucose	0.69	greenish grey
11	Xylose	0.80	grey-black
12	Galactose	0.59	light brown
13	Lactose	0.30	light greenish grey
14	Galacturonic Acid	0.63	grey brown
15	Glucuronic Acid	0.76	red-brown
16	Galactosamine HCL	0.20	light grey brown
17	Fructose	0.68	red
18	Starch	0.72	light grey

The TLC was performed with the EPS batch Sa1_D_1e, which was hydrolyzed by the selected enzymes A-amyla-Nov, Cellu-Sig, Cellu-Flk and Pect-Sig. The time points t_0 (at the beginning of the hydrolysis) and t_1 (after 24 hours of hydrolysis) were tested. The TLC plate is shown in Figure 21 and the calculated Rf-values are listed in Table 31.

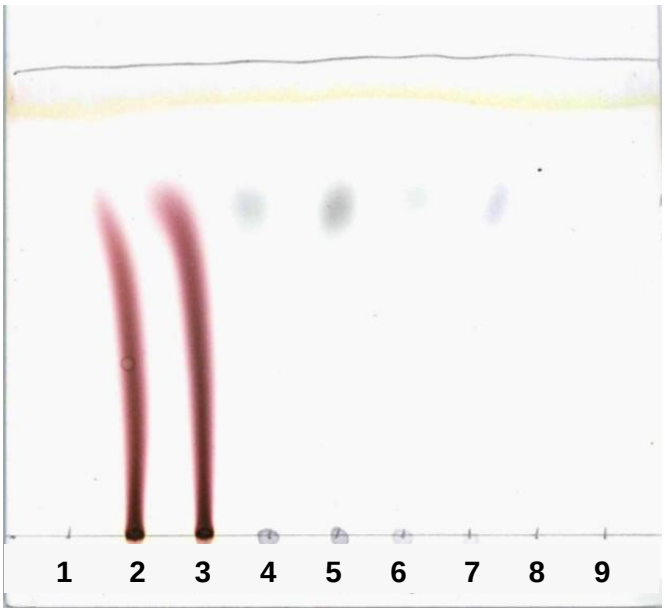

Figure 21: TLC of selected Sa1_D_1e hydrolysates (A-amyla-Nov, Cellu-Sig, Cellu-Flk, Pect-Sig)

Table 31: Rf-values of selected Sa1_D_1e hydrolysates

No.	Sample	Rf-value	Color of the spot
1	Blank	-	-
2	Sa1_D_1e+A-amyla-Nov t_0	-	red
3	Sa1_D_1e+A-amyla-Nov t_1	-	red
4	Sa1_D_1e+Cellu-Sig t_0	0.69	light grey
5	Sa1_D_1e+Cellu-Sig t_1	0.69	dark grey
6	Sa1_D_1e+Cellu-Flk t_0	0.69	light grey
7	Sa1_D_1e+Cellu-Flk t_1	0.69	light grey
8	Sa1_D_1e+Pect-Sig t_0	-	-
9	Sa1_D_1e+Pect-Sig t_1	-	-

The fascinating thing about this chromatographic separation is that in the case of the cellulases from *Aspergillus niger* (Cellu-Sig) and (Cellu-Flk) an enlargement of the spot was observed by comparing both time points t_0 and t_1. It can be concluded due to the color of the spots of both enzymes and the comparison of the Rf-value with the standard, that the respective spot probably contains glucose. The A-amyla-Nov hydrolysates could not be well separated, because of high sugar concentration and were repeated. The Pect-Sig hydrolysate showed no spot, it can be assumed that the enzyme wasn't able to cleave the EPS in mono- or disaccharides, which could be visualized by the spraying reagents. This method is an adequate method to get fast first information about the samples, but for an exact identification of the mono-, di-, or polysaccharide further methods should be used.

Due to the poor separation in the previous chromatogram the dialyzed (Sa1_D_1e) and not dialyzed (Sa1_U_1e) *S. aureus* EPS, hydrolyzed with A-amyla-Nov were spotted and run again by TLC in different dilutions (1:10, 1:20, 1:40, 1:60). The result of the TLC plate is shown in Figure 22.

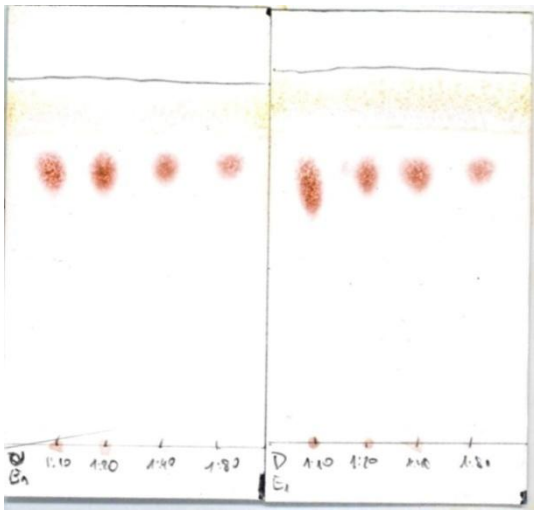

Figure 22: TLC of Sa1_U_1e/Sa1_D_1e+A-amyla-Nov tested in several dilutions

Based on the red color of the spots and the Rf-values, which were in the range of 0.69 to 0.74, it can be assumed that the spots contained fructose. Due to the adequate outcome of the previous plates the next step was the performance of the TLC of all EPS batches and hydrolysates. The TLC of the Sa1_D_1e, Ec1_D_1e and its hydrolysates of the time point t_1 (after 24 hours of hydrolysis) was performed, and is illustrated in Figure 23; the evaluation is shown in Table 32.

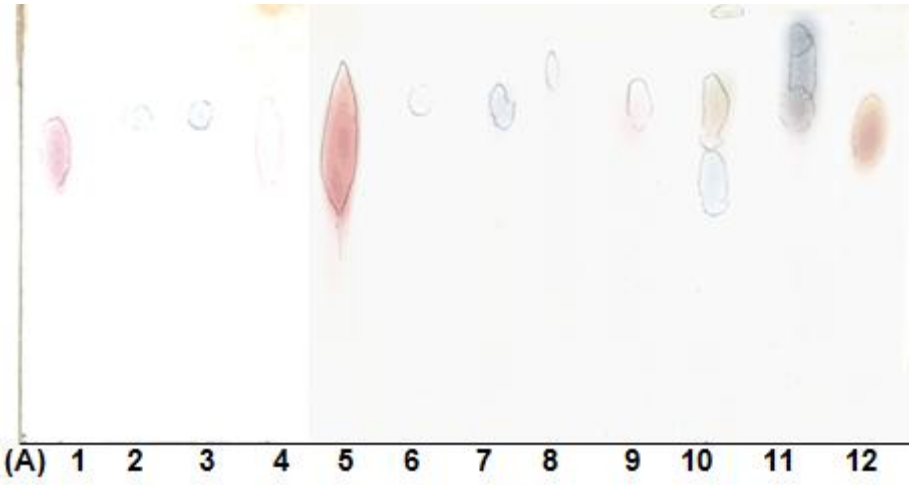

Figure 23: TLC plate (A) shows Sa1_D_1e, Ec1_D_1e, the hydrolysates at t_1 and three standards

Table 32: Evaluation of the TLC plate (A)

No.	Sample Name	Rf-value	Color
1	Sa1_D_1e+A-amyla-Nov (1:20)*	0.65	red
2	Sa1_D_1e+Cellu-Sig	0.71	blue-grey
3	Sa1_D_1e+Cellu-Flk	0.73	blue-grey
4	Sa1_D_1e+Pulp-Nov*	0.62	red
5	Ec1_D_1e+A-amyla-Nov (1:20)*	0.61	red
6	Ec1_D_1e+Cellu-Sig	0.66	blue-grey
7	Ec1_D_1e+Cellu-Flk	0.66	blue-grey
8	Ec1_D_1e+B-gluc-U	0.71	light grey
9	Ec1_D_1e+Pulp-Nov	0.65	red
10	STD II-Ribose	0.77	blue-grey
10	STD II-Arabinose	0.71	blue-grey
10	STD II-Fructose	0.63	red
11	STD I-Rhamnose	0.84	grey
11	STD I-Glucose	0.69	grey
11	STD I- Galacturonic acid	0.62	red
11	STD I-Maltose	0.51	blue-grey
12	Fructose	0.68	red

* no clear spot due to high sugar concentrations

The result of the Sa1_D_1e and Ec1_D_1e EPS and the hydrolysates of the time point t_1 (after 24 hours of hydrolysis) were nearly the same. All were run by TLC, the complete plates and tables with all samples are shown in the Appendix. Noteworthy, is the fact that always the same enzymes showed a positive TLC results. For both the enzymes A-amyla-Nov, Cellu-Sig, Cellu-Flk and Pulp-Nov the TLC was successful and carbohydrates could be identified. All had nearly the same Rf-value as above. The only difference was that beta glucanase of *E. coli* (sample: Ec1_D_1e+B-gluc-U) showed a light spot. According to the performed standards and the combination of the Rf-value and the color of the spot the carbohydrates could be identified. Fructose was detected in the hydrolysates of A-amyla-Nov and of the Pulp-Nov; due to the enlargement of the spot especially of A-amyla-Nov the clear identification by Rf-value was not possible. Nevertheless, the sugar fructose could be identified based on the spraying, because fructose was always the first sugar which appeared within several seconds while heating the plate. Both showed besides the same characteristic color reaction also the same Rf-value of 0.65.

The samples, which were hydrolyzed with the cellulases from *Aspergillus niger* (Cellu-Sig and Cellu-Flk) and the B-gluc-U showed all nearly the same Rf-value, but slight alteration in color. Based on the Rf-value two different carbohydrates are possible: glucose and starch. A clear identification was not possible, but due to the small difference it is conceivable that the Cellu-Sig-sample contained glucose, the B-gluc-U starch or glucose and the Cellu-Flk glucose or even a mix of glucose and starch. The chromatogram, which is illustrated in Figure 24 and evaluated in Table 33, shows the enzyme combinations of Sa1_D_1e and Ec1_D_1e EPS.

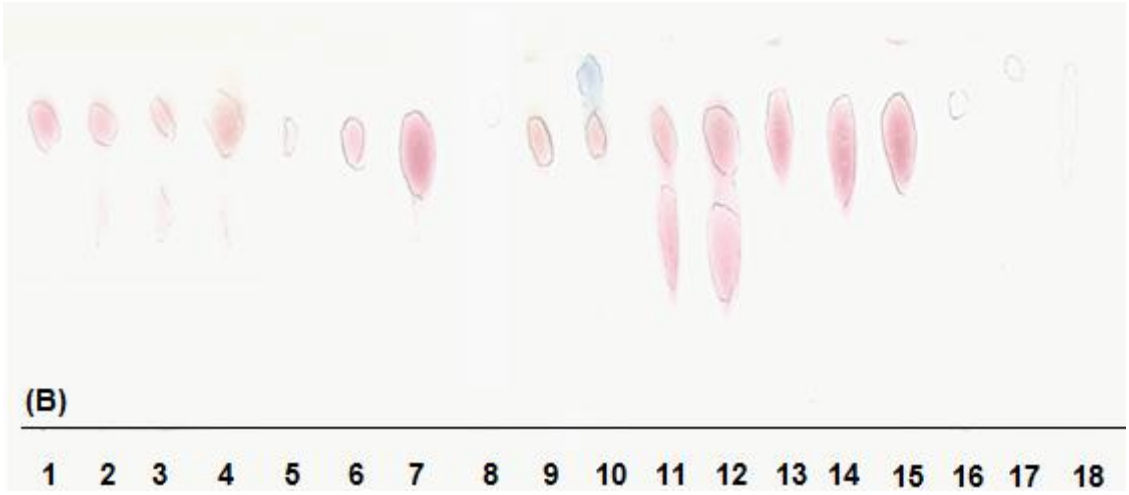

Figure 24: Evaluation of the TLC plate (B)

Table 33: Evaluation of the TLC plate (B)

No.	Sample Name	Rf-value	Color
1	Sa1_D_1e-Ek1 1:20*	0.70	red
2	Sa1_D_1e-Ek2 1:20*	0.70	red
3	Sa1_D_1e-Ek3 1:20*	0.70	red
4	Sa1_D_1e-Ek4 1:20*	0.69	red
5	Sa1_D_1e-Ek5 1:20*	0.65	red
6	Sa1_D_1e-Ek6 1:20*	0.63	red
7	Sa1_D_1e-Ek7 1:20*	0.61	red
8	Sa1_D_1e-Ek8	0.63	light grey
9	STD I-Rhamnose	0.81	green
9	STD I-Glucose	0.68	green
9	STD I-Galacturonic acid	0.63	red
10	STD II-Ribose	0.78	light grey
10	STD II-Arabinose	0.71	light grey
10	STD II-Fructose	0.63	red
11	Ec1_D_1e-Ek 1*	0.64	red
12	Ec1_D_1e-Ek 2*	0.63	red
14	Ec1_D_1e-Ek 4	0.61	red
15	Ec1_D_1e-Ek 5	0.61	red
16	Ec1_D_1e-Ek 6	0.68	light grey
17	Ec1_D_1e-Ek 8	0.71	light grey
18	Ec1_D_1e-Ek 9	0.64	red

* no clear spot due to high sugar concentrations

The interesting observation was that some of the enzyme combinations seemed to get a second spot, but this is hard to distinguish if it could be a second spot or only the spread of the spot above due to high sugar concentrations.

The outcome of the TLC of the Sa1_D_1e-Ek and Ec1_D_1e-Ek EPS, hydrolyzed by enzyme combinations, showed that the Sa1_D_1e-Ek1-8 and Ec1_D_1e-Ek1, 2, 3, 4, 5, 9 seemed to contain fructose due to the fast characteristic color reaction while spraying. All samples, which seemed to contain fructose, were hydrolyzed using the alpha amylase of Novozyme (A-amyla-Nov). Sa1_D_1e-Ek8 had a different color, which suggested that probably galacturonic acid was detected.

The sample Ec1_D_1e-Ek6 could not be identified for sure, but it is likely comprising the sugars starch, arabinose or glucose. It is worth mentioning that it was a combination of the cellulases from *Aspergillus niger* (Cellu-Sig and Cellu-Flk), additional to the color and Rf-value, it could be assumed that a mixture of arabinose and glucose was probably present. The sample Ec1_D_1e-Ek8 cannot be identified due to the Rf-value or the color.

The second batch of both organism (Sa2_D_1e and Ec2_D_1e) were tested by TLC and the plates are shown in Figure 25 and Table 34.

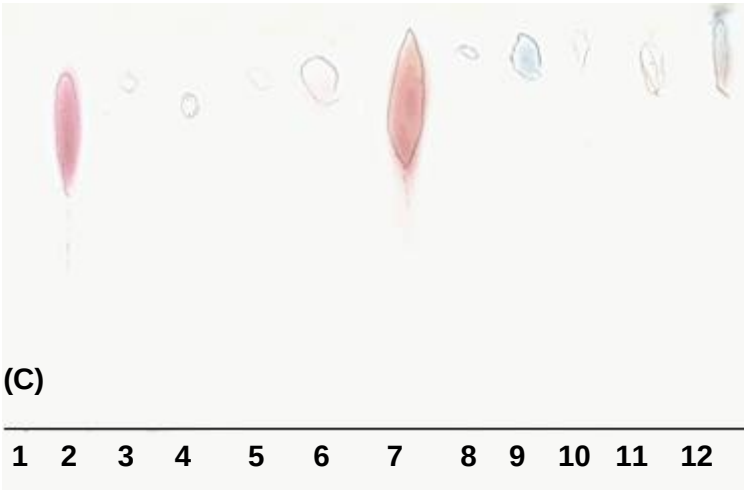

Figure 25: Evaluation of the TLC plate (C)

Table 34: Evaluation of the TLC plate (C)

No.	Sample Name	Rf-value	Color
1	Sa2_D_1e	-	-
2	Sa2_D_1e+A-amyla-Nov*	0.53	red
3	Sa2_D_1e+Cellu-Sig	0.68	grey
4	Sa2_D_1e+Cellu-Flk	0.62	grey
5	Sa2_D_1e+B-gluc-U	0.71	light grey
6	Sa2_D_1e+Pulp-Nov	0.68	red
7	Ec2_D_1e+A-amyla-Nov*	0.61	red
8	Ec2_D_1e+Cellu-Sig	0.69	grey
9	Ec2_D_1e+Cellu-Flk	0.67	grey
10	Ec2_D_1e+B-gluc-U	0.70	grey
11	Ec2_D_1e+Pulp-Nov	0.66	red
12	STD II-Ribose	0.78	light grey
12	STD II-Arabinose	0.71	light grey
12	STD II-Galacturonic acid	0.63	red

* no clear spot due to high sugar concentrations

The hydrolysates Sa2_D_1e+A-amyla-Nov, Sa2_D_1e+Pulp-Nov and Ec2_D_1e+A-amyla-Nov, Ec2_D_1e+Pulp-Nov seemed to contain fructose, because of the strong color reaction. The hydrolysates produced with Cellu-Sig and Cellu-Flk of both organisms probably contained glucose and the ones of B-gluc-U maybe starch or glucose. The results of the Sa2_D_1e batch were nearly similar compared to the Sa1_D_1e batch, because of the number of spots, the color of the spots and the calculated Rf-value. Except one difference that the EPS of the Sa2_D_1e, which was hydrolyzed with beta glucanase (B-gluc-U), showed a spot, it seemed to contain starch or glucose.

It can be summarized that the EPS itself shows no spot and that only the EPS hydrolysates, which were treated with A-amyla-Nov, Cellu-Sig, Cellu-Flk, B-gluc-U and Pulp-Nov showed in all samples a spot, the others seemed to contain no sugars, which were detectable by this method.

The EPS of both organisms, which was hydrolyzed using A-amyla-Nov, seemed to contain high amounts of fructose and could be distinguished due to the specific color reaction immediately after spraying and heating; based on Bales et al. [26] it can be assumed that it is hardly probable present in the EPS. Interestingly, they tested the EPS of several microorganisms by glycosyl composition analysis concerning the exopolysaccharides and in none of them fructose was detected. It is possible that either fructose is part of the sugar stabilizer of the enzyme preparation or a mixture of galacturonic acid and fructose was present, which could not be separated by TLC. However, the study of Savadogo et al. [67], showed that the EPS of lactic acid bacteria comprised fructose. Perhaps, the EPS of both studied microorganisms contained fructose as well. To confirm the carbohydrate in the EPS further analysis are necessary.

The hydrolysates, obtained by using the cellulases Cellu-Sig and Cellu-Flk, showed strong fluctuations in the Rf-values, but it is likely that they contained glucose. Based on Bales et al. [26] *S. epidermidis and E. coli* EPS comprises glucose. Therefore, it is very likely that glucose is existent in the two tested organisms considering that *S. epidermidis* is a relative of *S. aureus* and they belong to the same genus.

The EPS samples hydrolyzed using the beta glucanase (B-gluca-U) showed in all batches except Sa1_D_1e a spot with an Rf-value of 0.70 – 0.71 and could not be identified for sure, but possibly it can contain glucose (Rf-value of 0.69) or arabinose (Rf-value 0.70), unfortunately both showed almost the same color. Based on the glycosyl composition analysis, as already mentioned above, it can be assumed that only glucose was existent in the hydrolysates, because *S. epidermidis* and *E. coli* were tested of Bales et al. [26] to not contain the monosaccharide arabinose. The enzyme Pulp-Nov showed in all batches on the TLC sheets significant red colored spots and they had Rf-values in the range of 0.62 to 0.70. Unfortunately, based on the Rf-values it is possible that the sample comprises galacturonic acid (0.62) as well as fructose (0.68), but based on the specific color reaction as described above, it could be identified as fructose. As mentioned above fructose could be part of the sugar stabilizer of the enzyme preparation or in this case even a mixture of both sugars could be detected and maybe they are inadequately separated by TLC.

3.5 Production of H_2O_2 using CDH and enzymatically hydrolyzed EPS

The production of hydrogen peroxide was detected using several methods and their results are described in the following chapter.

3.5.1 Determination of the CDH activity using the DCIP assay

The enzyme activity of the batches of cellobiose dehydrogenase (CDH) was determined by using the DCIP assay. Formulas for calculation of enzyme activity are shown below in Figure 26. The enzyme activities of different CDH batches are shown in Table 35. The absorbance coefficient ε_{520} is 6.9 $mM^{-1}*cm^{-1}$ and the EF is 7.25.

$$Activity\ \left[\frac{U}{ml}\right] = (-1) * Slope * EF$$

$$EF = \frac{cuvette\ volume}{sample\ volume * \varepsilon}$$

Figure 26: Equations for the calculation of enzyme activity based on the DCIP assay

Table 35: Determination of different CDH batches I, III, IV, VI

No.	CDH Sample	Slope/min	Activity [U/ml]
1	CDH VI	-0.2457	1.78
2	CDH IV	-0.3974	2.88
3	CDH III	-0.6543	4.74
4	CDH I- oxyplus	-0.2248	1.63

Moreover, the DCIP assay was used to test the substrate specificity of the cellobiose dehydrogenase and the sugars lactose, N-acetyl-glucosamine, N-acetyl-galactosamine, glucosamine, galactosamine and cellotetraose. The reason for testing alternative substrates next to the common one was to get more information about the substrate usage of the CDH. The slopes of the spectrophotometric measurements are shown in Table 36.

Table 36: Substrate specificity testing of different carbohydrates using DCIP

No.	Sugar	Concentration [mM]	Slope	Activity	%relative activity
1	Lactose	300	-0.260	1.88	100
2	N-Acetyl-glucosamine	300	-0.020	0.14	7.5
3	N-Acetyl-glucosamine	300	-0.004	0.03	1.6
4	N-Acetyl-galactosamine	300	-0.002	0.01	0.7
5	Glucosamine HCl	300	-0.014	0.10	5.5
6	Cellotetraose	300	-0.196	1.42	75.6
7	Lactose	55.8	-0.282	2.05	100
8	Galactosamine HCl	55.8	-0.008	0.06	2.8

For a better evaluation of the data the percent of relative activity in relation to the lactose was calculated and is shown in Figure 27.

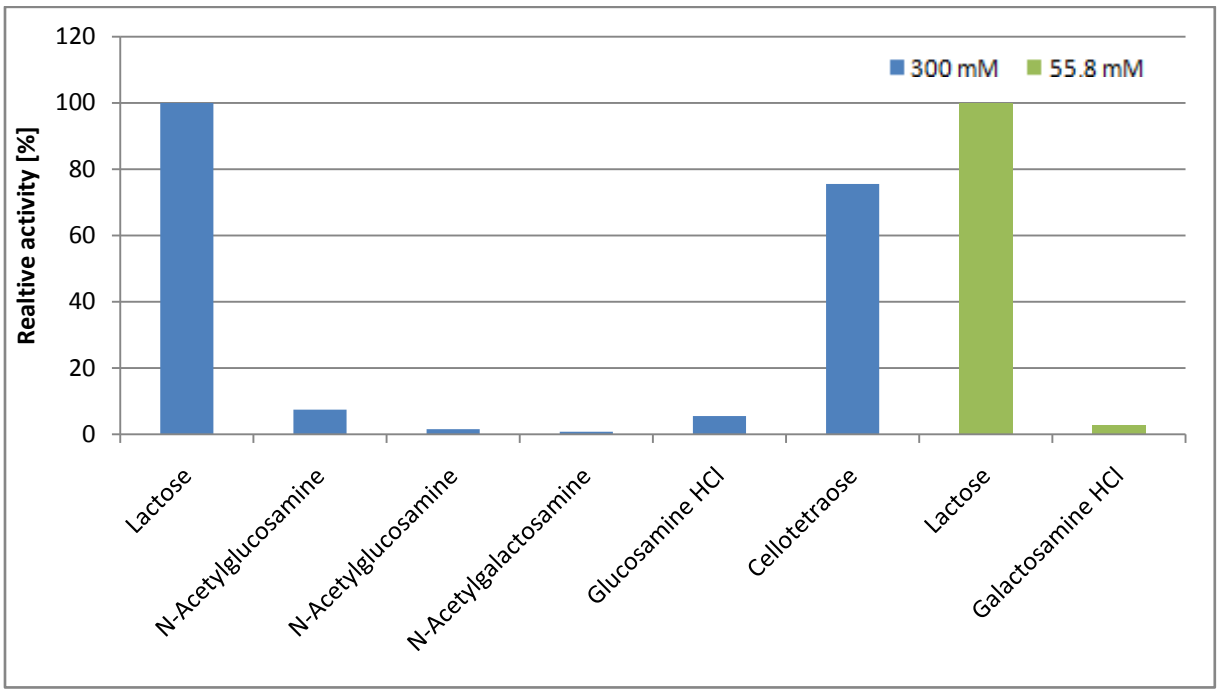

Figure 27: Relative activity of the tested sugars as electron donors in relation to lactose

The activity was calculated like the DCIP assay based on the slope, it was performed with lactose as standard. The lactose was measured in the respective concentration like the tested substrates to determine whether the sugar may be used by the CDH as substrate and the efficiency. Based on the results of the tested substrates, it can be assumed that cellotetraose is a good electron donor for the enzyme like lactose, but it is in comparison to lactose an expensive one. Moreover, it shows not as high efficiency as lactose. Henriksson et al. [38] already showed that cellotetraose can be used as substrate by the CDH. Moreover, they tested thiocellobiose as a better substrate than cellobiose or lactose.

3.5.2 Activity staining of catalase and CDH after electrophoresis

The gel electrophoresis was performed to analyze the CDH batches regarding their purity. It was suspected that the enzyme cellobiose dehydrogenase (batch III) was presumably contaminated with catalase, because if hydrogen peroxide was incubated with CDH, there was a decrease monitored by Quantofix ® hydrogen peroxide sticks as illustrated in Figure 28. The illustrated sample contained 35 mg/L hydrogen peroxide, 55 mM sodium phosphate buffer (pH 6.5) and CDH (batch III) and were monitored over the time.

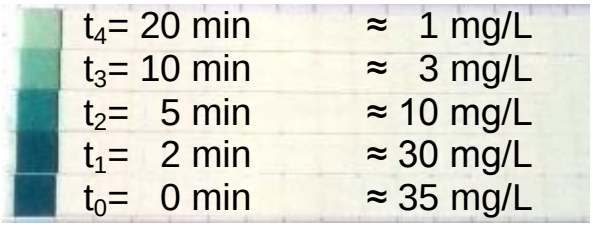

Figure 28: Hydrogen peroxide sticks to observe the H_2O_2 concentration over the time

The next step was the investigation of the remaining CDH batches and the result is shown in Figure 29. The samples contained 10 mg/L hydrogen peroxide and CDH, and two blanks to eliminate the buffer or water as potential source of contamination.

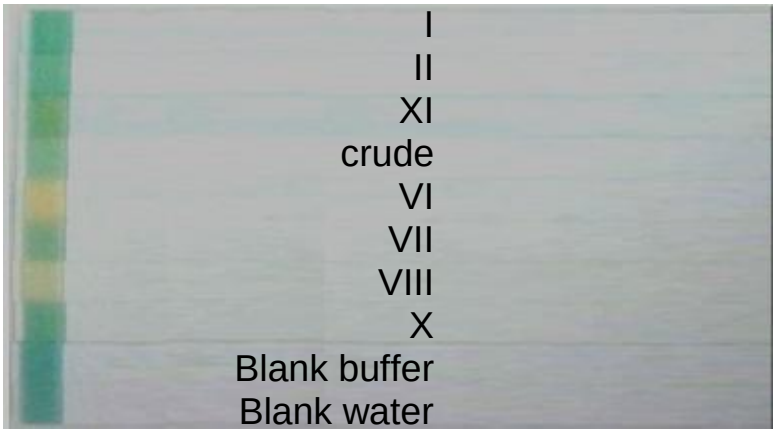

Figure 29: Hydrogen peroxide sticks used to observe the H_2O_2 decrease of the CDH batches

This testing with the hydrogen peroxide sticks resulted in a remarkable observation that not all batches seemed to contain this kind of impurity; especially, the CDH batches III, VI and VIII were contaminated. The other batches seemed to be free of catalase.

To investigate the suspicion that a contamination with catalase could be existent, a native gel electrophoresis was performed twice. The tested CDH batches III, VI, VII were unfiltrated and filtrated using low protein binding syringe filters (0.2 and 0.4 µm). The gel of the native gel electrophoresis was stained and is depicted in Figure 30 and the sample order is shown in Table 37.

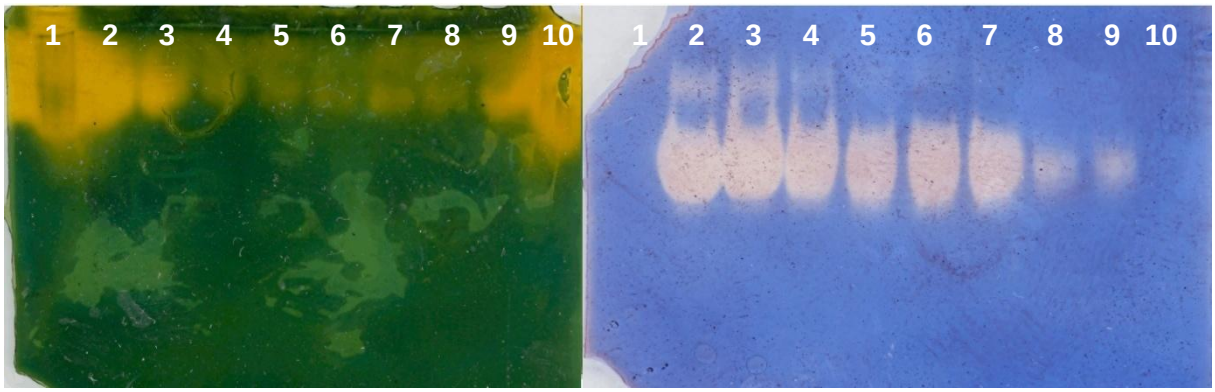

Figure 30: Native gel (8 % separating and 4 % stacking gel) for analyzing filtrated, not filtrated CDH samples and catalase as standard (left: Catalase staining; right: DCIP staining)

Table 37: Order of the samples analyzed by native gel electrophoresis

Slot-No.	1	2	3	4	5	6	7	8	9	10
Sample	Catalase 1:100 NF	VI NF	VIII NF	VII NF	Crude NF	VI NF	VIII SF	VII SF	Crude SF	Catalase 1:100 SF

SF-sterile filtrated NF-not filtrated

First of all, both staining methods worked well. The DCIP staining was like expected; it worked perfectly with the CDH samples, because it produced nice clear white bands in the blue-stained gel and didn't work with the catalase standard. In the stained gel the CDH samples showed two bands with CDH activity, this suggests the presence of two functional isoenzymes. The catalase staining worked perfectly with the standard, but also well with the CDH samples. The upper band of the CDH samples showed a positive staining, the lower one not. This suggests that in the CDH samples catalase is present. But it could be also possible, that the staining cannot properly distinguish between CDH and catalase, because both bands are approximately at the same height. An option for solving the problem would be to conduct more steps for purification or to test a highly pure CDH in comparison to the used batches. The SDS gel (6 % separating und 4% stacking gel) with the standard (Multicolor High Range Protein Ladder) is shown in Figure 31; the arrangement of the applied samples is listed in Table 38. The tested CDH batches III, VI, VII were not filtrated and filtrated as described above; additionally, two peaks, which were generated using size exclusion chromatography (SEC), were applied. By SEC the CDH batch VI was tested, the first peak was at 280 nm and the second one was a high conductivity peak. The chromatogram of the SEC is shown in the Appendix.

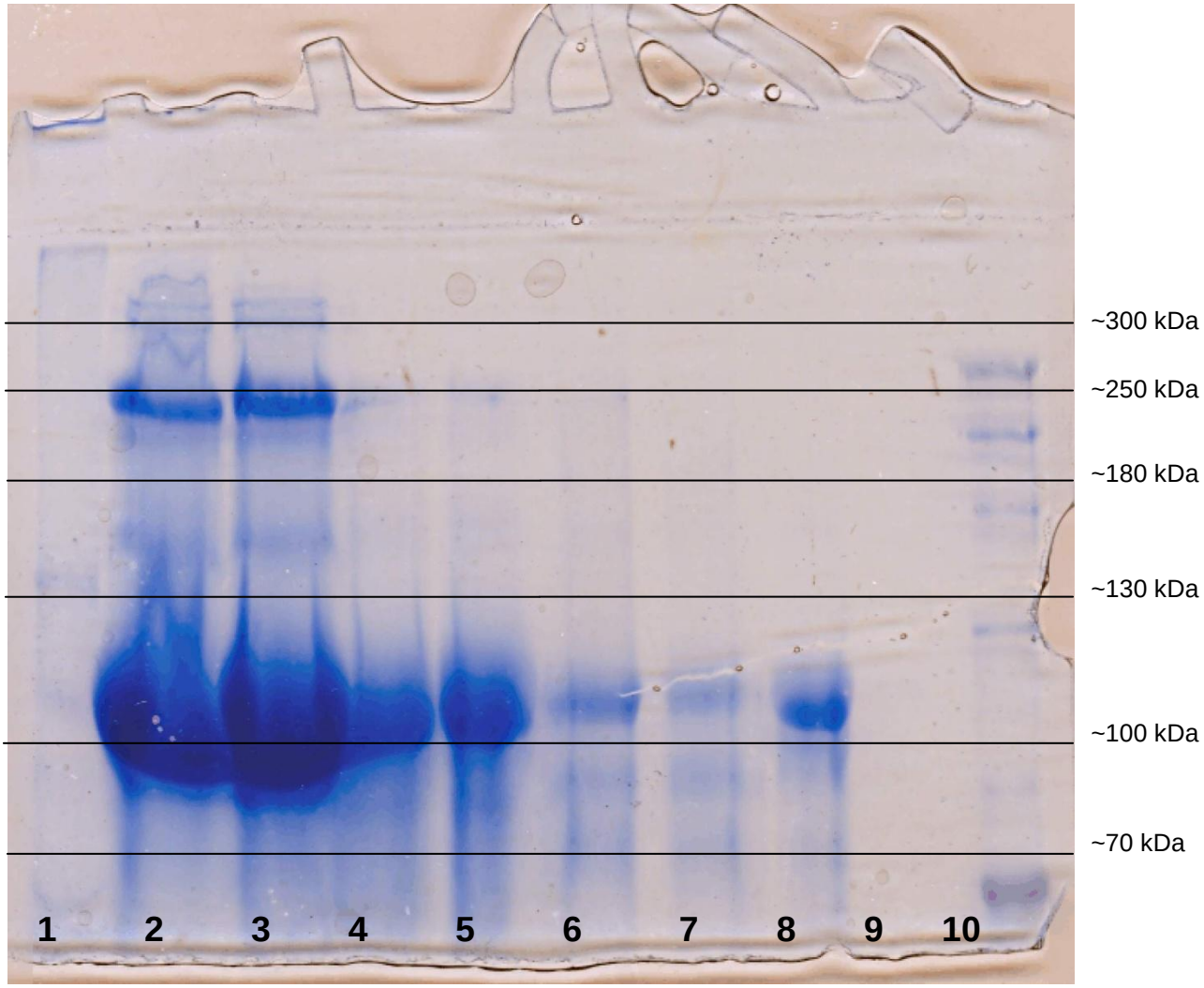

Figure 31: SDS gel electrophoresis (6 % separating and 4 % stacking gel) for analyzing the CDH and catalase

Table 38: Order of samples separated by gel electrophoresis and visualized by Kang staining

No.	1	2	3	4	5	6	7	8	9	10
Sample	Catalase 1:100 NF	VI NF	VI SF	VII NF	VII SF	Crude NF	Crude SF	Peak 1 VI-SF	Peak 2 VI-SF	STD

SF-sterile filtrated NF-not filtrated

3.5.3 Leuco crystal violet assay

The leuco crystal violet (LCV) assay was performed as described in the protocol. The calibration curve was obtained with hydrogen peroxide and leuco crystal violet, as illustrated in Figure 32 and was compared with the calibration curve generated with 2,2'-azino-bis-3-ethylbenzthiazoline-6-sulphonic acid (ABTS) as colorimetric substrate, which is shown in Figure 33.

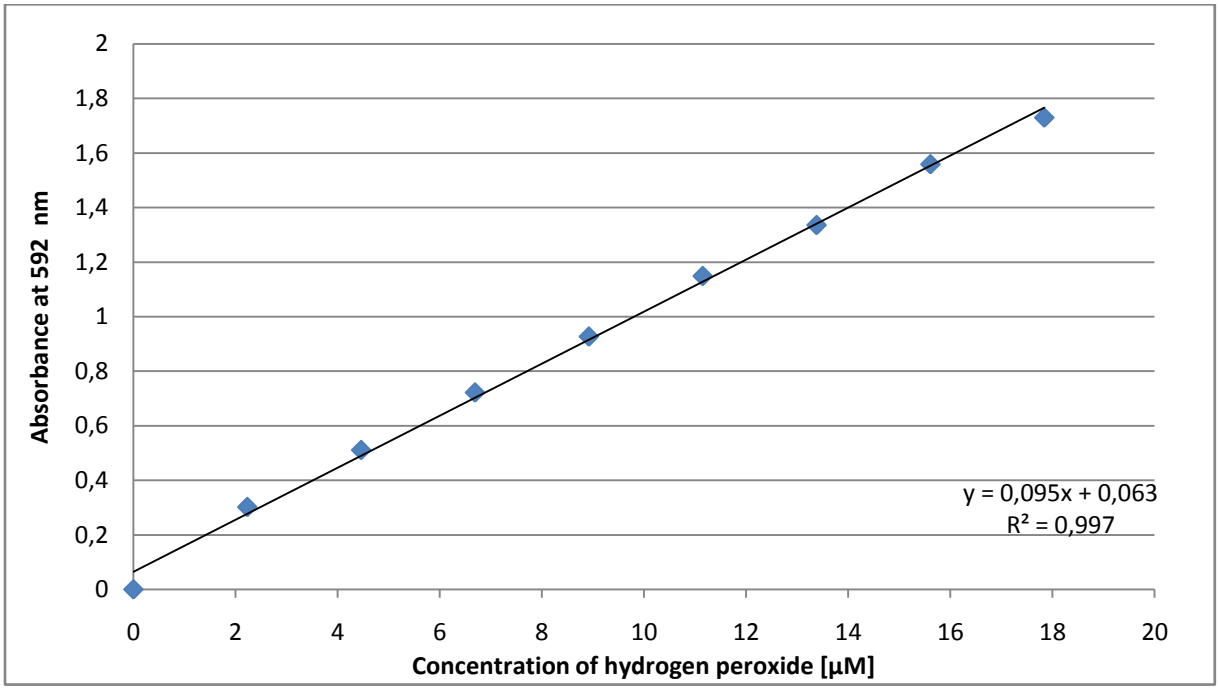

Figure 32: LCV assay for obtaining the calibration curve using leuco crystal violet

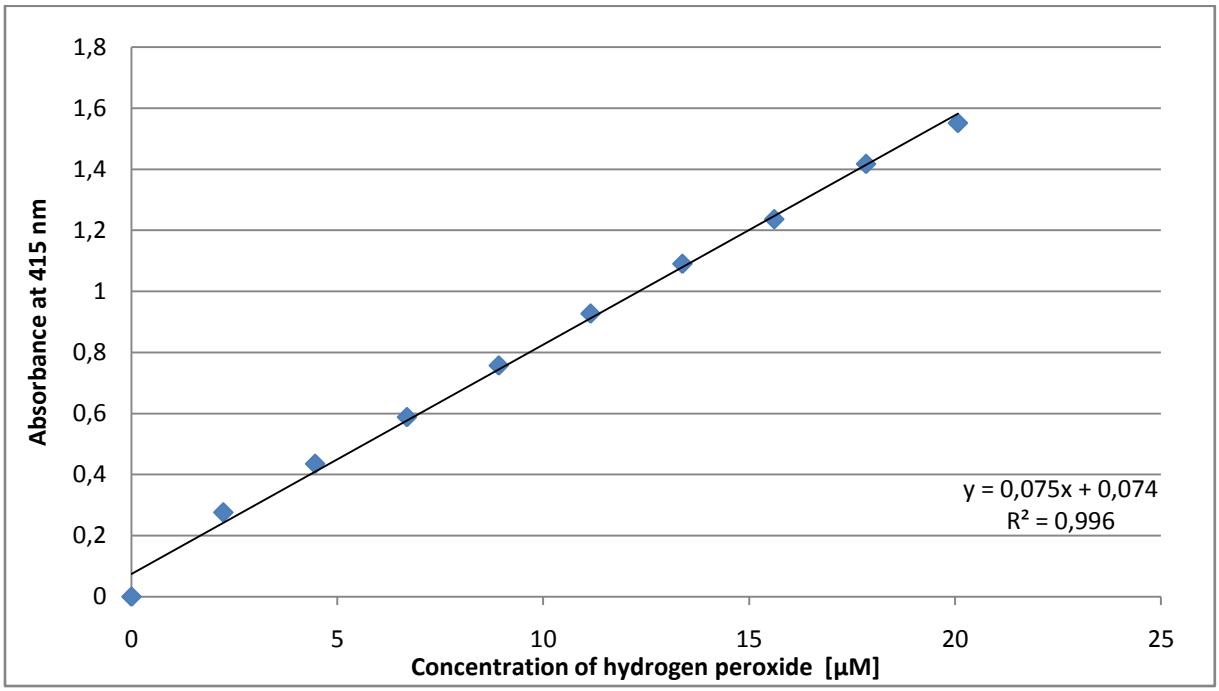

Figure 33: LCV assay for generating the calibration line using ABTS as colorimetric substrate

Even though both calibration curves were of satisfying quality the following assays were performed with LCV due to the reason that it was used as substrate in the original assay and less dangerous. The heating step in this assay is necessary to inactivate the CDH in order to avoid the reduction of the oxidized LCV back to its uncolored form. To make sure that not too much hydrogen peroxide would be lost throughout the heating process a CDH inactivation and a H_2O_2 stability study was performed as illustrated in Figure 34 and in Figure 35.

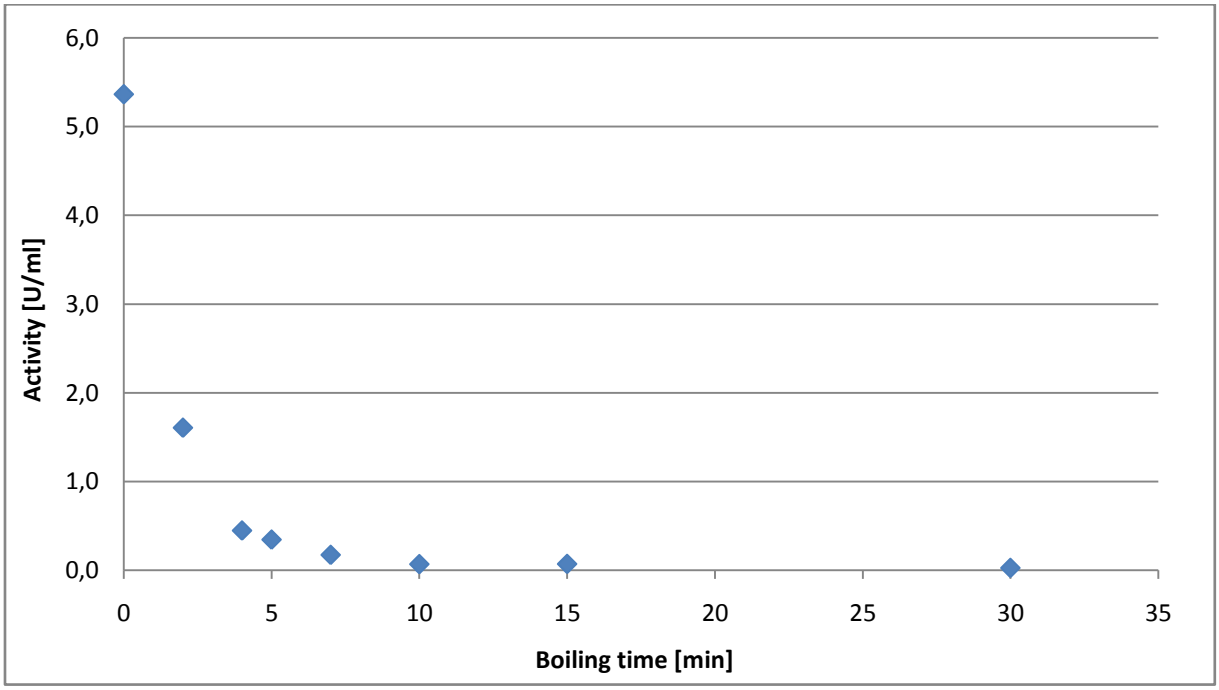

Figure 34: CDH activity loss over time

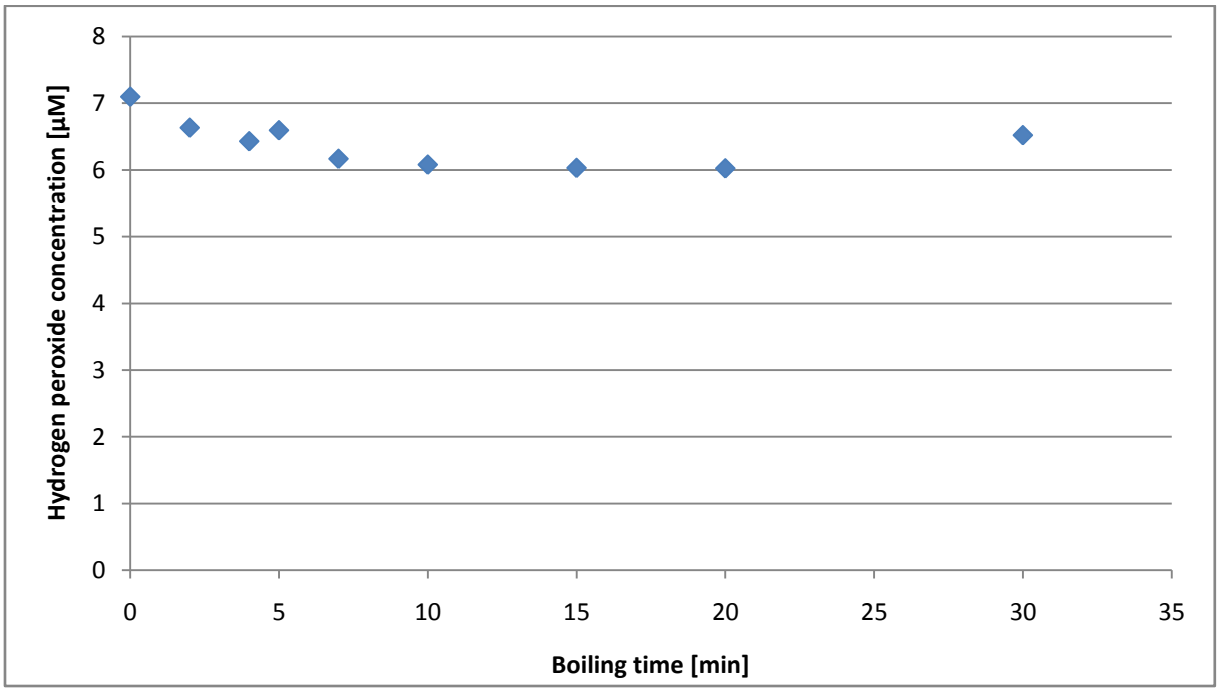

Figure 35: Stability test of the hydrogen peroxide over the time

The evaluation of the hydrogen peroxide stability over the heating time showed that after 20 minutes the enzyme was inactivated, due to the reason that the CDH was originally isolated from the thermophilic organism *Myriococcum thermophilum* and expressed in *Pichia pastoris* the original recommended heating time had to be prolonged. Nevertheless, the figure above shows that although decomposition of hydrogen peroxide occurred, this value was within a tolerable range. Using the line equation y = 0.095x + 0.063 of the calibration curve, as shown in Figure 32, the concentration of H_2O_2 was determined at several time points of the boiling experiment. Shown in Table 39, it can be seen that after 20 minutes about 15 percent of hydrogen peroxide already decomposed, but compared to the 2 minutes boiling step, which is recommended in the original protocol of the assay, the loss was 7 %. The small difference of 8 percent is tolerable and due to the thermostability of CDH it cannot be avoided, since it must be inactivated, because its activity interferes with the activity of the peroxidase.

Table 39: Stability testing of hydrogen peroxide over the time

Boiling time [min]	Absorption Measurement				H_2O_2 concentration [µM]	Standard deviation	H_2O_2 [%]
	1	2	3	Average			
0	0.760	0.958	0.715	0.738	7.10	0.33	100
2	0.692	0.693	0.695	0.693	6.64	0.02	93
4	0.675	0.675	0.672	0.674	6.43	0.02	91
5	0.689	0.702	0.678	0.690	6.60	0.13	93
7	0.666	0.621	0.660	0.649	6.17	0.26	87
10	0.630	0.646	0.646	0.641	6.08	0.10	86
15	0.644	0.603	0.661	0.636	6.03	0.31	85
20	0.635	0.626	0.645	0.635	6.02	0.10	85
30	0.695	0.631	0.722	0.663	6.52	0.49	92

Outlier: was not used for the calculations!

Using the modified assay some EPS hydrolysates of *S. aureus* (Sa1_D_1e and Sa1_U_1e) and *E. coli* (Ec1_D_1e and Ec1_U_1e) were measured. The concentration of the EPS, which was used in the LCV assay, was calculated by using the dry weight and the following performed dilution steps were considered and it is shown in Table 40.

Table 40: Determination of the concentration of *E. coli* and *S. aureus* EPS using the LCV assay

No.	Sample	Concentration of EPS in the LCV assay [mg/ml]	Amount of EPS in the LCV assay [mg]
1	Sa1_D_1e	0.0436	0.0645
2	Sa1_U_1e	0.3051	0.4515
3	Ec1_D_1e	0.0078	0.0115
4	Ec1_U_1e	0.5042	0.7462
5	Ec1_D_1e-Ek	0.2079	0.3077
6	Sa1_D_1e-Ek	0.0436	0.3077

Ek… the EPS was used for the enzyme combinations

The EPS and hydrolysates of Sa1_D_1e and Ec1_D_1e were measured by the LCV assay and the results can be seen in detail in the Appendix, and some selected samples of both organisms are shown in Table 41 and Table 42. The CDH batch III was used for all samples.

Table 41: LCV assay of Sa1_D_1e EPS, its hydrolysates and lactose as standard

No.	Sample	Average Adsorption	c(H_2O_2) [µM]	Standard deviation	c(H_2O_2) [µM]*
1	Lactose	0.462	4.20	0.10	4.94
2	Sa1_D_1e	0.000	0.00	0.00	0.00
3	Sa1_D_1e+A-amyla-Nov	0.531	4.93	1.35	5.80
4	Sa1_D_1e+A-amyla-Sig	0.248	1.94	0.53	2.29
5	Sa1_D_1e+Cellu-Sig	0.421	3.77	0.27	4.43
6	Sa1_D_1e+Cellu-Flk	0.184	1.27	0.08	1.49
7	Sa1_D_1e+Pulp-Nov	0.095	0.34	0.23	0.40

* 15% were added to the calculated hydrogen peroxide concentration, because of the decomposition generated by heating the samples

Table 42: LCV assay of Ec1_D_1e EPS, its hydrolysates and lactose as standard

No.	Sample	Average Adsorption	c(H_2O_2) [µM]	Standard deviation	c(H_2O_2) [µM]*
1	Lactose	0.444	4.01	0.26	4.71
2	Ec1_D_1e	0.003	0.00	0.02	0.00
3	Ec1_D_1e+A-amyla-Nov	0.551	5.14	0.19	6.05
4	Ec1_D_1e+A-amyla-Sig	0.145	0.87	0.22	1.02
5	Ec1_D_1e+Cellu-Sig	0.146	0.87	0.03	1.03
6	Ec1_D_1e+Cellu-Flk	0.373	3.26	0.37	3.83
7	Ec1_D_1e+Mann-Nov	0.319	2.70	0.55	3.17
8	Ec1_D_1e+Pulp-Nov	0.236	1.82	0.35	2.14

* 15% were added to the calculated hydrogen peroxide concentration, because of the decomposition generated by heating the samples

To compare both organisms the tables above are shown graphically in Figure 36.

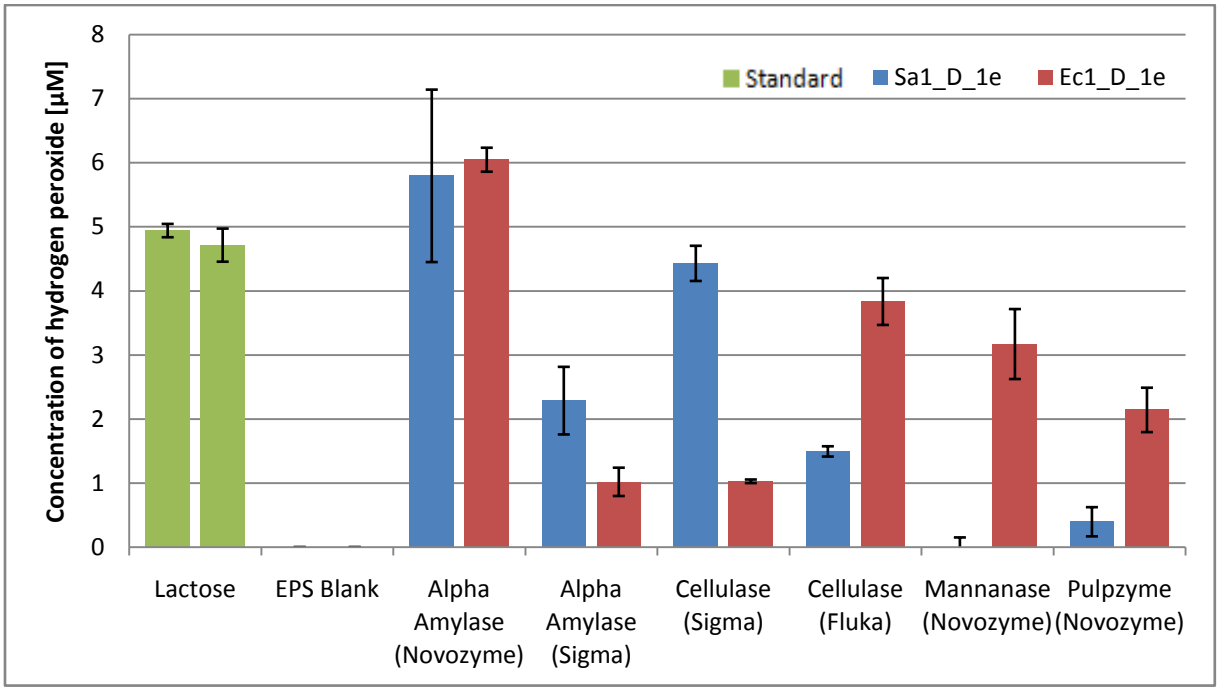

Figure 36: Comparison of selected hydrolysates of Sa1_D_1e and Ec1_D_1e

Between the concentration measurements of hydrogen peroxide, there was one connection. The similarity between the both organism was that the enzyme A-amyla-Nov worked for both very good even better than the standard substrate lactose, which was measured as standard to control the functionality of the assay. The four best hydrolyzing enzymes for *S. aureus* were A-amyla-Nov, Cellu-Sig, A-amyla-Sig and Cellu-Flk; for *E. coli* A-amyla-Nov, Cellu-Flk, Mann-Nov and followed by the Pulp-Nov.

The figure above shows the Sa1_D_1e and Ec1_D_1e EPS and hydrolysates, it points out the differences. Cellu-Sig and Cellu-Flk are both cellulases, but based on the results it can be assumed that both enzymes could hydrolyze the EPS. However, the interesting fact is that the LCV assay showed that Cellu-Sig cleaved the Sa1_D_1e more efficient to generate substrates for the CDH and Cellu-Flk the Ec1_D_1e. A possible explanation for the variation in the efficiency of cleavage could be that the composition of the biofilms is different. Moreover, the difference is confirmed due to the LCV assay, because of the reason that the Mann-Nov was very effective in the H_2O_2 production of the Ec1_D_1e and not of the Sa1_D_1e.

Furthermore, the enzyme combinations of both enzymes were tested, as well and can be seen in Table 43 and Table 44.

Table 43: LCV assay of Sa1_D_1e-Ek EPS, their enzyme combinations and lactose as standard

No.	Sample	Average Adsorption	c(H_2O_2) [µM]	standard deviation	c(H_2O_2) [µM]*
1	Sa1_D_1e EPS	0.037	0.00	0.03	0.00
2	Lactose	0.510	4.70	0.80	5.53
3	Sa1_D_1e-Ek1	0.245	1.92	0.79	2.26
4	Sa1_D_1e-Ek2	0.125	0.65	0.16	0.77
5	Sa1_D_1e-Ek3	0.174	1.16	0.02	1.37
6	Sa1_D_1e-Ek4	0.176	1.19	0.27	1.40
7	Sa1_D_1e-Ek5	0.419	3.74	0.15	4.40
8	Sa1_D_1e-Ek6	0.496	4.55	1.71	5.36
9	Sa1_D_1e-Ek7	0.124	0.64	0.07	0.75
10	Sa1_D_1e-Ek8	0.100	0.39	0.02	0.45
11	Sa1_D_1e-Ek9	0.010	0	0.00	0.00
12	Sa1_D_1e-Ek10	0.101	0.40	0.09	0.47

* 15% were added to the calculated hydrogen peroxide concentration, because of the decomposition generated by heating the samples

The enzyme combinations, which were hydrolyzing the *S. aureus* EPS reached partially higher values than the samples with a single hydrolyzing enzyme. Especially, the sample Sa1_D_1e-Ek6, which had the A-amyla-Nov combined with Pulp-Nov, achieved a high concentration. Very interesting was the fact, that all enzyme combinations, where the alpha amylase of Novozyme was combined with another enzyme, had produced hydrogen peroxide, but not in such a high amount as the single hydrolyzing enzyme. The data are shown in Figure 37.

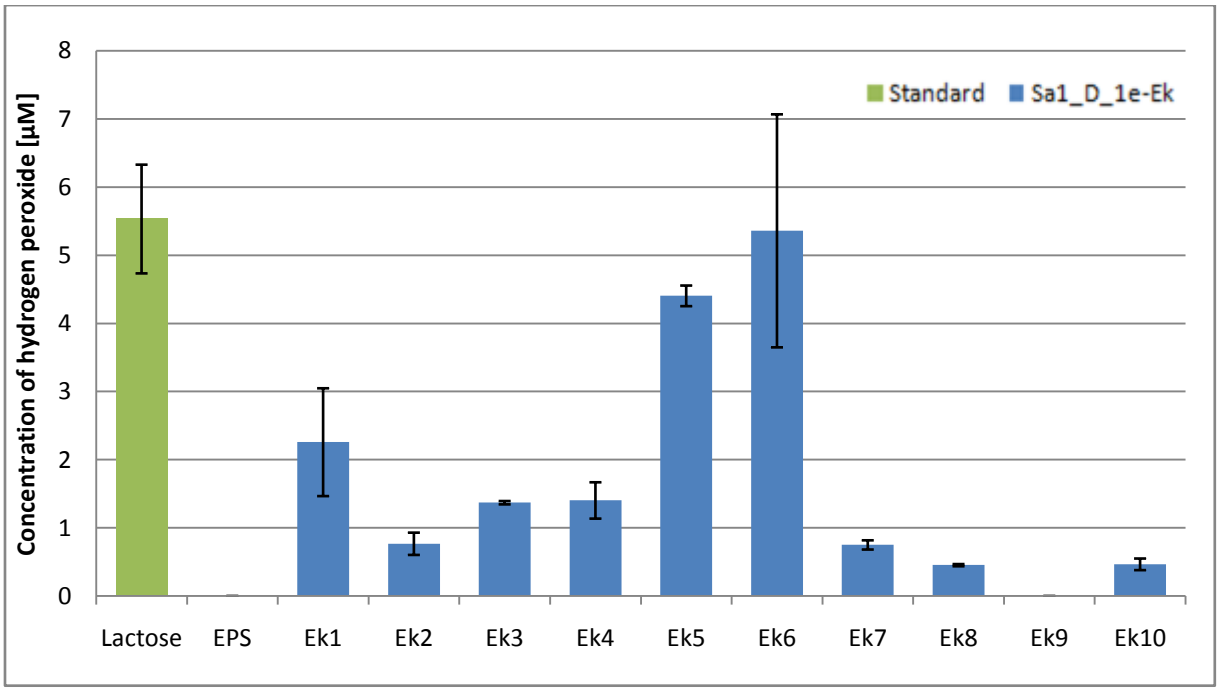

Figure 37: LCV assay of the Sa1_D_1e-Ek EPS, hydrolysates and lactose

Table 44: LCV assay of Ec1_D_1e-Ek, their hydrolysates and lactose as standard

No.	Sample	Average Adsorption	c(H_2O_2) [µM]	standard deviation	c(H_2O_2) [µM]*
1	Ec1_D_1e-EPS	0.161	0.14	0.28	0.16
2	Lactose	0.076	1.04	0.21	1.22
3	Ec1_D_1e-Ek1	0.429	3.85	0.31	4.53
4	Ec1_D_1e-Ek2	0.412	3.67	1.14	4.32
5	Ec1_D_1e-Ek3	0.300	2.50	0.11	2.94
6	Ec1_D_1e-Ek4	0.574	5.38	0.82	6.33
7	Ec1_D_1e-Ek5	0.564	5.28	2.01	6.21
8	Ec1_D_1e-Ek6	0.133	0.74	0.04	0.87
9	Ec1_D_1e-Ek7	0.110	0.50	0.28	0.59
10	Ec1_D_1e-Ek8	0.430	3.86	0.46	4.54
11	Ec1_D_1e-Ek9	1.511	15.24	1.39	17.93
12	Ec1_D_1e-Ek10	0.291	2.40	0.27	2.82

* 15% were added to the calculated hydrogen peroxide concentration, because of the decomposition generated by the heating of the samples

Two of the EPS samples, which were hydrolyzed with two or three hydrolytic enzymes, have achieved a high concentration of hydrogen peroxide, but the results were not trustworthy due to the fact that in this measurement set, the lactose standard was not as high as it should be. In the other measurements lactose resulted in concentration of H_2O_2 between 4.7 to 6 µM, but in this case it reached only 1.22 µM. Accordingly, the values were not trustable.

After trying to repeat the assay with lactose, there was not the typical color change of the samples as usual, so the assay was not reproducible any more. A possible explanation would be that LCV is very light sensitive and maybe an undesired reaction occurred or that the samples were contaminated with phenolic compounds. So the assay was tried to optimize again by changing several parameters. Therefore, it was tested which peroxidase, either the lignin peroxidase (LIP) or the horseradish peroxidase (HPO) and which metal chelator (EDTA or desferrioxaminemesylate) achieved better and more reproducible results. The LIP was compared with the HPO by obtaining a calibration curve using desferrioxaminemesylate (DM) as metal chelating agent, which can be seen in Figure 38 and Figure 39. Therefore hydrogen peroxide concentrations in the range of 0.68 to 274.9 µM were measured.

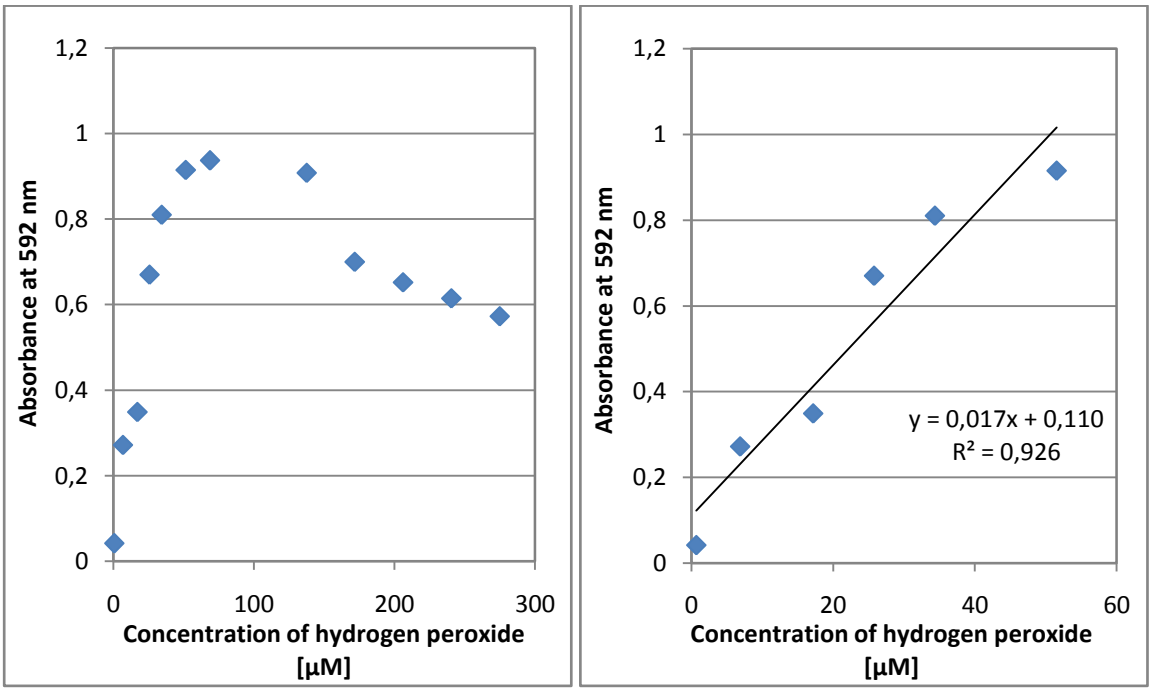

Figure 38: LCV assay prepared with lignin peroxidase and DM

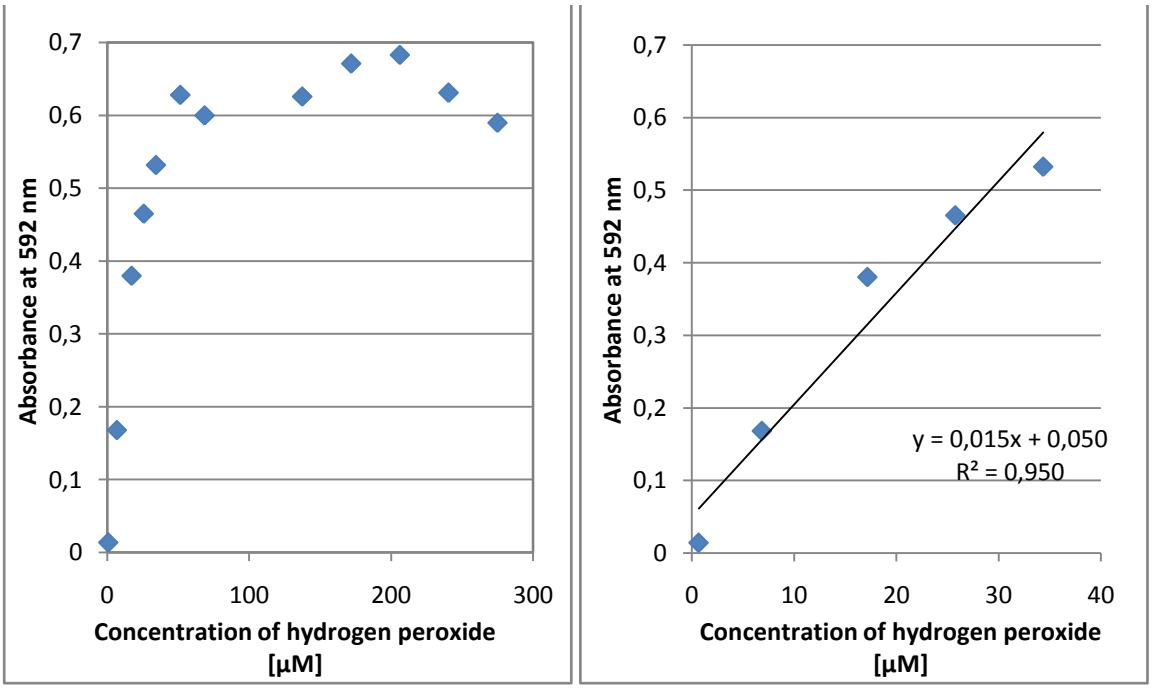

Figure 39: LCV assay prepared with horseradish peroxidase and DM

It has been reported that LCV is light sensitive. So the LCV was tested only with hydrogen peroxide and diluted with sodium phosphate buffer (55 mM; pH 6.5) as described in the optimized protocol and was measured over time, and, it has been found that the chemical compound was not stable. The first 400 seconds (approximately 7 minutes) the absorption increased over the time, afterwards it decreased again. It was not stable for more than 7 minutes in the light. The measurement is illustrated in the Appendix. Based on the knowledge of light sensitivity the optimization experiment was continued and for the following measurements the samples were incubated 20 minutes in the dark. Based on the calibration curve it can be said that both peroxidases are suitable for the assay for monitoring the hydrogen peroxide in the samples. So the optimization experiment was continued to test the two peroxidases each with EDTA and desferrioxaminemesylate to find out, which of the two is the more suitable metal chelator for the assay; the result of the experiment is shown in Table 45. It can be seen that there was a huge difference between the measurements, which contained desferrioxaminemesylate in comparison to them, which had EDTA as metal chelator. Because the amount of added hydrogen peroxide was the same, and somehow desferrioxaminemesylate seems to inhibit the peroxidases, compared to the other measurement with EDTA the dilution factor was very low. Moreover, the samples were measured for 20 minutes and the samples with desferrioxaminemesylate, had already after one minute a significant decrease. So desferrioxaminemesylate was tested and found to be an unsuitable metal chelating agent for the assay.

Table 45: LCV assay comparing two peroxidases with the metal chelators EDTA and DM

No.	Sample	Measured Adsorption	Adsorption after 60 sec	Dilution factor
1	LIP+ EDTA	0.818	0.805	10
2	HPO+ EDTA	0.810	0.807	10
3	LIP + DM	0.962	0.970	2
4	HPO + DM	0.401	0.401	2

The difference between LIP and HPO with EDTA was not significant, but the HPO was slightly a little more stable over the time, so the combination of HPO with EDTA was tested again as shown in Table 46 and the calibration line in Figure 40. But to get a higher range of the calibration curve the samples had to be diluted. Moreover, the combination of LIP was tested as well with EDTA and is shown in the Appendix. The assay had only a small range for the detection of hydrogen peroxide concentrations.

Table 46: Calibration curve of the optimized LCV assay

No.	measured OD	calculated OD	Dilution factor	H_2O_2 concentration [µM]
1	0.045	0.045	-	0.95
2	0.174	0.870	5	9.52
3	0.456	2.280	5	23.81
4	0.831	4.155	5	35.71
5	0.490	4.900	10	47.62
6	0.728	7.280	10	71.43
7	0.833	8.330	10	95.24
8	0.631	6.310	10	190.48

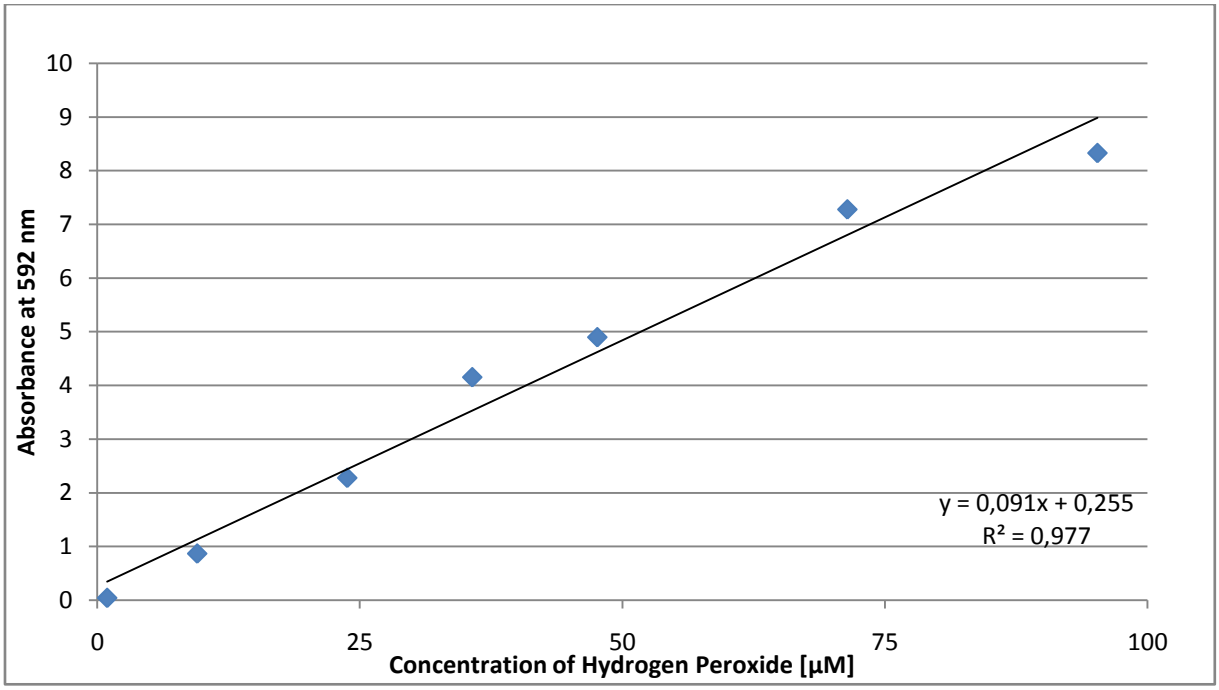

Figure 40: Calibration curve of the optimized LCV assay obtained using HPO and EDTA

However, the assay was still not suitable for the conducted measurements. Cohn et al. [62] tested the LCV with the focus on various factors such as pH, effects of EDTA in the presence of ferrous iron, and absorbance spectra and much more. Very remarkable in their experiments was the testing of the pH stability, because they identified a pH range of 3.6-4.2 as optimal, because they had created in this range nearly linear calibration curve. Moreover, they showed that at lower concentration the assay is not valid, and that at higher concentrations, there was a precipitation occurring.

Furthermore, the authors investigated the influence of EDTA in the presence of ferrous iron when measuring H_2O_2. This is a very important fact, because the measurement of the hydrogen peroxide of the untreated and hydrolyzed EPS was performed with various hydrolyzing enzymes and crude enzyme, it may be possible that the samples contained ferrous iron.

3.5.4 Amplex Red Assay

The Amplex Red assay was performed as an alternative to the leuco crystal violet assay. In comparison it has a big advantage, due to the fact that inactivation of CDH was not necessary, because Amplex Red dye does not act as an electron acceptor. Amplex Red itself was tested concerning the absorption maximum. As a consequence, the assay was performed with an excitation wavelength of 544 nm and an emission wavelength of 584 nm. The gain of 73 of the fluorescence readings was chosen for the fluorescence top reading measurements with the plate reader. The calibration curve was obtained by using 0.25 - 25 µM hydrogen peroxide and is illustrated in Figure 41.

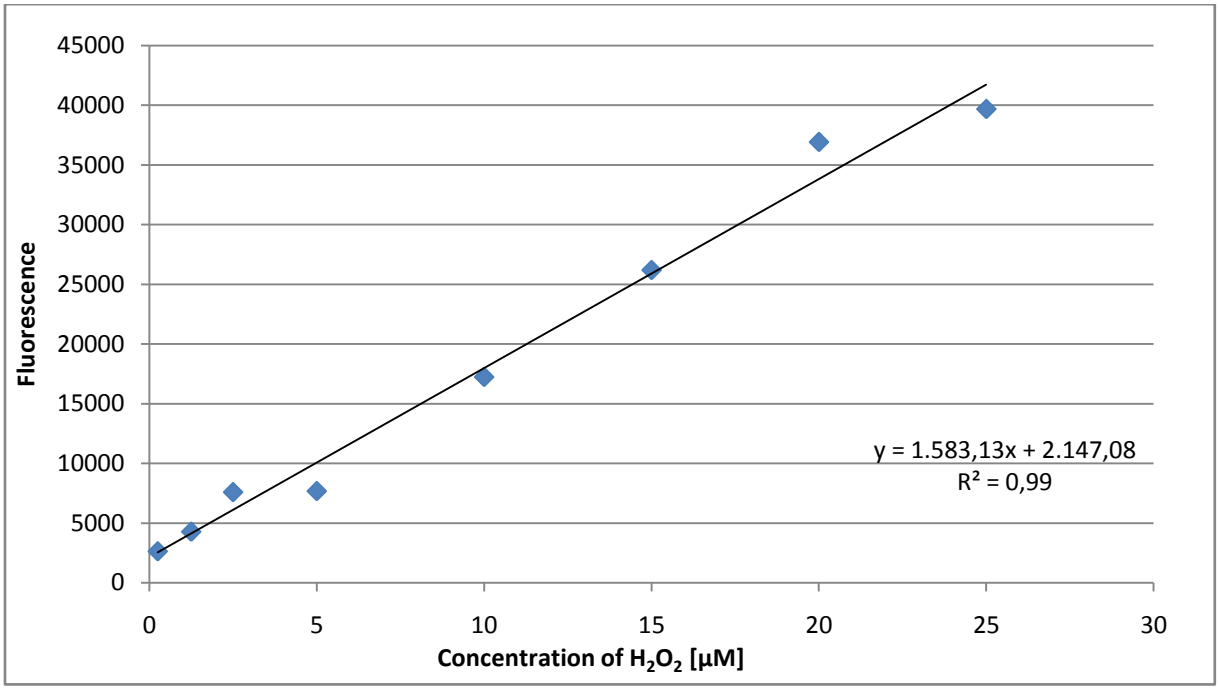

Figure 41: Calibration curve of the Amplex Red assay to determine H_2O_2 concentration

The reaction was stopped after 490 seconds, due to the fact that the peroxidase had already oxidized the previously produced hydrogen peroxide to molecular oxygen and in the same time, it had reduced the amplex red dye to resorufin. It can be concluded that the measured fluorescence increases rapidly at the beginning and then reaches a plateau. Afterwards, the fluorescence is still increasing slow, but steadily probably due to the auto-fluorescence of the used amplex red dye.

After reaching the plateau the measured values of the hydrolysates increased continuously over the time, but some samples showed no plateau formation. A possible explanation for this would be the fact that the hydrolytic enzymes were still active. They may have been able to hydrolyze more sugar over the time and consequently, the enzyme cellobiose dehydrogenase (CDH) was oxidizing more sugars and reducing molecular oxygen to hydrogen peroxide.

It is important for the measurement to prevent further production of substrates; based on this observation a boiling step was added to the protocol to avoid falsification of the results. As an example, the plateau formation and increasing fluorescence over the time was shown in Figure 42.

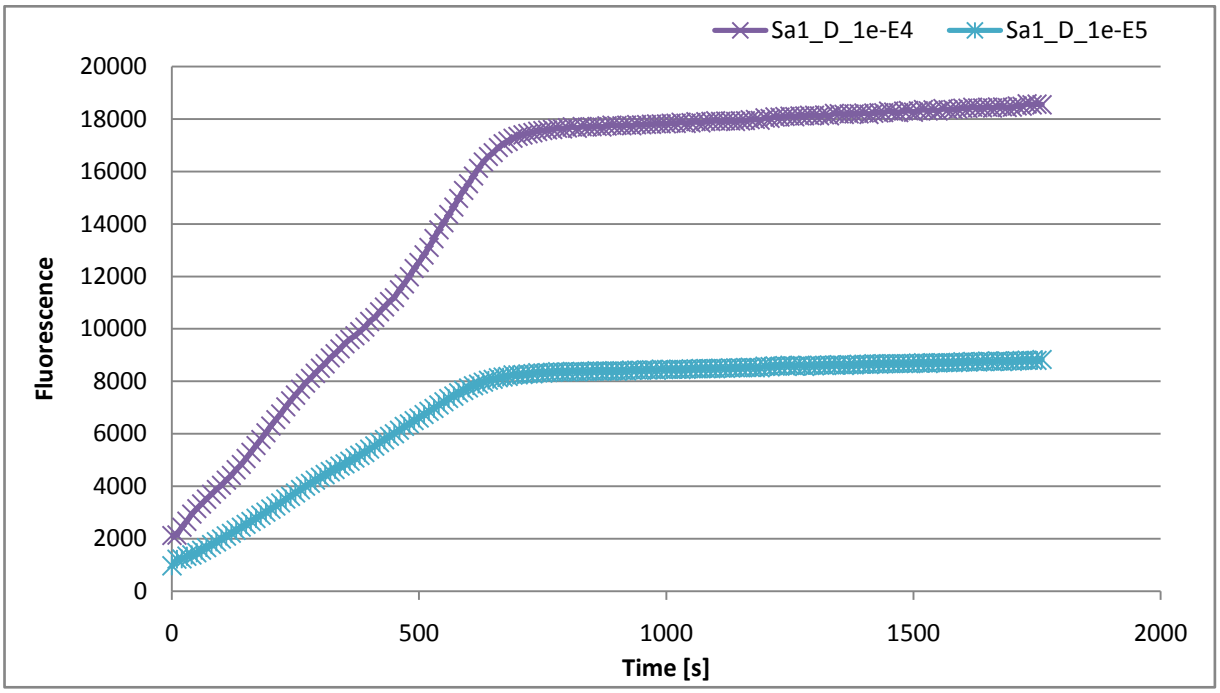

Figure 42: Example for the curve progression of the Amplex Red assay

The untreated EPS, hydrolysates and enzyme combinations were tested and the “oxyplus batch CDH I” was used for the assay; the measurements can be seen detailed in the Appendix. The “oxyplus” cellobiose dehydrogenase produces a higher amount of hydrogen peroxide in comparison to the *Mt*CDH. The concentration of hydrogen peroxide was determined of the untreated samples and hydrolysates, therefore the maximum value was used for the equation of the calibration curve to calculate the concentration of hydrogen peroxide in the assay. Due to the progression of the curves and the selected maximum value, it can be assumed that some enzymes were significantly more efficient in the cleavage of EPS, because they reached a higher concentration of hydrogen peroxide during incubation with CDH. First of all, the enzymes only were measured without adding EPS due to the previously observation that sugar stabilizers were present in some of the enzyme preparations. The result of the measurement is shown in Table 47. To compare the different batches of the respective organism, they are shown in Figure 43.

Table 47: Amplex Red assay of the enzyme blanks

No.	Sample	Fluorescence	Concentration of H_2O_2 [µM]
1	Blank A-amyla-Nov	6703	2.88
2	Blank A-amyla-Sig	1133	0.00
3	Blank A-amyla-U	2403	0.16
4	Blank Cellu-Sig	4490	1.48
5	Blank Cellu-Flk	5016	1.81
6	Blank Cellu-U	908	0.00
7	Blank Enz-mix-U	2570	0.27
8	Blank B-gluc-U	500	0.00
9	Blank Mann-Nov	847	0.00
10	Blank Pulp-Nov	798	0.00
11	Blank Pect-Sig	395	0.00
12	Blank Lyso-Sig	634	0.00

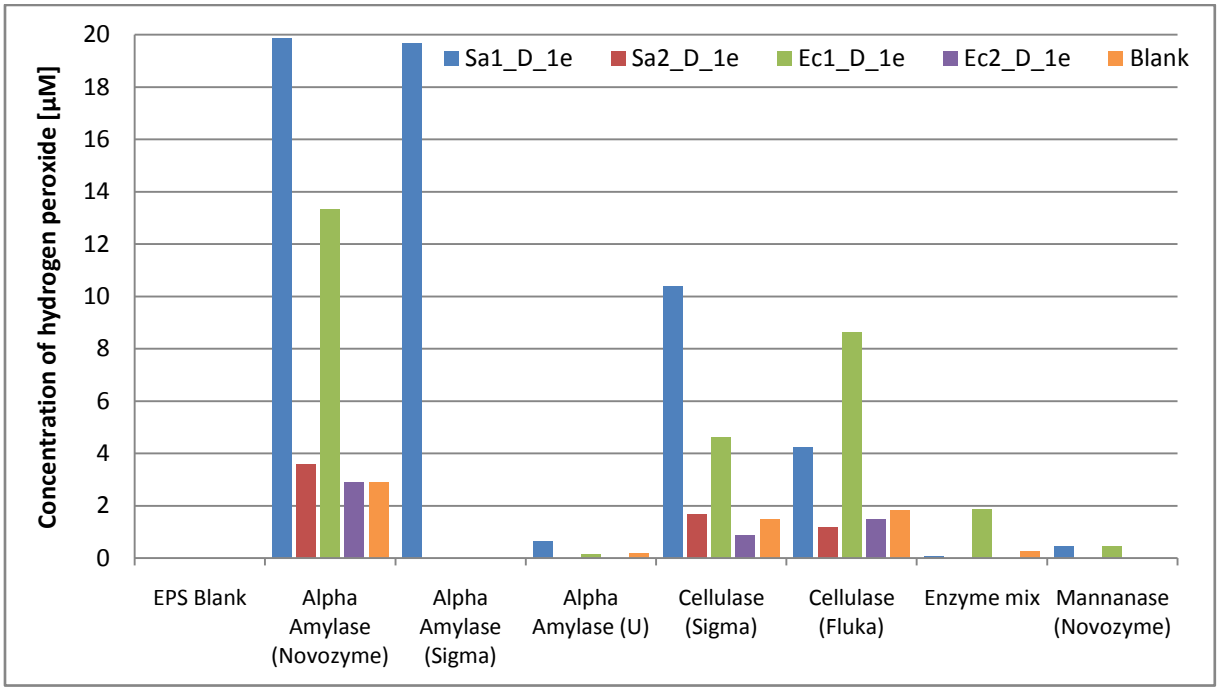

Figure 43: Amplex Red assay of the EPS batches, hydrolysates and enzyme blanks

First of all, it can be concluded due to the figure that the first batch of both organisms (Ec1_D_1e and Sa1_D_1e) are significantly better in hydrogen peroxide production than the second batch (Ec2_D_1e and Sa2_D_1e). The four best hydrolytic enzymes of the Sa1_D_1e for the production were the enzymes A-amyla-Nov, A-amyla-Sig, Cellu-Sig and Cellu-Flk. The four best hydrolytic enzymes for the hydrogen peroxide production of Ec1_D_1e were the enzymes A-amyla-Nov, Cellu-Flk, Cellu-Sig and Enz-mix-U. The results of the second batch (Ec2_D_1e and Sa2_D_1e) are consistent with those of the first, but for some reason, the measured concentrations are lower about a 5 to 6-fold.

In the measurements of Sa2_D_1e only the hydrogen peroxide concentration, generated by the A-amyla-Sig, was significantly lower. However, since only a simple determination was possible in this measurement, pipetting errors can also be a possible reason for this outlier.

But the significant difference of the whole batch cannot be explained, because the conditions of the cultivation, EPS production, harvesting and hydrolysis were performed according to the protocol.

Based on a comparison of the results of both organisms of the first batch, named Ec1_D_1e and Sa1_D_1e, it can be concluded that the A-amyla-Nov was the best hydrolytic enzyme. Furthermore, both cellulases Cellu-Sig and Cellu-Flk were very efficient as well. Interesting were the obvious differences of the amplex red assay results between the hydrolysates of the *E. coli* and *S. aureus* EPS. The assay showed for the *E. coli* EPS that the enzyme hydrolysis with the Enz-mix-U produced high levels of H_2O_2, and for the one of *S. aureus* the A-amyla-Sig from *Bacillus amyloliquefaciens*. Moreover, the EPS hydrolysis of the first batch was performed additionally to the single enzymes also with enzyme combinations for both *S. aureus* and *E. coli*, and the results are shown in Figure 44 and Figure 45.

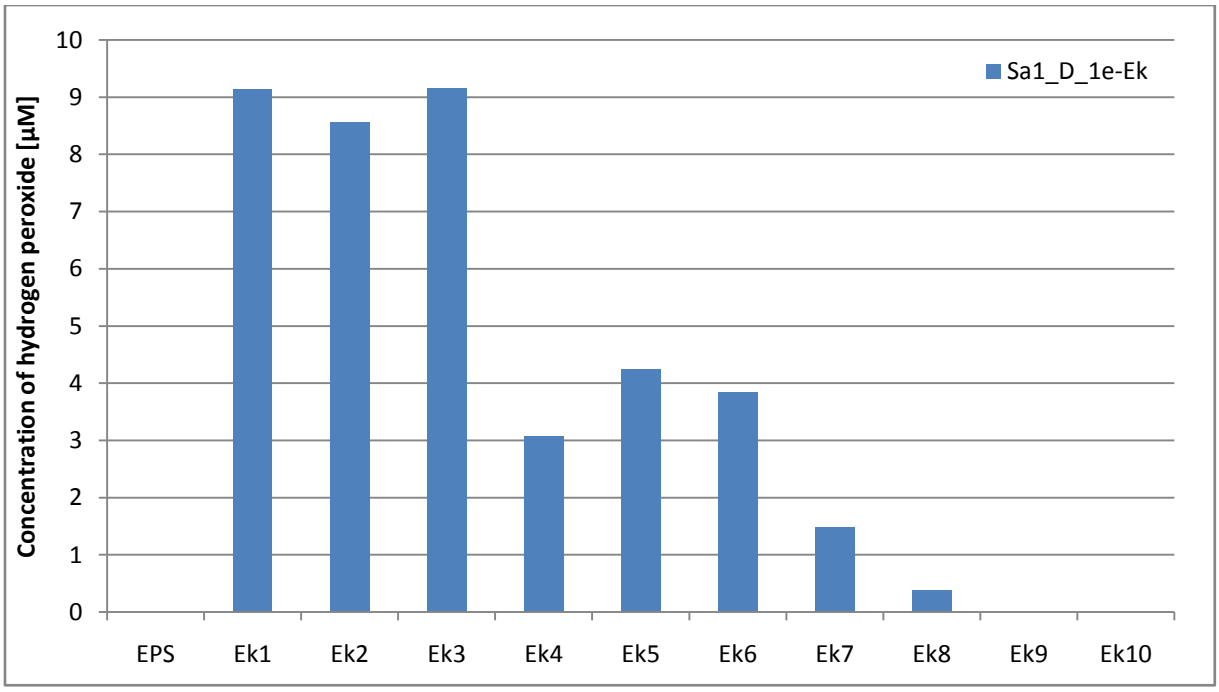

Figure 44: Amplex red assay of the Sa1_D_1e-Ek EPS and hydrolysates

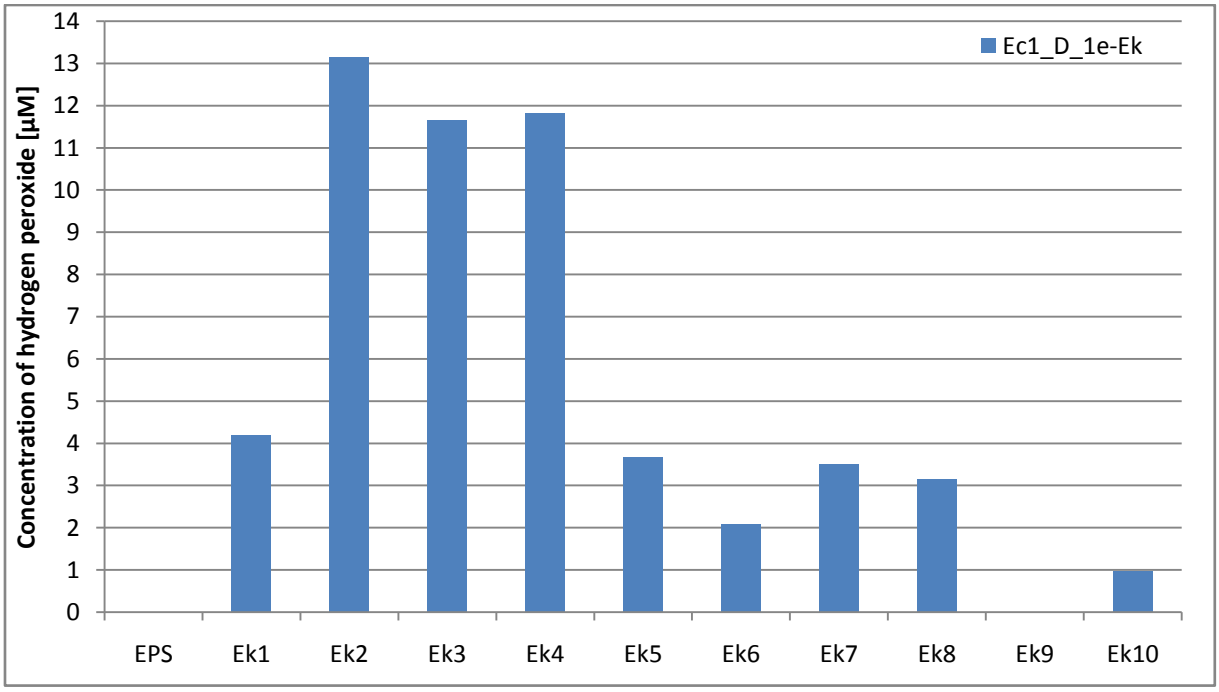

Figure 45: Amplex red assay of the Ec1_D_1e-Ek EPS and hydrolysates

The concentration of hydrogen peroxide used for the combination of two or more hydrolytic enzymes was not as high as expected. However, the enzyme combinations Ek1, Ek2, Ek3 of Sa1_D_1e-Ek and Ek2, Ek3, Ek4 of Ec1_D_1e-Ek were good. The activity of the enzymes was less than in the single enzyme hydrolysis, but the total activity of 1.5 U/ml was the same. Nevertheless, most of the combinations were not very efficient, but only the combination of Ec1_D_1e-Ek2 was outstanding, because all enzymes had only a third of activity in comparison with the single enzymes hydrolysates. The Ec1_D_1e-Ek3 and -Ek4 achieved high values, although the enzymes had only half of the activity as the single enzymes.

The Sa1_D_1e, Ec1_D_1e and the enzyme combinations were tested with two different methods; the comparison of some selected measurements conducted with the Amplex Red and LCV assay are shown in Figure 46 and Figure 47.

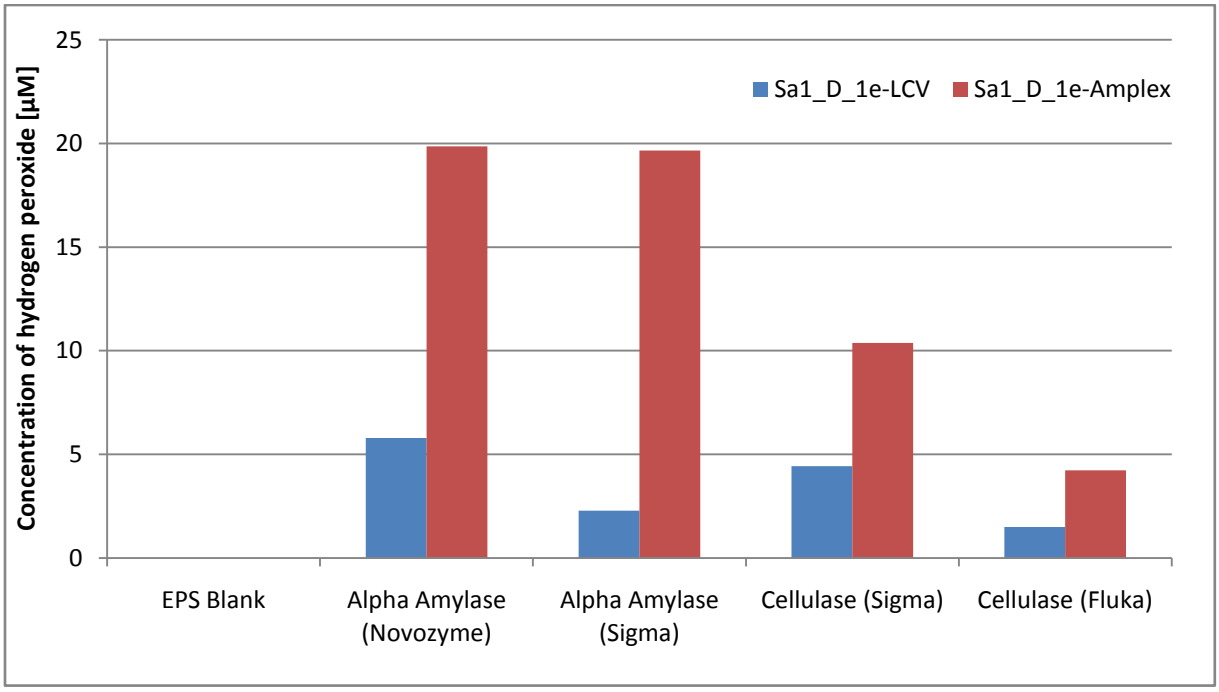

Figure 46: Comparison of H_2O_2 concentration of selected using LCV and Amplex Red assay

The comparison of the Amplex Red with the LCV assay measurements of the Sa1_D_1e shows that the results of the enzymes are similar and showed the same trend. They had just the difference that the LCV results were 2 to 3 times lower, but the one of A-amyla-Sig was significant lower.

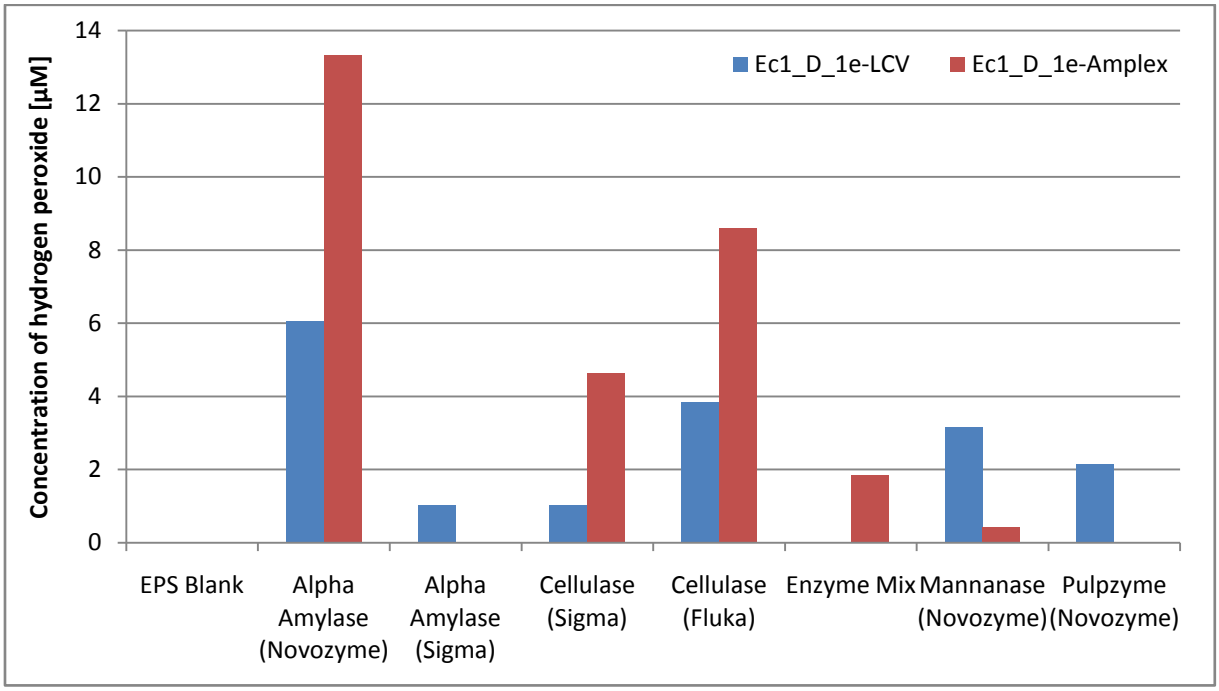

Figure 47: Comparison of Amplex Red and LCV assay results of Ec1_D_1e

The Ec1_D_1e samples were tested with both methods, but between both measurements were huge differences. The enzyme combination measurements were not comparable. However, it can be summarized that the A-amyla-Nov obtained in each batch the best result. Based on the Amplex Red Hydrogen Peroxide assay kit, the Amplex Red reagent reacts in a ratio of 1:1 with hydrogen peroxide. The evaluation of the assay showed that hydrogen peroxide and consequently, CDH substrates with a concentration of 10 to 20 µM, were determined using the alpha amylase of Novozyme (A-amyla-Nov) for hydrolysis. Interestingly, Christensen et al. [68] tested two different marine bacteria in a micro-annual reactor, it was especially developed to study biofilm processes. They showed that already low concentrations of hydrogen peroxide (1 to 5 mM) in combination with ferric iron (0.03 to 0.1 mM) resulted in a removal and detachment of already grown biofilm cells, although the growth of free cells was not completely inhibited. Furthermore, Alt et al. [31] identified that the antimicrobial agent possesses the ability to destroy gram-negative and gram-positive bacteria, fungi and yeasts. The authors detected that 3 % hydrogen peroxide resulted in a noticeable reduction concerning microbial growth. It can be concluded that the hydrogen peroxide testings results of different studies were very varying.

It suggests that the detected and reached concentrations would not be enough for the reduction of microbial growth. It is possible that different combinations of hydrolytic enzymes or prolongation of the hydrolysis would result in a higher yield. However, it can be concluded that the hydrogen peroxide concentration can possibly be insufficient and therefore the MIC of *E. coli* and *S. aureus* had to be determined to find out in which concentration range the future productions should yield.

3.5.5 H_2O_2 sensor

The sensor was tested as an alternative method for determining the concentration of hydrogen peroxide. Therefore a calibration curve was prepared with lactose as standard substrate in the range of 3.9 to 1000 µM. The measurements of the sensor are shown in Figure 48. The current is plotted against the time of various lactose concentrations.

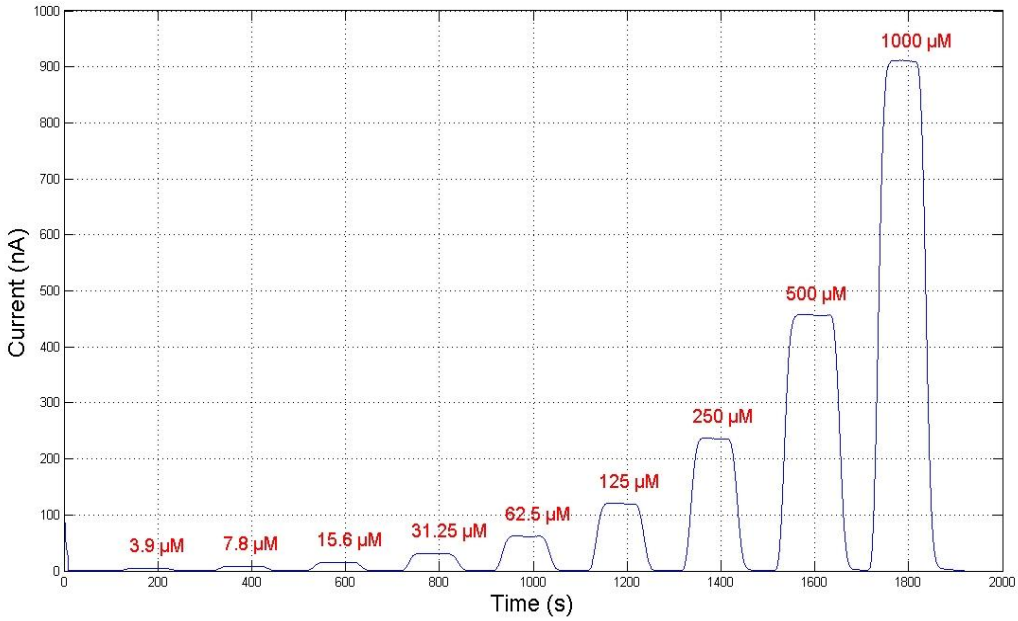

Figure 48: Measurement of the H_2O_2 sensor: the electric current is plotted against the time

For obtaining a calibration curve the current versus the concentration of lactose are plotted and the linear equation, which is depicted in Figure 49, is y = 0.90328 x + 3.6924.

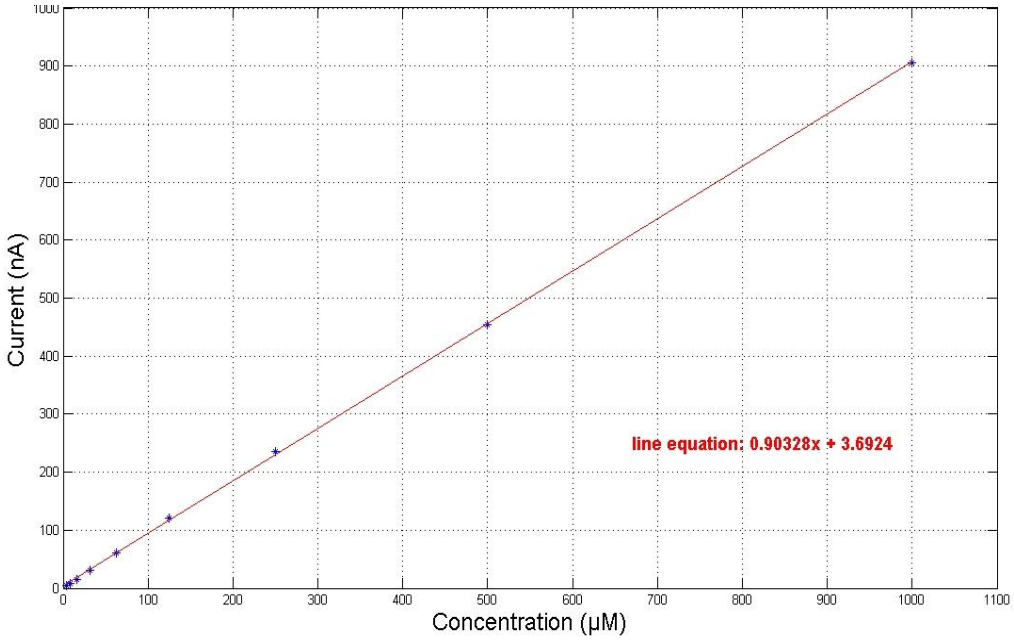

Figure 49: Measurement of the H_2O_2 sensor: the electric current versus lactose concentration

Then the calibration curve of lactose, illustrated in Figure 50, was used for the calculation of the hydrogen peroxide concentration using the results of the measurements.

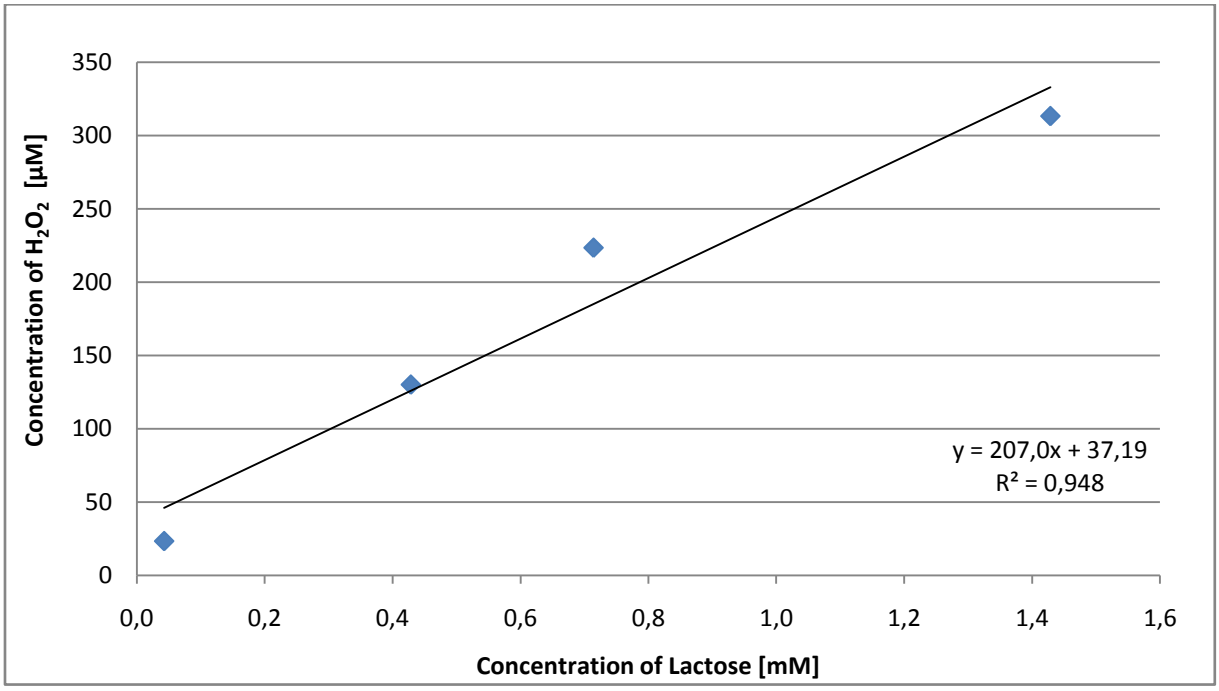

Figure 50: Calibration curve of the H_2O_2 sensor

The determined line equation was: y = 207.0 x + 37.19. The next step was the testing of the CDH with lactose as electron donor; the tested sugar concentrations were in the range of 0.03 to 30 mM. In Figure 51 the measurement of the current over the time is illustrated for different concentrations.

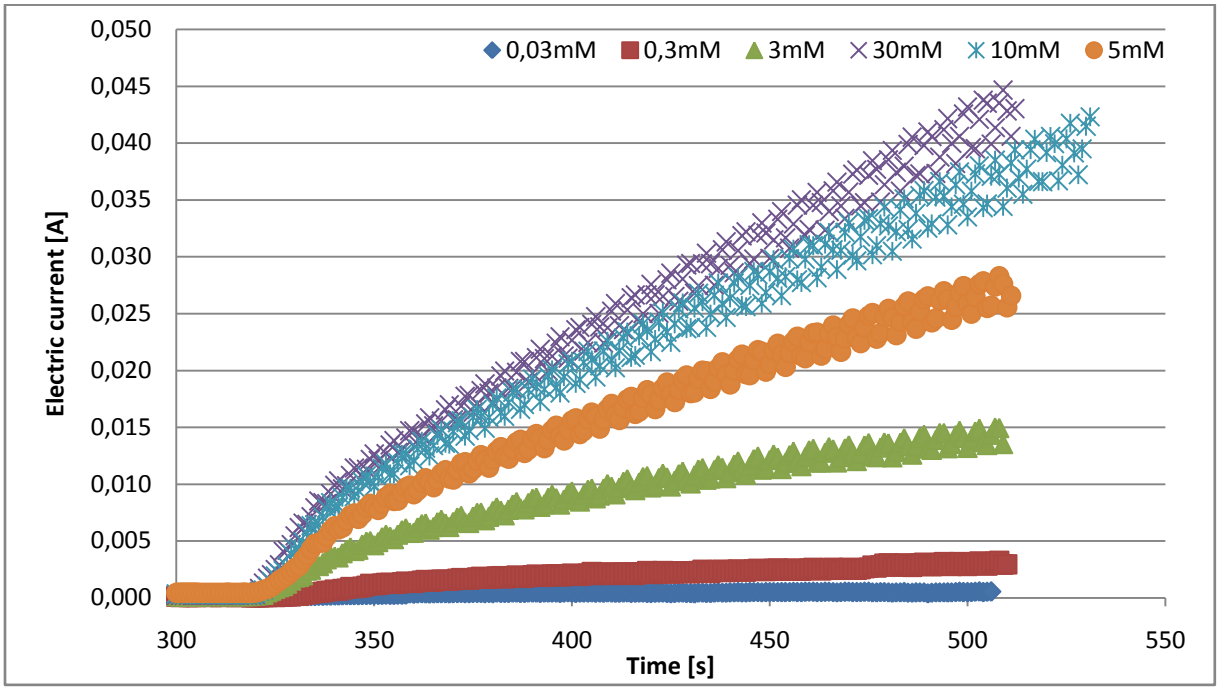

Figure 51: Measurement of the H_2O_2 using CDH and lactose electron donor

The observation of the measurement was that between the concentrations of 10 and 30 mM lactose, there was nearly no difference in the progression of the curve. Although the concentration was three times as high, the measurements were very close together. This suggests that the enzyme was already saturated with substrate lactose, because all active centers of the enzyme seem to be occupied, so that the reaction rate was nearly constant.

The next step would be to measure all untreated and hydrolyzed samples, but this was not carried out due to limited time.

However, it can be summarized that the best method for determination of the hydrogen peroxide concentration, in comparison to the sensor and LCV assay, is the Amplex Red assay, based on the convenient handling, the small sample quantity and quite accurate determination. Nevertheless the sensor has one big advantage in comparison to the other methods; it has a huge detection range.

3.6 Antibiofilm and antimicrobial activity assay

The antibiofilm and antimicrobial assay was tested using the crystal violet (CV) staining and the viability testing for *E. coli* and *S. aureus* to determine the minimal inhibitory concentration (MIC) for the antimicrobial agent hydrogen peroxide.

3.6.1 Testing of *E. coli*

The result of the performed CV staining is shown in Table 48. As growth inhibiting substances, hydrogen peroxide was tested in two different ways. The hydrogen peroxide was added or enzymatically produced by CDH using cellobiose as electron donor. The aim was to see an effect on cell growth.

Table 48: CV staining of *E. coli* (SC was used as blank for the calculations)

Sample	Average	standard deviation	Average-SC	inhibition [%]
Positive Control	1.0029	0.5098	0.76	
Sterile Control (SC)	0.2449	0.0426	Blank	
Cellobiose Control	0.5346		0.29	62
CDH Control	0.8863		0.64	15
0.5 mM Cellobiose	1.0987	0.1416	0.85	-13
2 mM Cellobiose	0.3561	0.0527	0.11	85
4 mM Cellobiose	0.8733	0.7991	0.63	17
500 µM H_2O_2	0.5317		0.29	62
1000 µM H_2O_2	0.3419		0.10	87
1500 µM H_2O_2	0.1456		0.00	113

SC… sterile control

The CV staining for *E. coli* was successful the effect of hydrogen peroxide as growth inhibiting substance was demonstrated. Based on the table above it can be assumed that the minimal inhibitory concentration (MIC) for 100 % inhibition was achieved within the range of 1000 and 1500 µM hydrogen peroxide. For the organism the MIC_{50} of hydrogen peroxide was lower than 500 µM. The measurement for the cellobiose combined with CDH was not successful. Due to the fact that only three concentrations of hydrogen peroxide and cellobiose were tested, the results of the staining and the viability testings are not significant based on a statistical point of view. The viability testing is shown in Table 49.

Table 49: Viability testing of *E. coli*

Sample	CFU/ml
Positive Control	61030
Sterile Control	0
Cellobiose Control	not countable
CDH Control	not countable
0.5 mM Cellobiose	not countable
2mM Cellobiose	8100
4 mM Cellobiose	100
500 µM H_2O_2	160
1000 µM H_2O_2	30
1500 µM H_2O_2	0

Nevertheless, the viability testing emerged a clear trend, because the colonies are decreasing with increasing cellobiose and hydrogen peroxide concentration. For the cellobiose testing no total inhibition was observed, with the hydrogen peroxide testing it could be determined at the concentration of 1500 µM. Based on both testings, it can be assumed that the total inhibition of *E. coli* is in the range of 1000 and 1500 µM hydrogen peroxide.

3.6.2 Testing of *S. aureus*

The crystal violet staining of *S. aureus* was tested twice. In detail the result of the first staining is shown in Table 50 and of the second one in Table 51.

Table 50: Evaluation of the first CV staining of *S. aureus* (SC was used as blank for calculation)

Sample	Average	Standard deviation	Average-SC	Inhibition [%]
Positive Control	1.2566	0.07	1.0885	
Sterile Control (SC)	0.1681	0.04	Blank	Blank
Cellobiose Control	1.1632	0.17	0.9951	9
CDH Control	0.7049	0.15	0.5368	51
0.5 mM Cellobiose	0.5243	0.19	0.3562	67
1 mM Cellobiose	0.2523	0.06	0.0843	92
2 mM Cellobiose	0.2666	0.11	0.0986	91
4 mM Cellobiose	0.1692	0.06	0.0011	100
5 mM Cellobiose	0.2612	0.10	0.0932	91
6 mM Cellobiose	0.2072	0.03	0.0391	96
125 µM H_2O_2	1.0694	0.17	0.9014	17
250 µM H_2O_2	0.5561	0.22	0.3880	64
500 µM H_2O_2	0.4085	0.41	0.2405	78
1000 µM H_2O_2	0.1517	0.02	-0.0164	102
1500 µM H_2O_2	0.1551	0.01	-0.0129	101
2000 µM H_2O_2	0.1021	0.01	-0.0659	106

Table 51: Evaluation of the second CV staining of *S. aureus* (CDH was calculated as blank)

Sample	Average	Standard deviation	Average-SC	inhibition [%]
Positive Control	0.6494	0.07		
Sterile Control (SC)	0.0686	0.02	0	
Cellobiose Control	0.8930	0.21	0.82	39
CDH Control	1.4109	0.14	1.34	0
0.5 mM Cellobiose	1.1103	0.06	1.11	17
1 mM Cellobiose	1.0872	0.32	1.09	19
2 mM Cellobiose	1.0772	0.07	1.08	20
4 mM Cellobiose	0.7376	0.40	0.74	45
5 mM Cellobiose	0.9580	0.27	0.96	29
6 mM Cellobiose	0.4816	0.16	0.48	64
125 µM H_2O_2	0.9295	0.04	0.86	35
250 µM H_2O_2	1.0031	0.15	0.93	30
500 µM H_2O_2	0.4059	0.06	0.34	74
1000 µM H_2O_2	0.0799	0.01	0.01	99
1500 µM H_2O_2	0.086	0.01	0.02	98
2000 µM H_2O_2	0.1042	0.02	0.04	97

In the second testing the staining of the positive control failed and a significant lower value was measured in comparison to the other samples. For evaluating the data of the hydrogen peroxide testings, the CDH blank was taken as positive control. Their result is shown in Figure 52.

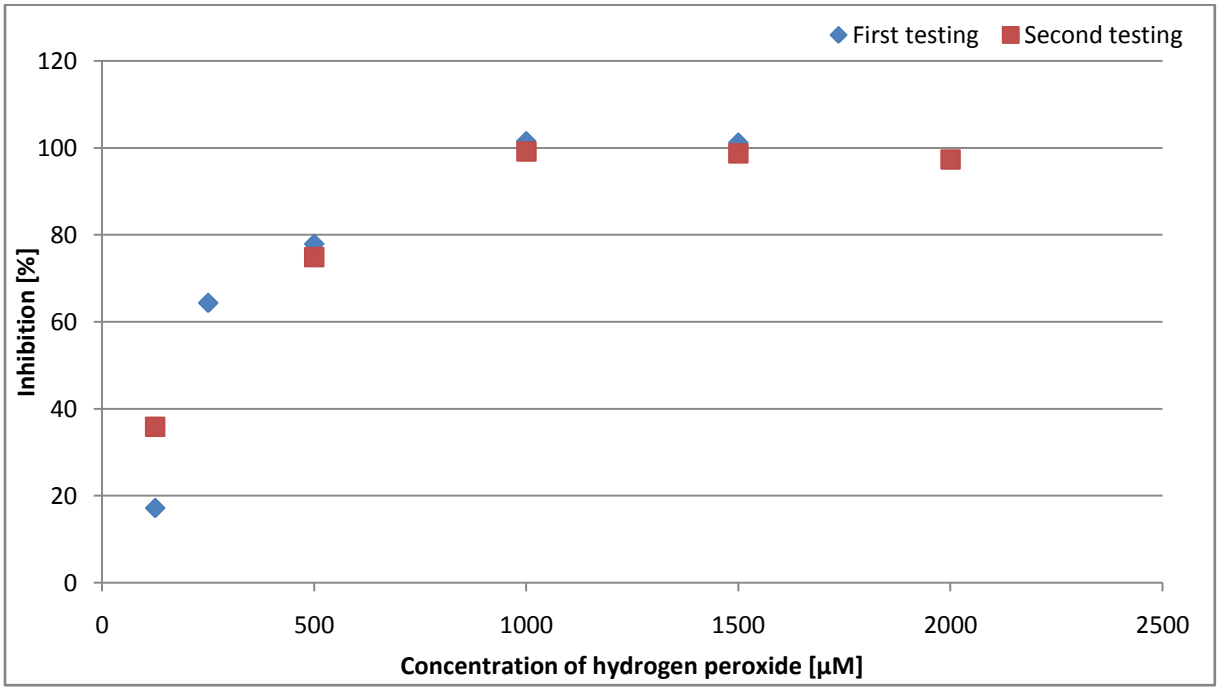

Figure 52: Comparison of both H_2O_2 testings of *S. aureus*

The result was very remarkable, because the antimicrobial effect of hydrogen peroxide could be observed. Based on the figure above, it can be assumed that the total inhibition was at 1000 µM. The MIC_{50} for this organism was approximately in the range of 200 to 300 µM. The

antibiofilm testing was performed for both, but only the first measurement achieved a nice result, which could be evaluated and is shown in Figure 53.

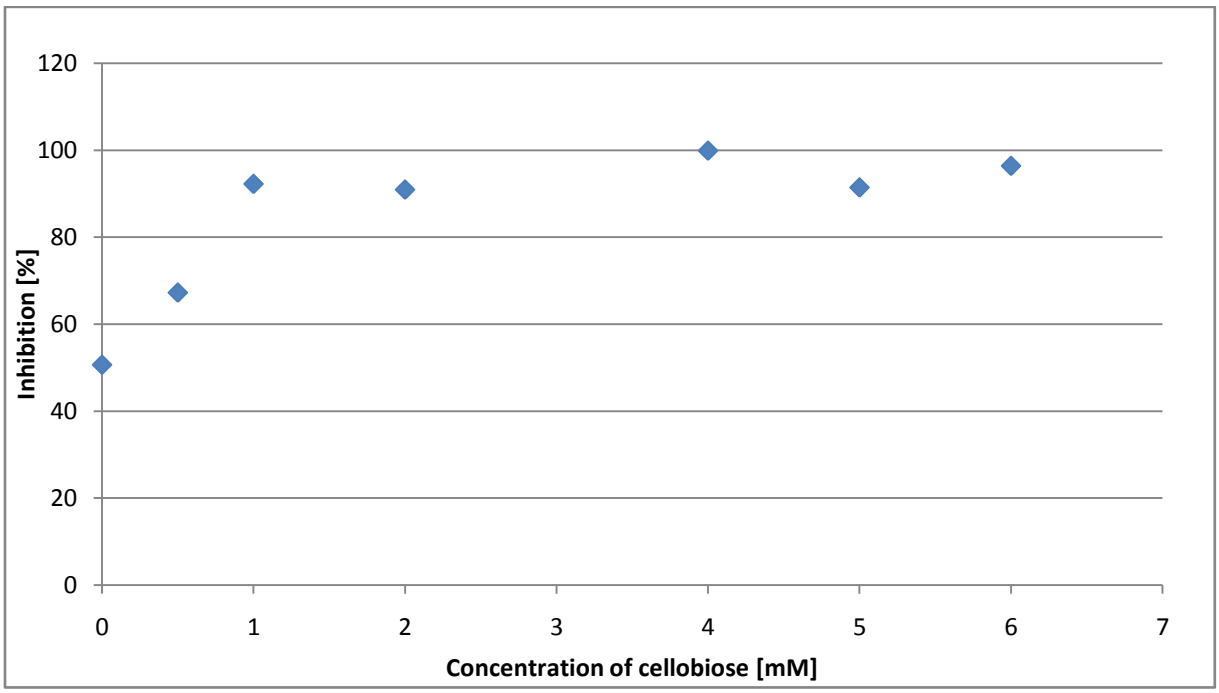

Figure 53: Cellobiose testing of *S. aureus*

As can be seen in the figure above, the results for the first measurement were varying, the MIC_{50} was at a concentration of 0 mM of cellobiose (CDH control). A possible explanation for this high value is the content of the sample, which consisted of CDH and TSB media containing glucose. As a consequence, it can be assumed that much glucose or other sugars were present, which could be used as electron donor for production of hydrogen peroxide by the enzyme. The strong fluctuation in the measurement can be explained due to the time, which was required by the cellobiose dehydrogenase for the generation of H_2O_2. Pricelius et al. [39] reported that the CDH from *M. thermophilum*, which was used for the antibiofilm assay was able in contrast to other CDHs such as *P. chrysosporium* to oxidize glucose or other monosaccharide. Based on the results of the authors, this would explain the high values that were measured. Moreover, they described that the dehydrogenase is not able to use the electron donor glucose as efficient as the original substrate cellobiose. Nevertheless, it is also possible that a potential presence of galactose, based on Henriksson et al. [38] could prevent the binding of cellobiose due to a competitive inhibition in cellobiose-galactose mixtures as they demonstrated with the CDH from *P. chrysosporium*.

It is entirely possible that the monosaccharide galactose was present in the produced biofilms, based on the glycosyl composition analysis of Bales et al. [26]. Interestingly, Pricelius et al. [39] studied the *Mt*CDH and they showed that the monosaccharide galactose alone can be used as substrate. However, it can be assumed that the MIC_{100} could possibly

be obtained by extension of the incubation time. The total inhibition was detected at 4 mM concentration. Nevertheless, the effect as growth inhibiting substance of hydrogen peroxide as well as newly formed one was confirmed. The ability of hydrogen peroxide as antimicrobial agent was shown by Alt et al. [31], it is already used as a disinfectant of wounds and they showed that local treatment with 3 % hydrogen peroxide reduced the microbial growth on polymer surface. Craigen et al. [28] studied with several testings the huge potential of the hydrolytic enzyme alpha amylase concerning the removal and growth inhibition of *Staphylococcus aureus* biofilms. In 96-well plates they tested the reduction of an existing biofilm. They achieved with the alpha amylase from *A. oryzae* (Sigma) a very significant reduction of 90 % after ten minutes and additionally, they tested the growth inhibition [28]. It can be assumed that the combination of alpha amylase and CDH for hydrogen peroxide production is more efficient in the destruction or growth inhibition of biofilms. On the one hand the alpha amylase can be used to destroy the complex matrix of the EPS and on the other hand CDH possesses the ability to use the smaller fragments produced by the hydrolytic enzyme such as mono-, di- and oligosaccharides as electron donor for the production of hydrogen peroxide.

The result of the viability testing is shown in Table 52.

Table 52: Viability testing of *S. aureus*

Sample	CFU/ml
Positive Control	50200000
Sterile Control	0
Cellobiose Control	18700000
CDH Control	35533333
0.5 mM Cellobiose	38633333
1 mM Cellobiose	38633333
2 mM Cellobiose	41800000
4 mM Cellobiose	17833333
5 mM Cellobiose	24900000
6 mM Cellobiose	7995000
125 µM H_2O_2	7266667
250 µM H_2O_2	6918333
500 µM H_2O_2	50000
1000 µM H_2O_2	0
1500 µM H_2O_2	0
2000 µM H_2O_2	0

There was a clear trend that above a concentration of 1000 µM hydrogen peroxide, no growth was detectable. This result correlated with the one of the CV staining. The CFU/ml for every plate had strong fluctuations within the triplicates in serial dilutions, so only the average was taken for calculation of the CFU/ml. This could be explained due to the ultrasonic method, which was previously used to remove the biofilm from the silicon plates.

For evaluation the efficiency of the method and the accuracy of the viability testing, the silicon plates were stained with CV after using ultrasonic. The result of the evaluation is shown in Table 53.

Table 53: CV staining for evaluation of the ultrasonic method

Sample	1.	2.	3.	Average	Standard deviation
Positive Control	0.1284	0.3359*	0.0716	0.18	0.14
Sterile Control (SC)	0.0866	0.0650	0.0641	0.07	0.01
Cellobiose Control	0.1643	0.1403	0.1898	0.16	0.02
CDH Control	0.1488	0.2039	0.2035	0.19	0.03
0.5 mM Cellobiose	0.1030	0.1022	0.0867	0.10	0.01
1 mM Cellobiose	0.1419	0.1130	0.2543	0.17	0.07
2 mM Cellobiose	0.1825	0.1282	0.1373	0.15	0.03
4 mM Cellobiose	0.1866	0.1145	0.7874*	0.36	0.05
5 mM Cellobiose	0.1056	0.2360	0.1546	0.17	0.07
6 mM Cellobiose	0.1758	0.1948	0.3006*	0.22	0.01
125 µM H_2O_2	0.0948	0.1515	0.1253	0.12	0.03
250 µM H_2O_2	0.1728	0.1397	0.1367	0.15	0.02
500 µM H_2O_2	0.0591	0.0559	0.0515	0.06	0.00
1000 µM H_2O_2	0.0925	0.1201	0.0871	0.10	0.02
1500 µM H_2O_2	0.0839	0.0720	0.0817	0.08	0.01
2000 µM H_2O_2	0.0699	0.0978	0.0767	0.08	0.01

* higher values (outliers)

Except three significant high measurements it seems, that the ultrasonic method was an efficient method to remove the biofilm from the silicon plates. Moreover, a relation could be observed between outliers of the plate counting and the staining. The samples that achieved high values at the staining seemed to contain still biofilm on the silicon plates and the same ones showed previously after streaked out on agar plates a lower CFU/ml in comparison to the others.

4 Conclusion

The aim of this thesis was to develop an in situ built system to destroy biofilms by using the EPS as substrate for CDH to produce the antimicrobial agent hydrogen peroxide in order to prevent microbial colonization of catheters. For this purpose *Staphylococcus aureus* and *Escherichia coli* were used as model organisms for investigating the effect of CDH.

Therefore to produce hydrogen peroxide the CDH was incubated with the untreated EPS of both organism and this resulted in a concentration up to 0.16 µM. The measured concentrations were very low, certainly after the performed dialysis, because all smaller fragments were removed. A new strategy, which involved a pre-hydrolysis step on the EPS in order to generate lower molecular weight fragments that can hopefully be used as substrates by the cellobiose dehydrogenase, was adopted for the purpose of boosting the hydrogen peroxide production. It was proven that the concentration of reducing sugars and generated hydrogen peroxide are not correlating. It can be explained due to the substrate specificity of cellobiose dehydrogenase; because it is possible that too large oligo- or polysaccharides or monosaccharides with reducing ends were hydrolyzed, which cannot be used as electron donor.

The routine accurate measurement of hydrogen peroxide is problematic. Several methods were tested to determine the hydrogen peroxide concentration such as H_2O_2 sensor, leuco crystal violet assay and the Amplex Red assay, but the Amplex Red assay was found to be the best method with an easy handling. The H_2O_2 sensor exhibited an interesting observation that lactose concentrations between 10 and 30 mM showed at the beginning no different progression of the curve. This can be explained based on the fact that the active centers seemed to be already occupied.

The Amplex Red assay showed that the best three hydrolytic enzymes for the hydrogen peroxide production for *S. aureus* EPS (first batch) were cellulase from *Aspergillus niger* (Sigma), alpha amylase of Novozyme and Sigma. The concentrations of H_2O_2 were in the range of 10 to 20 mM. The same enzymes were effective in hydrolyzing the *E. coli* EPS (first batch) and reached 5 and 13 mM H_2O_2. However, the alpha amylase (Novozyme) was for both organisms the most effective enzyme for hydrolysis. The LCV assay had due to the light sensitiveness problems with the reproducibility; it measured mainly lower hydrogen peroxide values than the Amplex Red assay, but they showed a similar trend. It was detected with both assays that the cellulase (Sigma) worked better for the production of hydrogen peroxide for *S. aureus* than *E. coli.* For the other cellulase (Fluka) it was the other way round. This suggests that both cellulases from *Aspergillus niger* have different hydrolytic mechanisms.

The MIC_{50} of hydrogen peroxide was for both model microorganisms in the range of 200 to 500 µM. A complete inhibition was detected for both at concentrations between 1000 to 1500 µM and higher for the newly formed one. It can be concluded that CDH, in combination with one or more hydrolytic enzymes, is needed to reach such high concentrations. Based on the performed viability testing and the CV staining it can be assumed that the total inhibition for *Escherichia coli* was is in the range of 1000 to 1500 µM. The viability and CV testings of *Staphylococcus aureus* showed that a total inhibition was at the concentration of 1000 µM hydrogen peroxide. The MIC_{50} for this organism was approximately in the range of 200 to 300 µM. In the cellobiose testing the MIC_{50} was reached at a concentration of 0 mM cellobiose. The total inhibition was obtained at 4 mM cellobiose, nevertheless it was possible to detect for both organisms that hydrogen peroxide possesses the ability to destroy biofilms. It can be assumed that a prolongation of the hydrolysis could possibly increase the yield of hydrogen peroxide. Its concentration has to be increased about a 50 to 100-fold, presumably other combinations of enzymes could be more efficient.

The next step would be to develop an enzyme system for destroying biofilms based on the antimicrobial agent hydrogen peroxide by combining one or more hydrolytic enzyme with cellobiose dehydrogenase. Principally, the implementation of the enzyme system should be possible, also for indwelling medical devices. The focus of subsequent studies can possibly be on the combination of different alpha amylase and CDH for hydrogen peroxide production, especially because it can be expected that this approach can result in a more effective destruction or growth inhibition of biofilms. Moreover, it can be assumed that the EPS can be hydrolyzed by the amylase to ensure that the hydrogen peroxide can penetrate easier into the biofilm to obtain a more favorable result. It can be a possible future objective to test different microorganism and other hydrolytic enzymes as well as enzyme combinations.

5 Literature

[1] Vu B, Chen M, Crawford RJ, Ivanova EP: **Bacterial extracellular polysaccharides involved in biofilm formation.** *Molecules* 2009, **14**(**7**):2535–54.

[2] Kokare CR, Chakraborty S, Khopade AN, Mahadik KR: **Biofilm : Importance and applications.** *Indian J Biotechnol* 2009, **8**(**2**):159–68.

[3] Denkhaus E, Meisen S, Telgheder U, Wingender J: **Chemical and physical methods for characterisation of biofilms.** *Microchim Acta* 2007, **158**(**1-2**):1–27.

[4] Watnick P, Kolter R: **Biofilm , City of Microbes.** *J Bacteriol* 2000, **182**(**10**):2675–9.

[5] Klapper I, Dockery J: **Mathematical Description of Microbial Biofilms.** *SIAM Rev* 2010, **52**(**2**):221–65.

[6] Donlan RM: **Biofilms: microbial life on surfaces.** *Emerg Infect Dis* 2002, **8**(**9**):881–90.

[7] Sutherland I: **Biofilm exopolysaccharides: a strong and sticky framework.** *Microbiology* 2001, **147**(**1**):3–9.

[8] Lazar V: **Quorum sensing in biofilms - How to destroy the bacterial citadels or their cohesion/power?** *Anaerobe* 2011, **17**(**6**):280–5.

[9] Marić S, Vraneš J: **Characteristics and significance of microbial biofilm formation.** *Period Biol* 2007, **109**(**2**):115–21.

[10] Costerton JW, Lewandowski Z, Caldwell DE, Korber DR, Lappin-Scott HM: **Microbial biofilms.** *Annu Rev Microbiol* 1995, **49**(**1**):711–45.

[11] Hall-Stoodley L, Costerton JW, Stoodley P: **Bacterial biofilms: From the natural environment to infectious diseases.** *Nat Rev Microbiol* 2004, **2**(**2**):95–108.

[12] Thallinger B, Prasetyo EN, Nyanhongo GS, Guebitz GM: **Antimicrobial enzymes: An emerging strategy to fight microbes and microbial biofilms.** *Biotechnol J* 2013, **8**(**1**):97–109.

[13] Simões M, Simões LC, Vieira MJ: **A review of current and emergent biofilm control strategies**. *LWT - Food Sci Technol* 2010, **43**(**4**):573–83.

[14] Nikaido H: **Multidrug Resistance in Bacteria.** *Annu Rev Biochem* 2010, **78**:119–46.

[15] Donlan RM: **Biofilms and device-associated infections.** *Emerg Infect Dis* 2001, **7**(**2**):277–81.

[16] Mah TF, O'Toole GA: **Mechanisms of biofilm resistance to antimicrobial agents.** *Trends Microbiol* 2001, **9**(**1**):34–9.

[17] Darouiche RO: **Treatment of infections associated with surgical implants.** *N Engl J Med* 2004, **350**(**14**):1422–9.

[18] Mack D, Fischer W, Krokotsch A, Leopold K, Hartmann R, Egge H, Laufs R: **The intercellular adhesin involved in biofilm accumulation of Staphylococcus epidermidis**

is a linear beta-1,6-linked glucosaminoglycan: purification and structural analysis. *J Bacteriol* 1996, **178**(**1**):175–83.

[19] Bouza E, Guembe M, Muñoz P: **Selection of the vascular catheter: can it minimise the risk of infection?** *Int J Antimicrob Agents* 2010, **36**(**S2**):22–5.

[20] Eboigbodin KE, Biggs CA: **Characterization of the extracellular polymeric substances produced by Escherichia coli using infrared spectroscopic, proteomic, and aggregation studies.** *Biomacromolecules* 2008, **9**(**2**):686–95.

[21] Tian Y, Zheng L, Sun D: **Functions and behaviors of activated sludge extracellular polymeric substances (EPS): a promising environmental interest.** *J Environ Sci* 2006, **18**(**3**):420–7.

[22] Bahat-Samet E, Castro-Sowinski S, Okon Y: **Arabinose content of extracellular polysaccharide plays a role in cell aggregation of Azospirillum brasilense.** *FEMS Microbiol Lett* 2004, **237**(**2**):195–203.

[23] Rättö M, Verhoef R, Suihko M-L, Blanco A, Schols HA, Voragen AGJ, Wilting R, Siika-Aho M, Buchert J: **Colanic acid is an exopolysaccharide common to many enterobacteria isolated from paper-machine slimes.** *J Ind Microbiol Biotechnol* 2006, **33**(**5**):359–67.

[24] Cerca N, Maira-Litrán T, Jefferson KK, Grout M, Goldmann DA, Pier GB: **Protection against Escherichia coli infection by antibody to the Staphylococcus aureus poly-N-acetylglucosamine surface polysaccharide.** *Proc Natl Acad Sci U S A* 2007, **104**(**18**):7528–33.

[25] Danese PN, Pratt LA, Kolter R: **Exopolysaccharide Production Is Required for Development of Escherichia coli K-12 Biofilm Architecture Exopolysaccharide Production Is Required for Development of Escherichia coli K-12 Biofilm Architecture.** *J Bacteriol* 2000, **182**(**12**):3593–6.

[26] Bales PM, Renke EM, May SL, Shen Y, Nelson DC: **Purification and Characterization of Biofilm-Associated EPS Exopolysaccharides from ESKAPE Organisms and Other Pathogens.** *PLoS One* 2013, **8**(**6**):1–8.

[27] Arvaniti A, Karamanos N, Dimitracopoulos G, Anastassiou E: **Isolation and Characterization of a Novel 20-kDa Sulfated Polysaccharide from the Extracellular Slime Layer of Staphylococcus epidermidis.** *Arch Biochem Biophys* 1994, **308**(**2**):432–8.

[28] Craigen B, Dashiff A, Kadouri DE: **The Use of Commercially Available Alpha-Amylase Compounds to Inhibit and Remove Staphylococcus aureus Biofilms.** *Open Microbiol J* 2011, **5**:21–31.

[29] Hansen EH, Schembri MA, Klemm P, Scha T, Molin S, Gram L: **Elucidation of the Antibacterial Mechanism of the Curvularia Haloperoxidase System by DNA Microarray Profiling.** *Appl Environ Microbiol* 2004, **70**(**3**):1749–57.

[30] Fux C a, Costerton JW, Stewart PS, Stoodley P: **Survival strategies of infectious biofilms.** *Trends Microbiol* 2005, **13**(**1**):34–40.

[31] Alt E, Leipold F, Milatovic D, Lehmann G, Heinz S, Schömig A: **Hydrogen peroxide for prevention of bacterial growth on polymer biomaterials.** *Ann Thorac Surg* 1999, **68**(**6**):2123–8.

[32] Curtis J, Klykken P: **A Comparative Assessment of Three Common Catheter Materials.** *Dow Corning Corp* 2008:1–8.

[33] Anon: **http://ec.europa.eu/research/health/infectious-diseases/antimicrobial-drug-resistance/projects/084_en.htm**.

[34] Yoshida M, Ohira T, Igarashi K, Nagasawa H, Samejima M: **Molecular cloning and characterization of a cDNA encoding cellobiose dehydrogenase from the wood-rotting fungus Grifola frondosa.** *FEMS Microbiol Lett* 2002, **217**(**2**):225–30.

[35] Sygmund C, Santner P, Krondorfer I, Peterbauer CK, Alcalde M, Nyanhongo GS, Guebitz GM, Ludwig R: **Semi-rational engineering of cellobiose dehydrogenase for improved hydrogen peroxide production.** *Microb Cell Fact* 2013, **12**(**38**):1–10.

[36] Ludwig R, Harreither W, Tasca F, Gorton L: **Cellobiose Dehydrogenase: A versatile Catalyst for Electrochemical Applications.** *ChemPhysChem* 2010, **11**(**13**):2674–97.

[37] Henriksson G, Johansson G, Pettersson G: **A critical review of cellobiose dehydrogenases.** *J Biotechnol* 2000, **78**(**2**):93–113.

[38] Henriksson G, Sild V, Szabó IJ, Pettersson G, Johansson G: **Substrate specificity of cellobiose dehydrogenase from Phanerochaete chrysosporium.** *Biochim Biophys Acta* 1998, **1383**(**1**):48–54.

[39] Pricelius S, Ludwig R, Lant N, Haltrich D, Guebitz GM: **Substrate specificity of Myriococcum thermophilum cellobiose dehydrogenase on mono-, oligo-, and polysaccharides related to in situ production of H2O2.** *Appl Microbiol Biotechnol* 2009, **85**(**1**):75–83.

[40] Zámocký M, Schümann C, Sygmund C, O'Callaghan J, Dobson ADW, Ludwig R, Haltrich D, Peterbauer CK: **Cloning, sequence analysis and heterologous expression in Pichia pastoris of a gene encoding a thermostable cellobiose dehydrogenase from Myriococcum thermophilum.** *Protein Expr Purif* 2008, **59**(**2**):258–65.

[41] Hammel KE, Kapich AN, Jensen Jr KA, Ryan ZC: **Reactive oxygen species as agents of wood decay by fungi**. *Enzyme Microb Technol* 2002, **30**:445–53.

[42] Henriksson G, Zhang L, Li J, Ljungquist P, Reitberger T, Pettersson G, Johansson G: **Is cellobiose dehydrogenase from Phanerochaete chrysosporium lignin degrading enzyme?** *Biochim Biophys Acta* 2000, **1480**(**1**):83–91.

[43] Vasil'chenko L, Khromonygina V, Karapetyan K, Vasilenko O, Rabinovich M: **Cellobiose dehydrogenase formation by filamentous fungus Chaetomium sp. INBI 2-26(-).** *J Biotechnol* 2005, **119**(**1**):44–59.

[44] Hallberg BM, Henriksson G, Pettersson G, Vasella A, Divne C: **Mechanism of the reductive half-reaction in cellobiose dehydrogenase.** *J Biol Chem* 2003, **278**(**9**):7160–6.

[45] Hallberg BM, Bergfors T, Bäckbro K, Pettersson G, Henriksson G, Divne C: **A new scaffold for binding haem in the cytochrome domain of the extracellular flavocytochrome cellobiose dehydrogenase.** *Structure* 2000, **8**(**1**):79–88.

[46] Flitsch A, Prasetyo EN, Sygmund C, Ludwig R, Nyanhongo GS, Guebitz GM: **Cellulose oxidation and bleaching processes based on recombinant Myriococcum thermophilum cellobiose dehydrogenase.** *Enzyme Microb Technol* 2013, **52**(**1**):60–7.

[47] Maischberger T, Nguyen T-H, Sukyai P, Kittl R, Riva S, Ludwig R, Haltrich D: **Production of lactose-free galacto-oligosaccharide mixtures: comparison of two cellobiose dehydrogenases for the selective oxidation of lactose to lactobionic acid.** *Carbohydr Res* 2008, **343**(**12**):2140–7.

[48] Nyanhongo GS, Sygmund C, Ludwig R, Prasetyo EN, Guebitz GM: **An antioxidant regenerating system for continuous quenching of free radicals in chronic wounds.** *Eur J Pharm Biopharm* 2013, **83**:396–404.

[49] Pan X, Liu J, Zhang D, Chen X, Li L, Song W, Yang J: **A comparison of five extraction methods for extracellular polymeric substances (EPS) from biofilm by using three-dimensional excitation-emission matrix (3DEEM) fluorescence spectroscopy.** *Water SA* 2010, **36**(**1**):111–6.

[50] Dubois M, Gilles K, Hamilton J, Rebers P, Smith F: **Colorimetric Method for Determination of Sugars and Related Substances.** *Anal Chem* 1956, **28**(**3**):350–6.

[51] Dreywood R: **Qualitative Test for Carbohydrate Material.** *Ind Eng Chem Anal Ed* 1946, **18**(**8**):499–499.

[52] Foster JS, Green SJ, Ahrendt SR, Golubic S, Reid RP, Hetherington KL, Bebout L: **Molecular and morphological characterization of cyanobacterial diversity in the stromatolites of Highborne Cay, Bahamas.** *ISME J* 2009, **3**(**5**):573–87.

[53] King BC, Donnelly MK, Bergstrom GC, Walker LP, Gibson DM: **An optimized microplate assay system for quantitative evaluation of plant cell wall-degrading enzyme activity of fungal culture extracts.** *Biotechnol Bioeng* 2009, **102**(**4**):1033–44.

[54] Anon: **http://www.eng.umd.edu/~nsw/ench485/lab4a.htm**.

[55] Anon: **http://www.brechbuehler.ch/fileadmin/redacteur/pdf/columns-sampleprep/lc-columns/zhlun.pdf**.

[56] Bailey RW, Bourne EJ: **Colour Reactions given by sugars and diphenylamine-aniline spray reagents on paper chromatograms.** *J Chromatogr* 1960, **4**:206–13.

[57] Buchan JL, Savage RI: **Paper chromatography of some starch conversion products.** *Analyst* 1952, **77**(**917**):401–6.

[58] Mottola HA, Simpson BE, Gorin G: **Absorptiometric determination of hydrogen peroxide in submicrogram amounts with leuco crystal violet and peroxidase as catalyst.** *Anal Chem* 1970, **42**(**3**):410–1.

[59] Stoica L, Ruzgas T, Gorton L: **Electrochemical evidence of self-substrate inhibition as functions regulation for cellobiose dehydrogenase from Phanerochaete chrysosporium.** *Bioelectrochemistry* 2009, **76**(**1**):42–52.

[60] Kandukuri SS, Noor A, Ranjini SS, Vijayalakshmi MA: **Purification and characterization of catalase from sprouted black gram (Vigna mungo) seeds.** *J Chromatogr B Analyt Technol Biomed Life Sci* 2012, **889-890**:50–4.

[61] Woodbury W, Spencer A, Stahmann M: **An Improved Procedure Using Ferricyanide for Detecting Catalase Isoenzymes.** *Anal Biochem* 1971, **44**(**1**):301–5.

[62] Cohn CA, Pak A, Strongin D, Schoonen MA: **Quantifying hydrogen peroxide in iron-containing solutions using leuco crystal violet.** *Geochem Trans* 2005, **6**(**3**):47–51.

[63] Harrich DR: **Entwicklung eines Sensors zur frühzeitigen Detektion von Wundinfektionen.** 2013.

[64] Comte S, Guibaud G, Baudu M: **Relations between extraction protocols for activated sludge extracellular polymeric substances (EPS) and EPS complexation properties Part I. Comparison of the efficiency of eight EPS extraction methods.** *Enzyme Microb Technol* 2006, **38**(**1**):237–45.

[65] Dogsa I, Kriechbaum M, Stopar D, Laggner P: **Structure of bacterial extracellular polymeric substances at different pH values as determined by SAXS.** *Biophys J* 2005, **89**(**4**):2711–20.

[66] Meisen S, Wingender J, Telgheder U: **Analysis of microbial extracellular polysaccharides in biofilms by HPLC. Part I: Development of the analytical method using two complementary stationary phases.** *Anal Bioanal Chem* 2008, **391**(**3**):993–1002.

[67] Savadogo A, Ouattara CA, Savadogo PW, Barro N, Aboubacar S, Traoré AS: **Identification of exopolysaccharides-producing lactic acid bacteria from Burkina Faso fermented milk samples.** *African J Biotechnol* 2004, **3**(**3**):189–94.

[68] Christensen BE, Trønnes HN, Vollan K, Smidsrød O, Bakke R: **Biofilm removal by low concentrations of hydrogen peroxide.** *Biofouling* 1990, **2**(**2**):165–75.

6 Abbreviations

Abbreviation	?
%	percent
(w/v)	weight/volume
°C	degree centigrade
µ	micro
Å	angstrom
ACN	acetonitrile
Amplex	10-acetyl-3,7-dihydroxyphenoxazine
BCA	bicinchoninic acid
BSA	bovine serum albumin
CDH	cellobiose dehydrogenase
cm	centimeter
Cu	Copper
CV	crystal violet
Da	dalton
DCIP	2,6-dichloroindophenol
ddH_2O	double distilled water
dH_2O	destilled water
DM	desferrioxaminemesylate
DNS	3,5-dinitrosalicylic acid
e^-	electron
EDTA	Ethylenediaminetetraacetic acid
Ek	enzyme combination
EPS	extracellular polymeric substances or exopolysaccharide
Fe	iron
g	gramm
H^+	hydrogen
H_2O_2	hydrogen peroxide
HGT	horizontal gene transfer
HPLC	high performance liquid chromatography
HPO	horseradish peroxidase
l	liter
K	kilo
LCV	leuco crystal violet
LIP	Lignin Peroxidase
µ	micro
m	milli
M	molar concentration [mol/L]
mg/ml	milligram per milliliter
MIC	minimal inhibitory concentration
min	minute
ml/min	milliliter per minute
MS	mass spectrophotometer
*Mt*CDH	cellobiose dehydrogenase from *Myriococcum thermophilum*
MWCO	molecular weight cut-off
nm	nanometer
NaCl	sodium chloride
NaOH	sodium hydroxide
nm	nanometer
o-	ortho-
O_2	molecular oxygen
OD	optical density
ONC	overnight culture

MPa	Mega Pascal
RI detector	refraction index detector
Rf	retardation factor
rpm	rotations per minute
SC	sterile control
spp.	species pluralis
SDS	sodium dodecyl sulfate
TEMED	tetramethylethylenediamine
TLC	thin layer chromatography
Tris	2-amino-2-hydroxymethyl-propane-1,3-diol
TSB	tryptic soy broth
U	enzyme unit
U/ml	unit per milliliter
UV	ultraviolet

7 Chemicals

Chemicals	Company
10-acetyl-3,7-dihydroxyphenoxazine (Amplex Red)	Invitrogen
2,6-dichloroindophenol (DCIP)	Hoffman La Roche
2-Propanol	Carl Roth GmbH
Acetic acid	Carl Roth GmbH
Acetone	Carl Roth GmbH
Acetonitrile (ACN)	Merck
Acrylamide Bis	Merck
Agar Agar	Carl Roth GmbH
Aniline	Sigma Aldrich
Anthrone	Merck
Ammonium persulfate (APS)	Merck
Bicinchoninic acid (BCA)	EMD Millipore chemicals
Bovine serum albumin (BSA)	Sigma Aldrich
Bromphenol blue	Merck
Cellobiose	Carl Roth GmbH
Cellohexaose	Megazyme
Cellotetraose	Megazyme
Cellulose	Merck
Crystal violet (CV)	Fluka
Cupric sulfate	EMD Millipore chemicals
D (+)-Galactose	Merck
D(-)-Fructose	Sigma Aldrich
D(+)-Mannose	Carl Roth GmbH
D(+)-Saccarose	Carl Roth GmbH
D(+)-Trehalose dihydrate	Carl Roth GmbH
D(+)-Xylose	Carl Roth GmbH
Desferrioxaminemesylate(DM)	Sigma Aldrich
Diphenylamine	Sigma Aldrich
Disodium hydrogen phosphate	Carl Roth GmbH
D-Ribose	Merck
Ethylenedinitrilo-tetraacetic acid tetrasodium salt Tetrahydrate	Merck
Ferric chloride	Merck
Hydrogen peroxide	Sigma Aldrich
Formic acid	Carl Roth GmbH
Galacturonic acid	Fluka
D(+)-Glucosamine	Sigma Aldrich
Glucuronic acid	Sigma Aldrich
Glycerol	Carl Roth GmbH
Glycin	Carl Roth GmbH
Hydrochloric acid	Sigma Aldrich
L (+)-Arabinose	Sigma Aldrich
Lactose monohydrate	Carl Roth GmbH
Leuco crystal violet (LCV)	Sigma Aldrich
L-Rhamnose monohydrate	Fluka
Maltose (monohydrate)	Merck
N-Acetyl-Galactosamine	Sigma
N-Acetyl-Glucosamine	Sigma
D-(+)Galactosamine hydrochloride	Sigma
o-Phosphoric acid	Merck
Phenol	Fluka

Potassium ferricyanide	Merck
Sodium chloride	Carl Roth GmbH
Sodium citrate	Sigma Aldrich
Sodium dodecyl sulfate (SDS)	Carl Roth GmbH
Sodium dihydrogen phosphate	Carl Roth GmbH
Starch	Sigma Aldrich
Sulfuric acid	Merck
Tetramethylethylenediamine (TEMED)	Sigma Aldrich
2-Amino-2-hydroxymethyl-propane-1,3-diol (Tris)	Carl Roth GmbH
Tryptic soy broth (TSB) = Caso Bouillon	Carl Roth GmbH
Yeast extract	Carl Roth GmbH
α-D (+)-Glucose monohydrate	Carl Roth GmbH
2,2'-azino-bis(3-ethylbenzthiazoline-6-sulphonic acid) (ABTS)	Sigma Aldrich
aluminum sulfate 18 hydrate	Merck
Coomassie Blue CBB G-250	Biorad
Ethanol	Carl Roth GmbH

8 Equipment

Equipment	Company
96-well plates	Carl Roth GmbH
AEKTA purifier	Amersham Pharmacia Biotech, Model
analytic balance	Sartorius 2004 MP
analytic balance	Sartorius laboratory
analytic balance	KERN 440-35A
analytic balance	Ohaus Adventurer Pro
autoclav	Varioklav hp-med.com
autoclav	Systec 50
BCA-Assay-Kit	EMD millipore chemicals
centrifuge	Eppendorf mini spin
centrifuge	Hermle Z2056A
centrifuge	Heraeus, Biofuge primo
ddH_2O supply	Barnstead NANOpure
drying oven	Memmert
electrophoresis power supply	BIO-RAD, PowerPAC 1000
electrophoresis power supply	BIO-RAD, PowerPac HV
filter (low protein binding)	Sartorius stedim syringe filters
filters- Acrodisc ® Premium (25mm Syringe Filter with 0.2 µm GHP membrane)	Pall life sciences
HPLC	Pump: Dionex UltiMate 3000 Autosampler: ASI 100 Automated Sample Injector Thermostated Column Compartment: Dionet UltiMate 3000 Column Compartement RI Detector: Shodex
ice machine	Elma Ziegra Eis Maschinen
lamina flow	Faster Ultra Safe
Luna NH_2 (Amino)-HPLC column	Phenomenex
magnetic stirrer	IKA RCT standard
mass spectrometer	Aglient 1100 Series LC/MSD Trap
multicolor High Range Protein Ladder	Thermo Scientific
peroxide sticks	Sigma Aldrich Quantofix Peroxide 25
peroxide sticks	Sigma Aldrich Quantofix Peroxide 100
pH-meter	METTLER TOLEDO, Seven Easy
photometer	HITACHI, Spectrophotometer U2001
pipette	Carl Roth GmbH
pipette	Socorex, ACURA 825
pipette	Gilson
plate reader	TECAN infinite M200
plate shaker	JANKE & KUNKEL, IKA, KS 250
scanner	HP Scanjet 4890
thermomixer	Eppendorf Thermomixer comfort
TLC sheets	Pre-coated TLC sheets ALUGRAM ® Xtra SIL G/UV254 with 60 Å mean pore size
ultrasonic	Transsonic DigitalS
vortex	JANKE & KUNKEL, IKA, vortex genius 3
zellutrans (nominal MWCO: 3,500, flat width: 46mm, wall thickness: 28µm, vol/cm: 6.74ml, diameter: 29.3mm)	Carl Roth

9 Appendix

Composition of the used buffers

Buffer	Properties	Chemical	Amount
Sodium phosphate	55 mM, pH 6.7	NaH_2PO_4	4.51 g
		Na_2HPO_4	5.99 g
		destilled water	fill up to 500 ml
Sodium phosphate	20 mM, pH 6.9 6.7 mM NaCl	NaH_2PO_4	1.32 g
		Na_2HPO_4	2.79 g
		NaCl	0.20 g
		destilled water	fill up to 500 ml
Sodium phosphate	500 mM, pH 7	NaH_2PO_4	29.18 g
		Na_2HPO_4	77.33 g
		destilled water	fill up to 500 ml
Sodium acetate	100 mM, pH 4	Acetic acid (99 %)	2.86 ml
		distilled water	400 ml
		NaOH	add until pH 4
		distilled water	fill up to 500 ml
Sodium acetate	200 mM, pH 4	Acetic acid (99 %)	5.72 ml
		distilled water	400 ml
		NaOH	add until pH 4
		distilled water	fill up to 500 ml

BCA

		Absorbance				Protein concentration [mg/ml]				
No.	sample name	1.	2.	3.	Average	1.	2.	3.	Average	standard deviation
1	Sa1_U_1e	1.5684	1.6559	1.6778	1.6340	1.5374	1.625	1.647	1.603	0.058
2	Sa1_D_1e	0.9849	1.0166	1.0348	1.0121	0.9539	0.986	1.004	0.981	0.025
3	Ec1_U_1e	1.9422	1.9583	2.0820	1.9942	1.9112	1.927	2.051	1.963	0.076
4	Ec1_D_1e	1.1682	1.8418	1.2580	1.4227	1.1372	1.811	1.227	1.392	0.366
5	Ec2_D_1e	1.1476	1.1124	1.1489	1.1363	0.694	0.670	0.695	0.686	0.014
6	Ec2_D_2e	1.0357	1.0342	1.0223	1.0307	0.618	0.617	0.609	0.615	0.005
7	Ec2_D_3e	0.7418	0.7277	0.7666	0.7454	0.418	0.408	0.435	0.420	0.013
8	Sa2_D_1e	0.9990	0.9409	0.9612	0.9670	0.593	0.553	0.567	0.571	0.020
9	Sa2_D_2e	0.6209	0.6109	0.6005	0.6108	0.335	0.329	0.322	0.329	0.007
10	Sa2_D_3e	0.4948	0.4911	0.4532	0.4797	0.25	0.247	0.221	0.239	0.016
11	Sa2_D_1e-b	0.8552	0.8115	0.8273	0.8313	0.495	0.465	0.476	0.479	0.015
12	Sa2_D_2e-b	0.6576	0.6358	0.6302	0.6412	0.36	0.346	0.342	0.349	0.010
13	Sa2_D_3e-b	0.5062	0.4996	0.4956	0.5005	0.257	0.253	0.25	0.253	0.004

Dubois

		Absorbance				Uronic acid concentration [mM]				
No	**Sample name**	**1.**	**2.**	**3.**	**Average**	**1.**	**2.**	**3.**	**Average**	**standard deviation**
1	Ec1_D_1e	0.6524	0.7031	0.6016	0.6524	1.03	1.09	0.97	1.03	0.32
2	Sa1_D_1e	0.3753	0.2107	0.3585	0.3148	0.70	0.51	0.68	0.63	0.37
3	Ec2_D_1e	0.2674	0.3706	0.1854	0.2745	0.58	0.70	0.48	0.59	0.37
4	Ec2_D_2e	0.1600	0.3729	0.1506	0.2278	0.45	0.70	0.44	0.53	0.41
5	Ec2_D_3e	0.2252	0.2574	0.2218	0.2348	0.53	0.57	0.52	0.54	0.29
6	Sa2_D_1e	0.7101	0.7207	0.3641	0.5983	1.09	1.11	0.69	0.96	0.50
7	Sa2_D_2e	0.3022	0.3378	0.3686	0.3362	0.62	0.66	0.70	0.66	0.30
8	Sa2_D_3e	0.2287	0.2170	0.2189	0.2215	0.53	0.52	0.52	0.52	0.27
9	Sa2_D_1e-b	0.9399	0.9401	0.8908	0.9236	1.36	1.36	1.31	1.34	0.30
10	Sa2_D_2e-b	0.4236	0.3985	0.3677	0.3966	0.76	0.73	0.69	0.73	0.30
11	Sa2_D_3e-b	0.2891	0.3280	0.2541	0.2904	0.60	0.65	0.56	0.60	0.31

Anthrone

		Absorbance				Sugar concentration [mM]				
No	**Sample name**	**1.**	**2.**	**3.**	**Average**	**1**	**2**	**3**	**Average**	**Standard deviation**
1	Sa1_D_1e	0.2394	0.2576	0.2553	0.2507	0.62	0.66	0.66	0.65	0.02
2	Ec1_D_1e	0.1693	0.2001	0.1603	0.1765	0.45	0.53	0.43	0.47	0.05
3	Ec2_D_1e	0.8327	0.5763	0.6085	0.6725	2.03	1.42	1.50	1.65	0.33
4	Ec2_D_2e	0.2572	0.2568	0.2321	0.2487	0.66	0.66	0.60	0.64	0.03
5	Ec2_D_3e	0.1101	0.1471	0.1368	0.1313	0.31	0.40	0.38	0.36	0.05
6	Sa2_D_1e	0.6736	0.6942	0.6787	0.6821	1.65	1.70	1.67	1.67	0.03
7	Sa2_D_2e	0.2122	0.2702	0.2378	0.2400	0.55	0.69	0.62	0.62	0.07
8	Sa2_D_3e	0.1439	0.1750	0.1401	0.1530	0.39	0.47	0.38	0.41	0.05
9	Sa2_D_1e-b	0.9897	0.8191	0.9004	0.9030	2.41	2.00	2.19	2.20	0.20
10	Sa2_D_2e-b	0.3303	0.3821	0.3601	0.3575	0.84	0.96	0.91	0.90	0.06
11	Sa2_D_3e-b	0.1617	0.2326	0.2239	0.2060	0.43	0.60	0.58	0.54	0.09

DNS-Assay

a)untreated EPS

No.	**Sample name**	**Average of Absorbance**	**Reducing Sugar [mM]**
1	Ec1_D_1e	0.082	0.314
2	Sa1_D_1e	0.075	0.281
3	Ec2_D_1e	0.073	0.273
4	Ec2_D_2e	0.070	0.258
5	Ec2_D_3e	0.069	0.253
6	Sa2_D_1e	0.078	0.296
7	Sa2_D_2e	0.071	0.260
8	Sa2_D_3e	0.069	0.251
9	Sa2_D_1e-b	0.083	0.321
10	Sa2_D_2e-b	0.072	0.267
11	Sa2_D_3e-b	0.074	0.275

b)Ec2_D_1e

No.	Sample Name	Measurement 1	Measurement 2	Dilution	Average	Reducing sugar [mM]	Reducing sugar [mM]
1	Ec2_D_1e+A-amyla-Nov	0.9764	1.0443	10	1.0103	4.87	48.69
2	Ec2_D_1e+A-amyla-Sig	0.2808	0.2462	-	0.2635	1.21	1.21
3	Ec2_D_1e+A-amyla-U	0.2315	0.2388	10	0.2351	1.07	10.67
4	Ec2_D_1e+Cellu-Sig	0.2467	0.2598	10	0.2532	1.16	11.56
5	Ec2_D_1e+Cellu-Flk	0.2851	0.3737	10	0.3294	1.53	15.29
6	Ec2_D_1e+Cellu-U	0.0824	0.0824	-	0.0824	0.32	0.32
7	Ec2_D_1e+Enz-mix-U	0.0853	0.0843	-	0.0848	0.33	0.33
8	Ec2_D_1e+B-gluc-U	0.2868	0.2912	4	0.2890	1.33	5.32
9	Ec2_D_1e+Mann-Nov	0.1582	0.1711	-	0.1646	0.72	0.72
10	Ec2_D_1e+Pulp-Nov	0.1786	0.1652	4	0.1719	0.76	3.03
11	Ec2_D_1e+Pect-Sig	0.0971	0.0955	-	0.0963	0.39	0.39
12	Ec2_D_1e+Lyso-Sig	0.0706	0.0735	-	0.0720	0.27	0.27

c)Sa2_D_1e

No.	Sample Name	Measurement 1	Measurement 2	Dilution	Average	Reducing sugar [mM]	Reducing sugar [mM]
1	Sa2_D_1e+A-amyla-Nov	0.5130	0.4728	20	0.4929	2.33	46.62
2	Sa2_D_1e+A-amyla-Sig	0.1826	0.1912	-	0.1869	0.83	0.83
3	Sa2_D_1e+A-amyla-U	0.2419	0.2856	10	0.2637	1.21	12.07
4	Sa2_D_1e+Cellu-Sig	0.2529	0.2274	10	0.2401	1.09	10.91
5	Sa2_D_1e+Cellu-Flk	0.3110	0.2994	10	0.3052	1.41	14.10
6	Sa2_D_1e+Cellu-U	0.0779	0.0812	-	0.0795	0.30	0.30
7	Sa2_D_1e+Enz-mix-U	0.0881	0.0933	-	0.0907	0.36	0.36
8	Sa2_D_1e+B-gluc-U	0.8537	0.8103	-	0.8320	3.99	3.99
9	Sa2_D_1e+Mann-Nov	0.1818	0.1557	-	0.1687	0.74	0.74
10	Sa2_D_1e+Pulp-Nov	0.7993	0.7411	-	0.7702	3.69	3.69
11	Sa2_D_1e+Pect-Sig	0.0783	0.0923	-	0.0853	0.33	0.33
12	Sa2_D_1e+Lyso-Sig	0.0764	0.0771	-	0.0767	0.29	0.29

d)Sa1_D_1e

No.	Sample Name	Measurement 1	Measurement 2	Dilution	Average	Reducing sugar [mM]	Reducing sugar [mM]
1	Sa1_D_1e+A-amyla-Nov	0.4695	0.4905	20	0.48	2.27	45.36
2	Sa1_D_1e+A-amyla-Sig	0.1746	0.2035	-	0.18905	0.84	0.84
3	Sa1_D_1e+A-amyla-U	0.2396	0.1857	10	0.21265	0.96	9.57
4	Sa1_D_1e+Cellu-Sig	0.2594	0.2721	10	0.26575	1.22	12.17
5	Sa1_D_1e+Cellu-Flk	0.4205	0.4052	10	0.41285	1.94	19.38
6	Sa1_D_1e+Cellu-U	0.0736	0.0731	-	0.07335	0.27	0.27
7	Sa1_D_1e+Enz-mix-U	0.0736	0.0826	-	0.0781	0.30	0.30
8	Sa1_D_1e+B-gluc-U	0.6563	0.6617	-	0.659	3.15	3.15
9	Sa1_D_1e+Mann-Nov	0.0828	0.0884	-	0.0856	0.33	0.33
10	Sa1_D_1e+Pulp-Nov	0.8457	0.7507	-	0.7982	3.83	3.83
11	Sa1_D_1e+Pect-Sig	0.1337	0.0759	-	0.1048	0.43	0.43
12	Sa1_D_1e+Lyso-Sig	0.0746	0.074	-	0.0743	0.28	0.28

e)Ec1_D_1e

No.	Sample Name	Measurement 1	Measurement 2	Dilution	Average	Reducing sugar [mM]	Reducing sugar [mM]
1	Ec1_D_1e+A-amyla-Nov	1.2079	1.3795	20	1.2937	6.26	125.17
2	Ec1_D_1e+A-amyla-Sig	0.2135	0.1956	-	0.20455	0.92	0.92
3	Ec1_D_1e+A-amyla-U	0.2621	0.2335	10	0.2478	1.13	11.29
4	Ec1_D_1e+Cellu-Sig	0.6458	0.6721	10	0.65895	3.15	31.45
5	Ec1_D_1e+Cellu-Flk	0.3489	0.2984	20	0.32365	1.50	30.02
6	Ec1_D_1e+Cellu-U	0.0733	0.0723	-	0.0728	0.27	0.27
7	Ec1_D_1e+Enz-mix-U	0.0877	0.0832	-	0.08545	0.33	0.33
8	Ec1_D_1e+B-gluc-U	0.5244	0.4837	-	0.50405	2.39	2.39
9	Ec1_D_1e+Mann-Nov	0.1359	0.1145	-	0.1252	0.53	0.53
10	Ec1_D_1e+Pulp-Nov	0.8596	0.8607	-	0.86015	4.13	4.13
11	Ec1_D_1e+Pect-Sig	0.0845	0.0864	-	0.08545	0.33	0.33
12	Ec1_D_1e+Lyso-Sig	0.0714	0.0708	-	0.0711	0.26	0.26

f)Sa1_D_1e-Ek

No.	Sample	Measurement 1	Measurement 2	Dilution	Average	Reducing sugar [mM]	Reducing sugar [mM]
1	Sa1_D_1e-Ek1	1.1271	1.0114	20	1.069	5.16	103.15
2	Sa1_D_1e-Ek2	1.2982	1.4123	20	1.355	6.56	131.21
3	Sa1_D_1e-Ek3	1.1999	1.0796	20	1.140	5.50	110.07
4	Sa1_D_1e-Ek4	1.1449	0.8975	20	1.021	4.92	98.44
5	Sa1_D_1e-Ek5	1.0203	0.9958	20	1.008	4.86	97.15
6	Sa1_D_1e-Ek6	0.6185	1.0566	20	0.838	4.02	80.43
7	Sa1_D_1e-Ek7	1.2285	1.2317	10	1.230	5.95	59.47
8	Sa1_D_1e-Ek8	1.107		2	1.107	5.34	5.34
9	Sa1_D_1e-Ek9	0.2068		unv	0.207	0.93	0.93
10	Sa1_D_1e-Ek10	0.5737		unv	0.574	2.73	2.73

g)Ec1_D_1e-Ek

No.	Sample	Measurement 1	Measurement 2	Dilution	Average	Reducing sugar [mM]	Reducing sugar [mM]
1	Ec1_D_1e-Ek1	0.497	0.511	100	0.504	2.38	238.38
2	Ec1_D_1e-Ek2	0.749	0.739	50	0.744	3.56	178.04
3	Ec1_D_1e-Ek3	1.004	1.077	50	1.040	5.02	250.80
4	Ec1_D_1e-Ek4	0.580	0.520	50	0.550	2.61	130.58
5	Ec1_D_1e-Ek5	0.744	0.608	50	0.676	3.23	161.49
6	Ec1_D_1e-Ek6	0.306	0.283	10	0.294	1.36	13.57
7	Ec1_D_1e-Ek7	0.352	0.181	10	0.267	1.22	12.21
8	Ec1_D_1e-Ek8	0.202	0.177	10	0.189	0.84	8.42
9	Ec1_D_1e-Ek9	0.078	0.084	10	0.081	0.31	3.10
10	Ec1_D_1e-Ek10	0.069	0.072	10	0.070	0.26	2.58

h)DNS enzyme blanks

No.	Enzyme Blank	Measurement	Reducing sugar [mM]
1	A-amyla-Nov	1.664	8.10
2	A-amyla-Sig	0.1882	0.59
3	A-amyla-U	2.7052	12.93
4	Cellu-Sig	0.9763	4.45
5	Cellu-Flk	0.9193	4.17
6	Cellu-U	0.0727	0.02
7	Enz-mix-U	0.099	0.15
8	B-Gluc-U	1.2544	5.82
9	Mann-Nov	0.1441	0.37
10	Pulp-Nov	0.7017	3.11
11	Pect-Sig	0.0782	0.05
12	Lyso-Sig	0.0689	0.00

Dubois

No.	Sample Name	Measurements			Average	Standard deviation	Uronic acid [mM]
		1.	2.	3.			
1	Ec1_D_1e	0.652	0.651	0.703	0.602	0.072	1.02
2	Sa1_D_1e	0.315	0.375	0.211	0.359	0.091	0.69
3	Ec2_D_1e	0.267	0.371	0.185	0.275	0.093	0.64
4	Ec2_D_2e	0.160	0.373	0.151	0.228	0.126	0.59
5	Ec2_D_3e	0.225	0.257	0.222	0.235	0.020	0.59
6	Sa2_D_1e	0.710	0.721	0.364	0.598	0.203	1.02
7	Sa2_D_2e	0.302	0.338	0.369	0.336	0.033	0.71
8	Sa2_D_3e	0.229	0.217	0.219	0.222	0.006	0.58
9	Sa2_D_1e-b	0.940	0.940	0.891	0.924	0.028	1.40
10	Sa2_D_2e-b	0.424	0.399	0.368	0.397	0.028	0.78
11	Sa2_D_3e-b	0.289	0.328	0.254	0.290	0.037	0.66

HPLC-RI

a)Sugar Standards measured at 130 bar

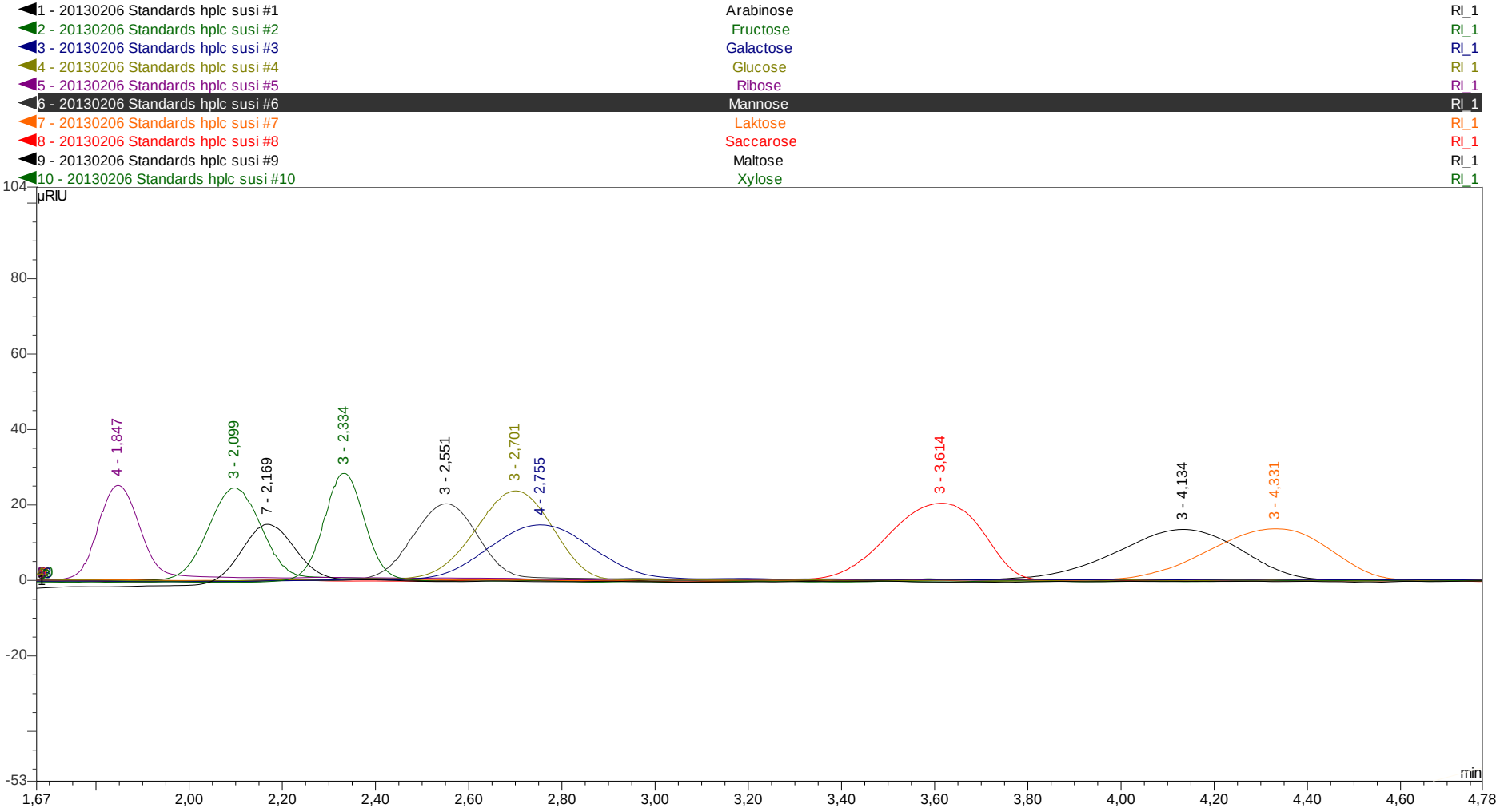

b)Sugar Standards measured at 130 bar

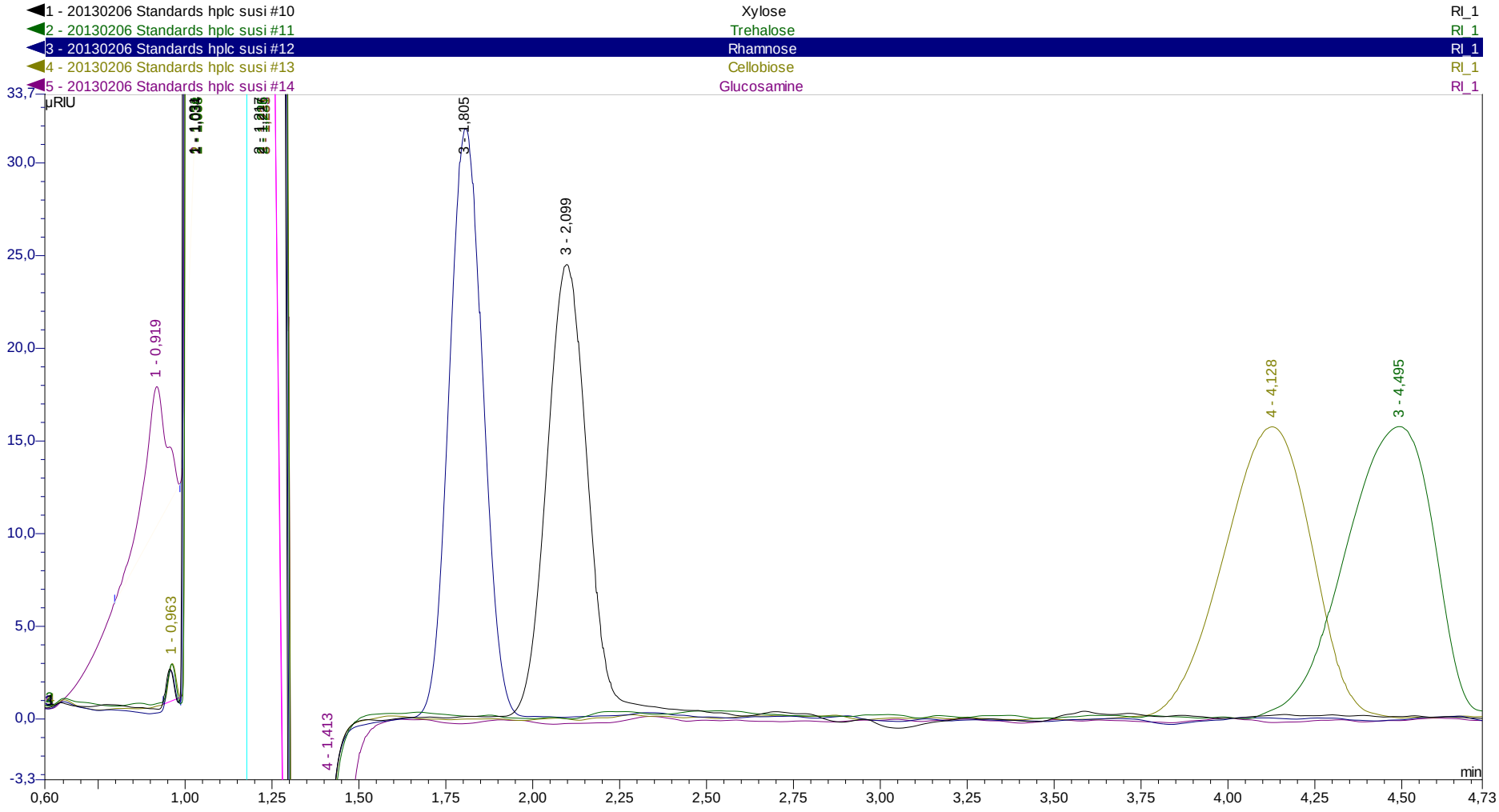

c) HPLC analysis of Sa_D_1e+A-amyla-Nov at t_0 and t_1

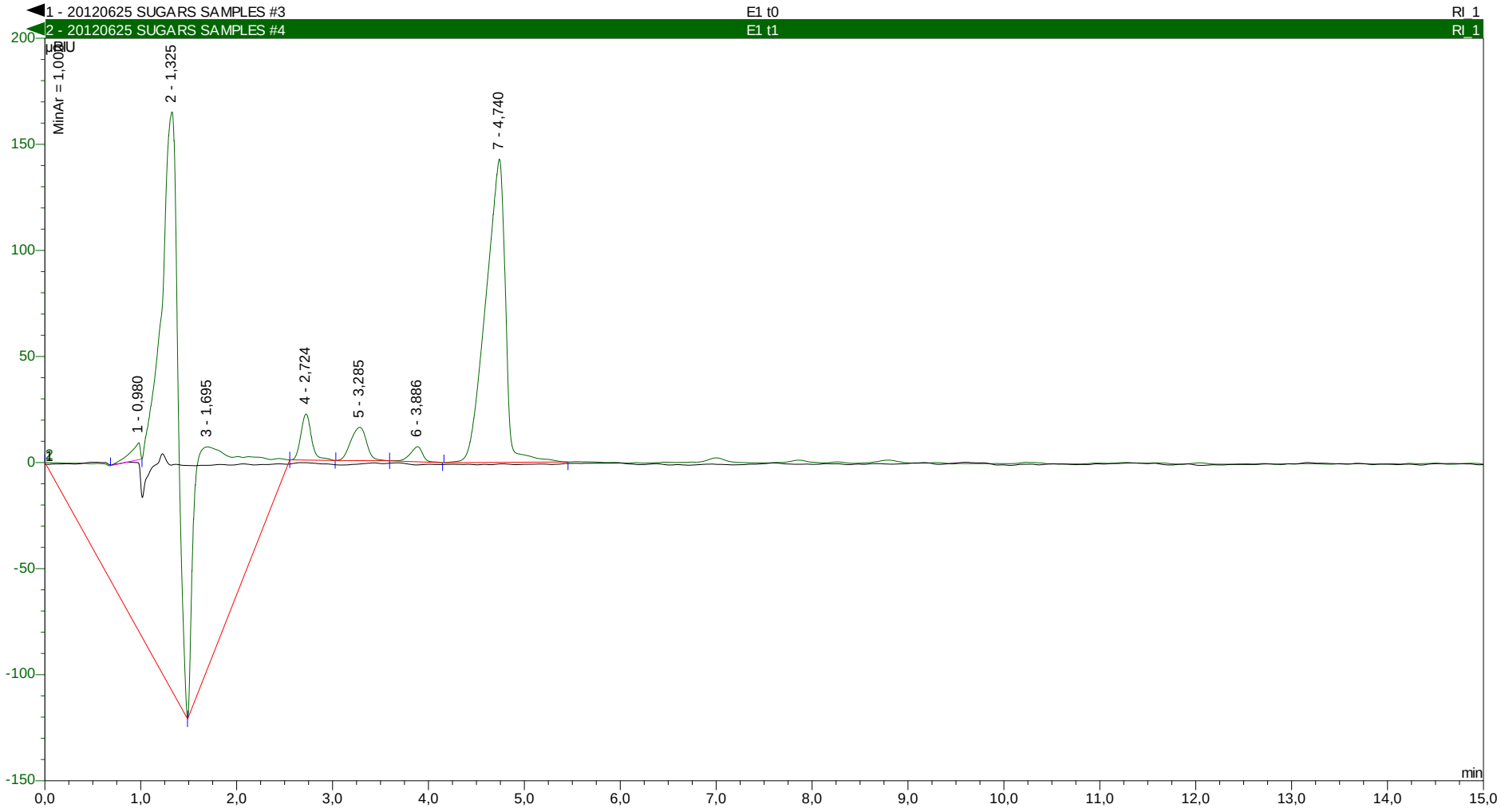

d)HPLC analysis of Sa_D_1e+Cellu-Sig at t_0 and t_1

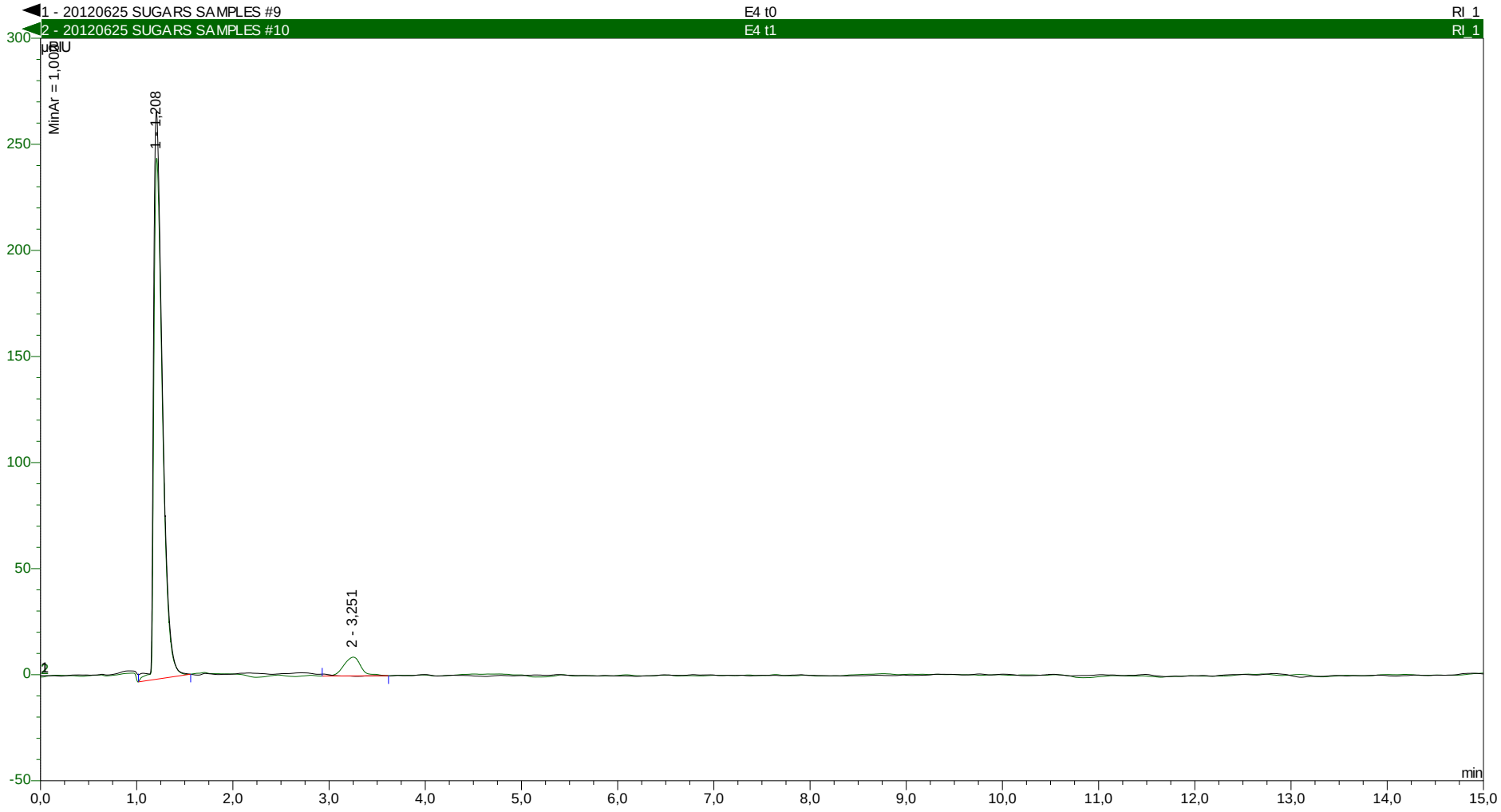

e)HPLC analysis of Sa_D_1e+Enz-Mix-U at t_0 and t_1

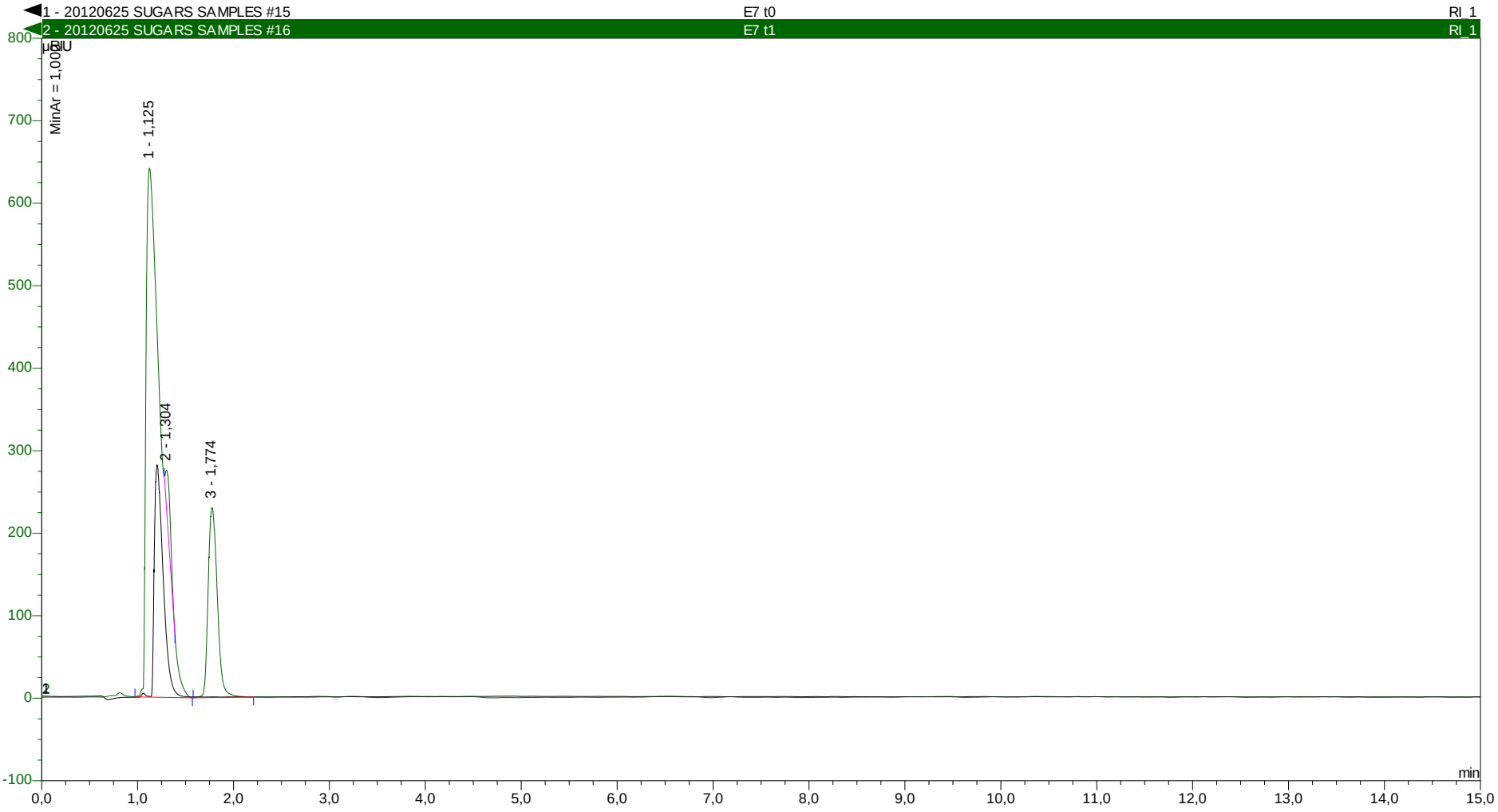

f)HPLC analysis of the Sa_D_1e+Cellu-Flk at t_0 and t_1

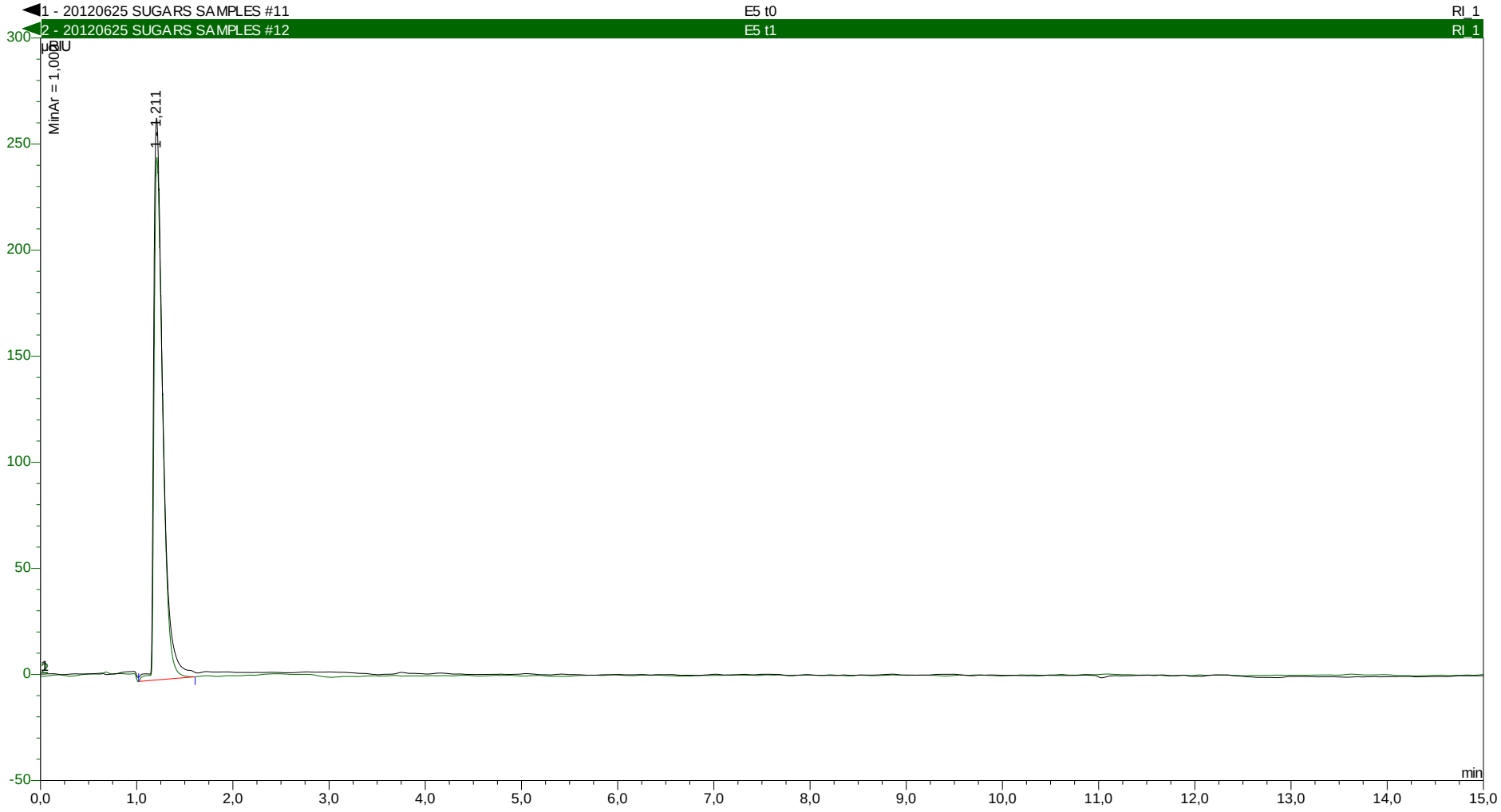

g)HPLC analysis of the Sa_D_1e+B-Gluc-U at t_0 and t_1

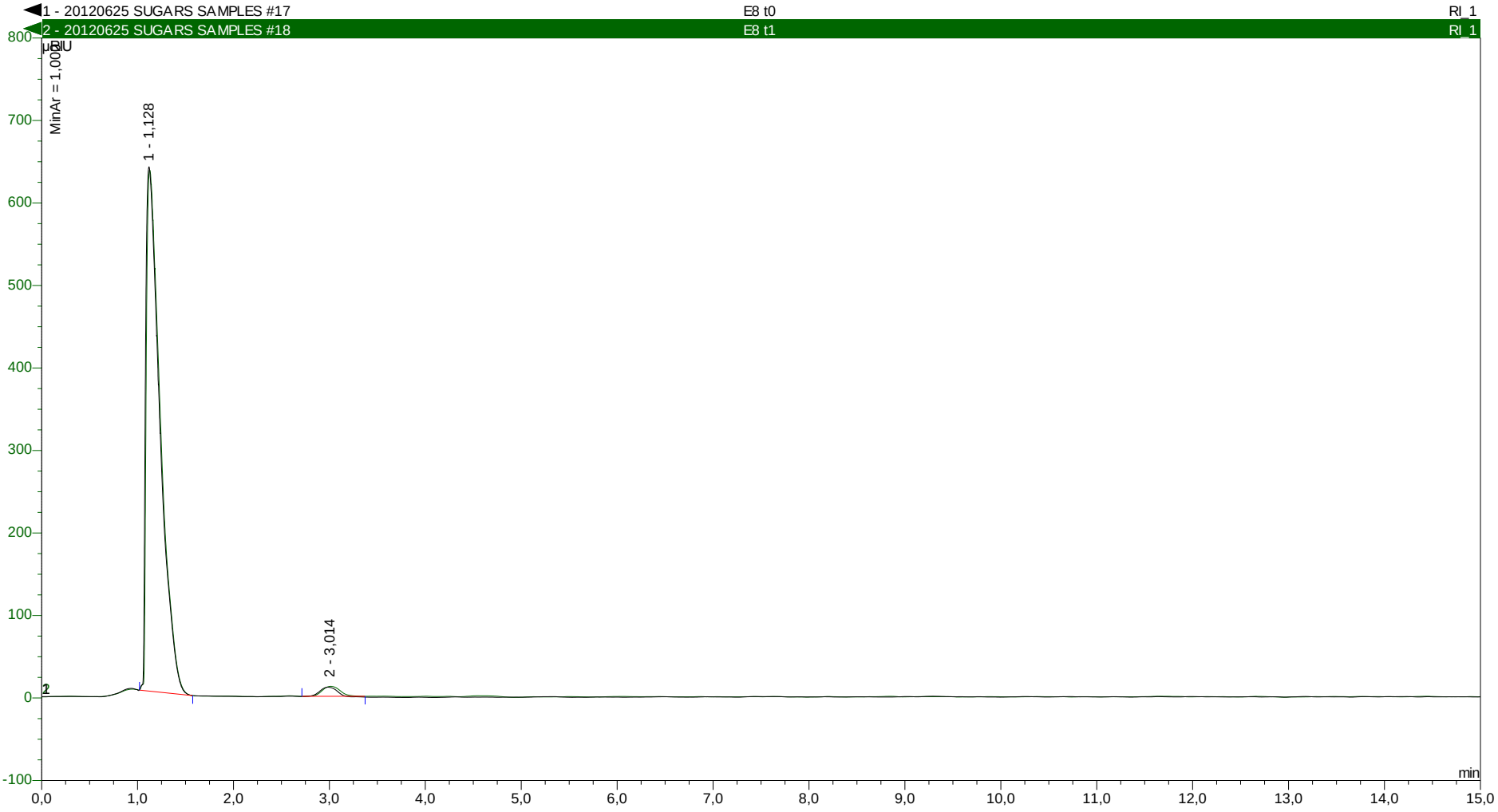

h)HPLC analysis of Sa1_D_1e+A-amyla-Nov (+CDH) and the enzyme only (+CDH)

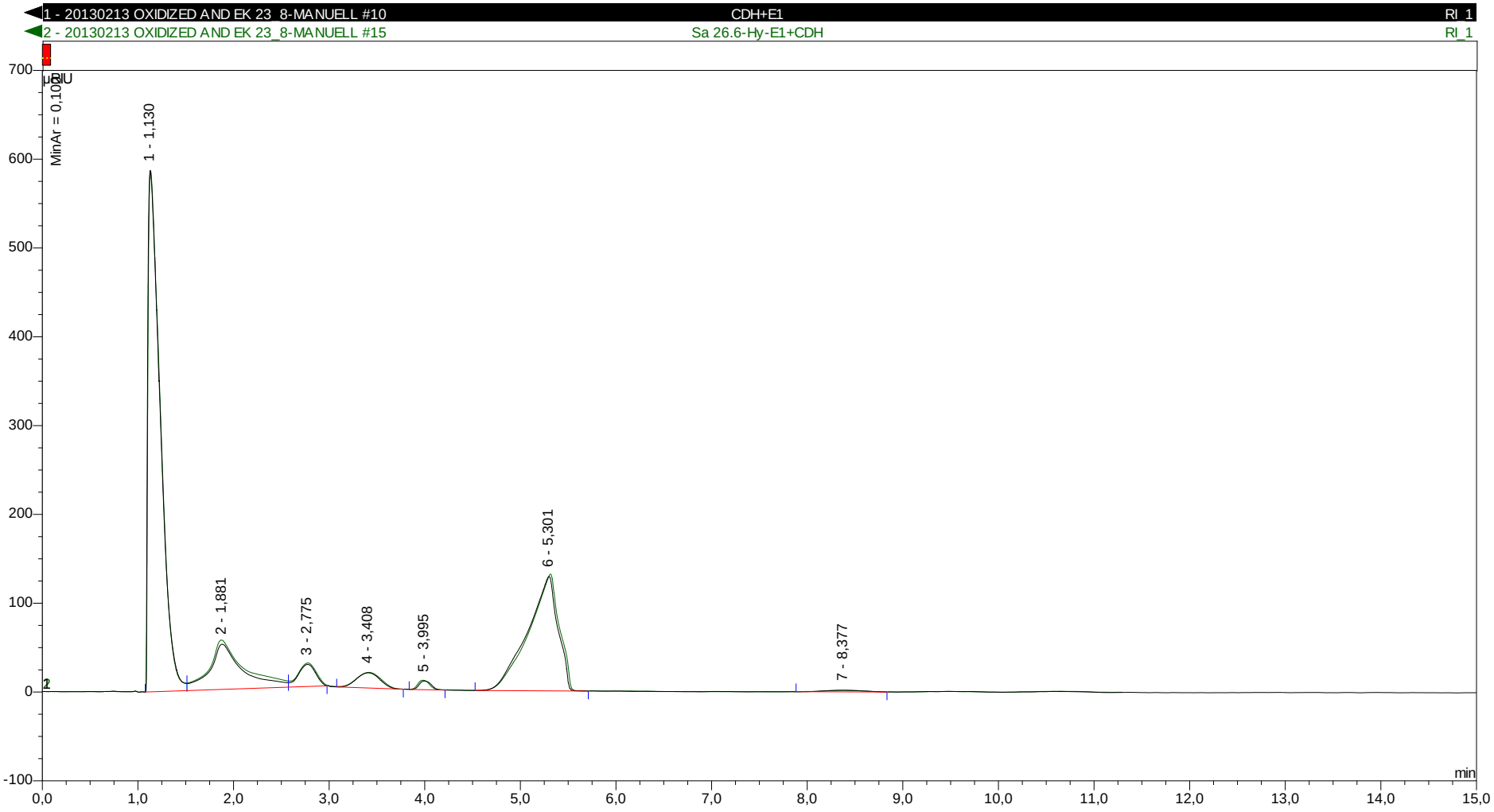

HPLC/MS

a)Sa1_D_1e + Alpha amylase from *Bacillus amyloliquefaciens* (Sigma): peak 1

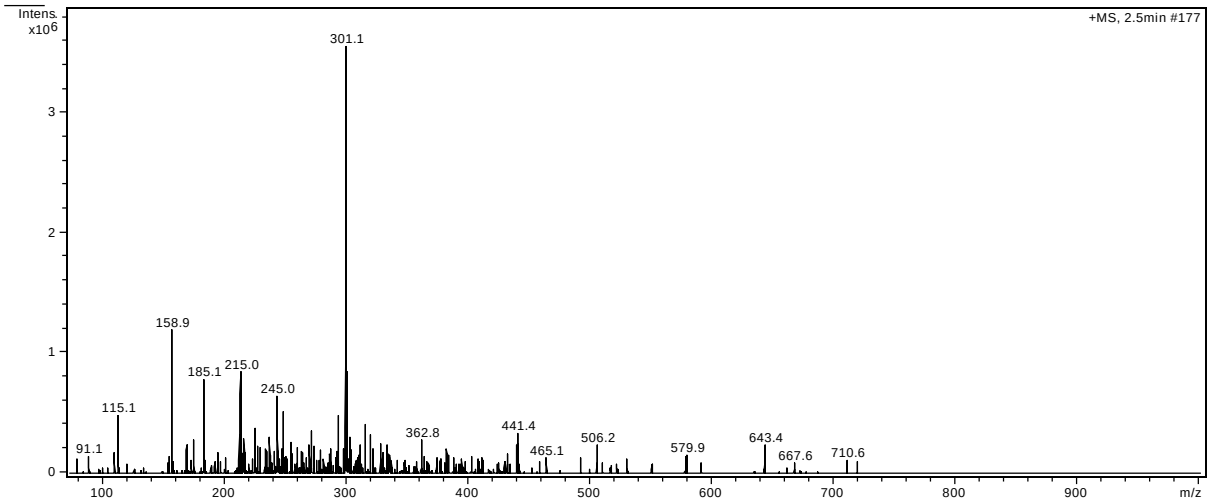

b)Sa1_D_1e + Alpha amylase of *Bacillus amyloliquefaciens* (Sigma): peak 2

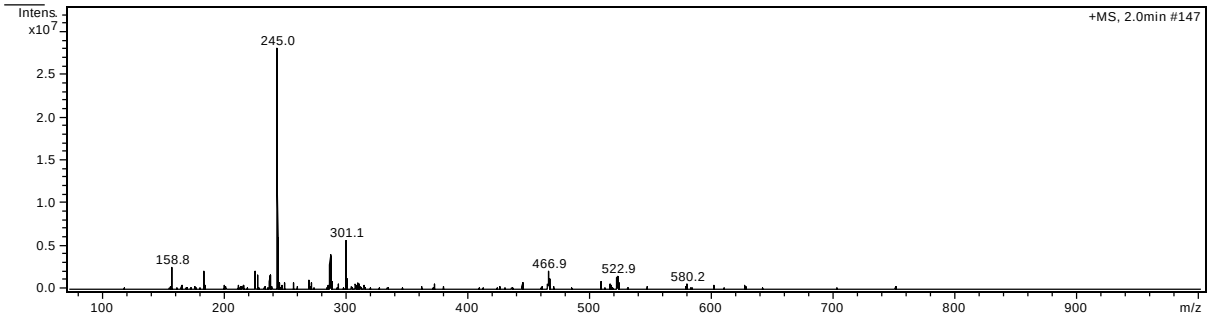

c)Sa1_D_1e + Alpha amylase (Unk.): peak 1

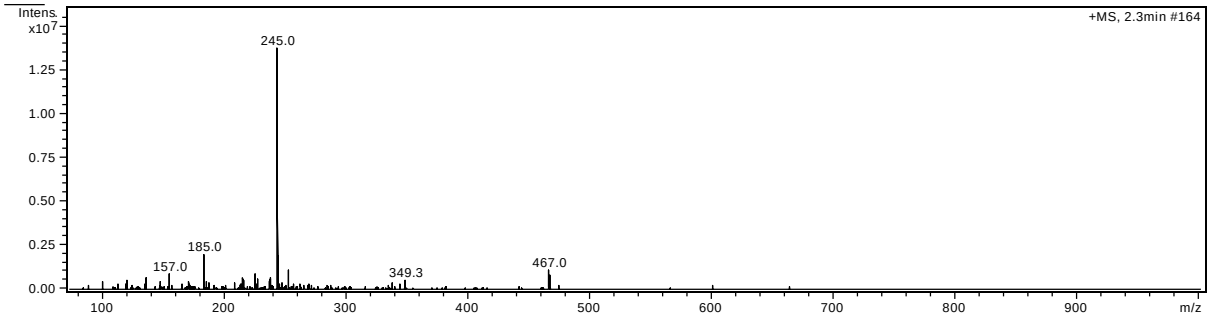

d)Sa1_D_1e + Alpha amylase (Unk.): peak 2 _1

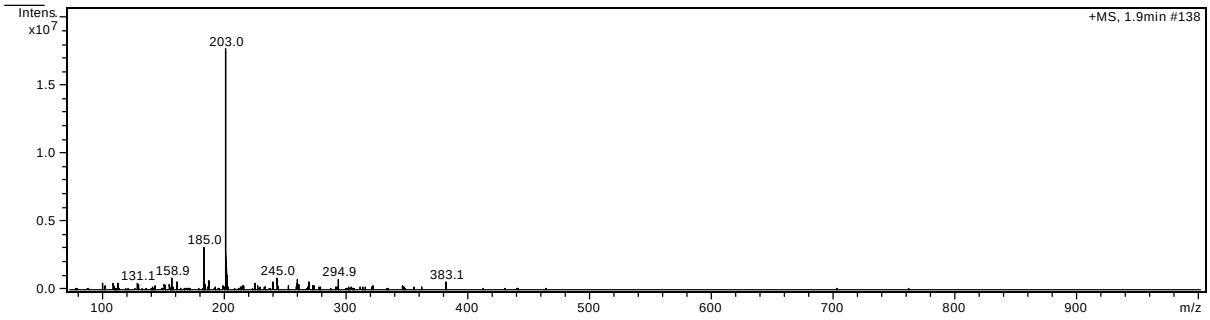

e)Sa1_D_1e + Alpha amylase (Unk.): peak 2_2

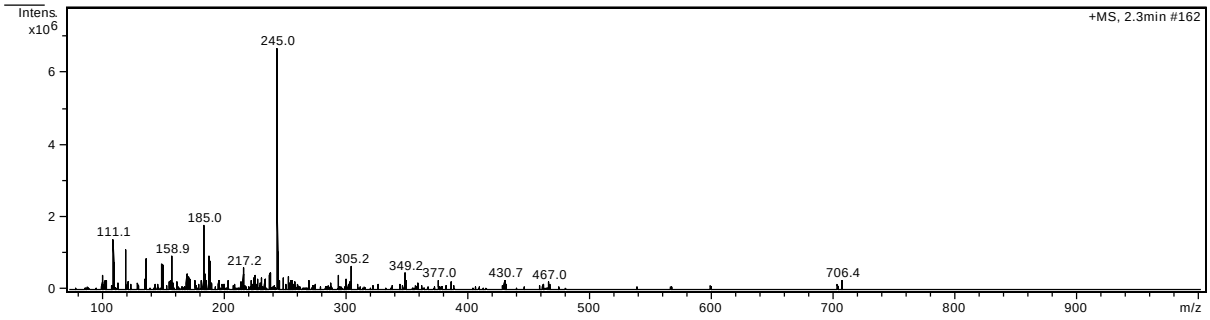

f)Sa1_D_1e + Alpha amylase (Unk.): peak 3:_1

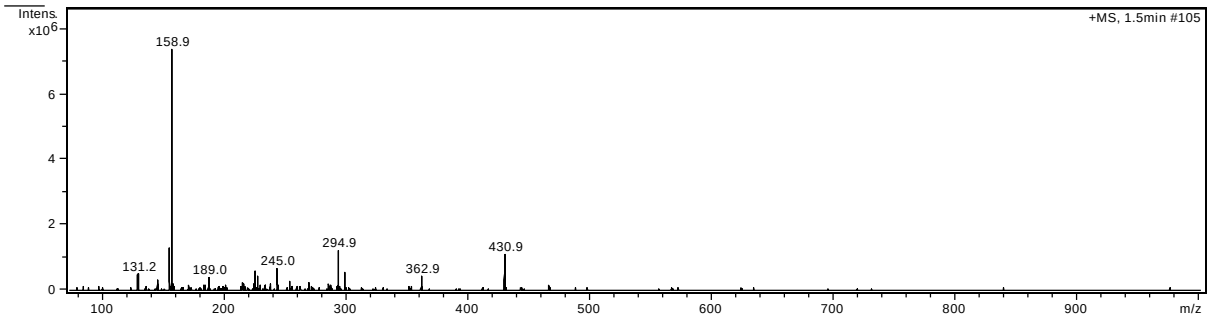

g)Sa1_D_1e + Alpha amylase (Unk.): peak 3_2

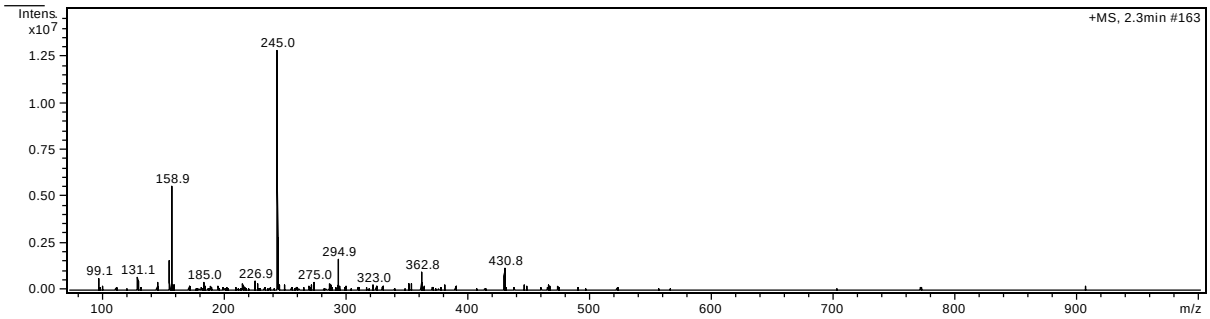

h)Sa1_D_1e + Alpha amylase (Unk.): peak 4_1

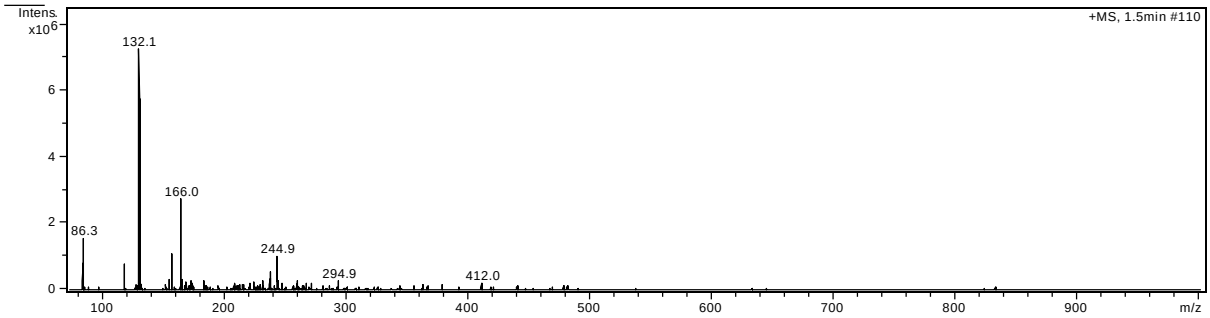

i)Sa1_D_1e + Alpha amylase (Unk.): peak 4_2

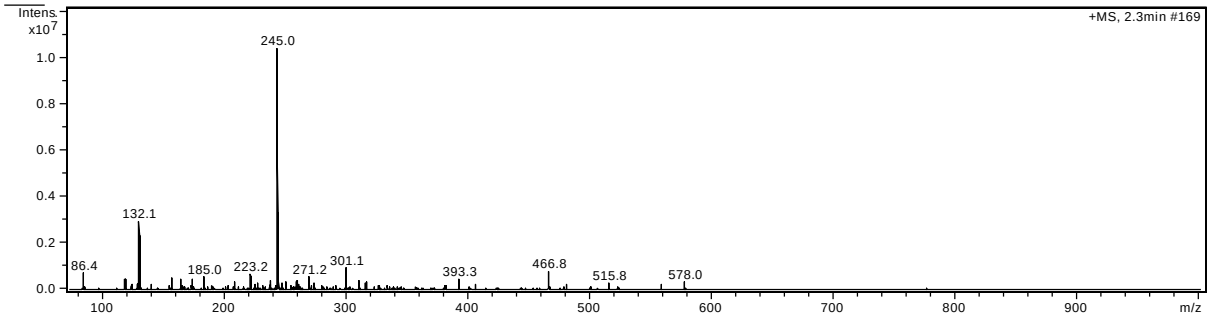

j)Sa1_D_1e + Alpha amylase (Unk.): peak 5

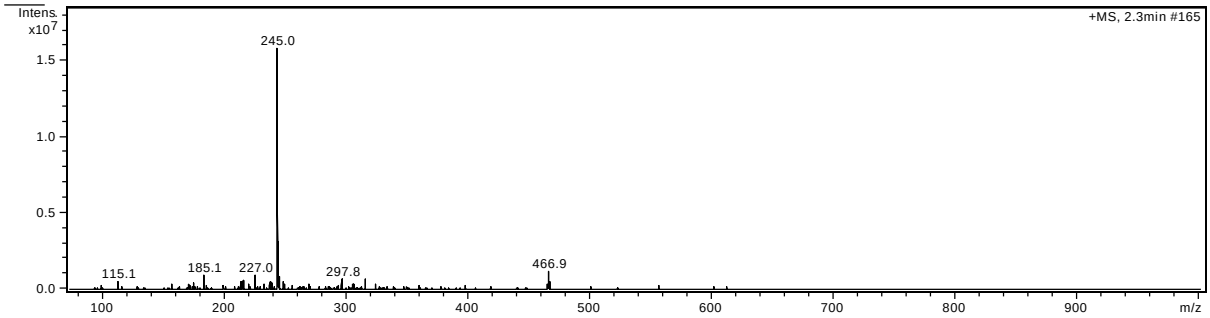

k)Sa1_D_1e + Alpha amylase (Unk.): peak 6

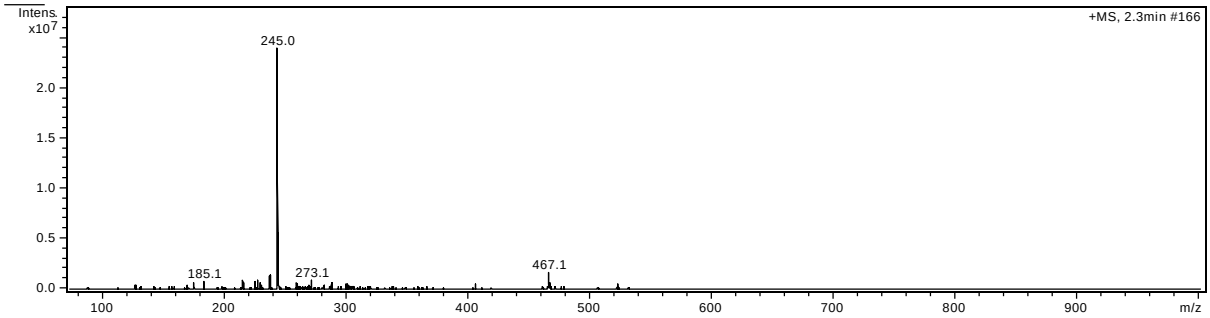

l)Sa1_D_1e + Alpha amylase (Unk.): peak 7

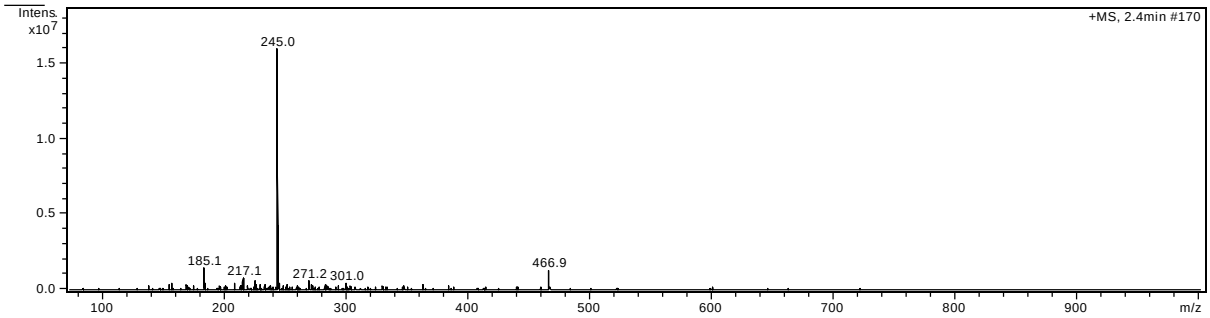

m)Sa1_D_1e + Alpha amylase (Unk.): peak 8

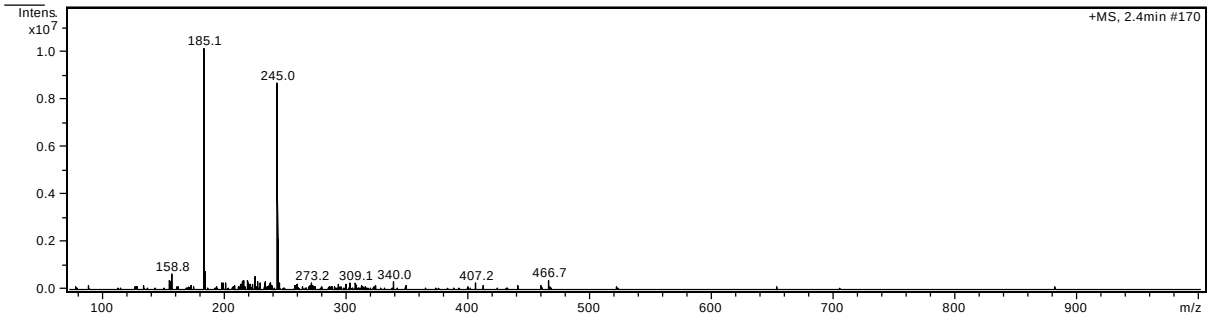

n)Sa1_D_1e + Cellulase from *Aspergillus niger* (Sigma) peak 1

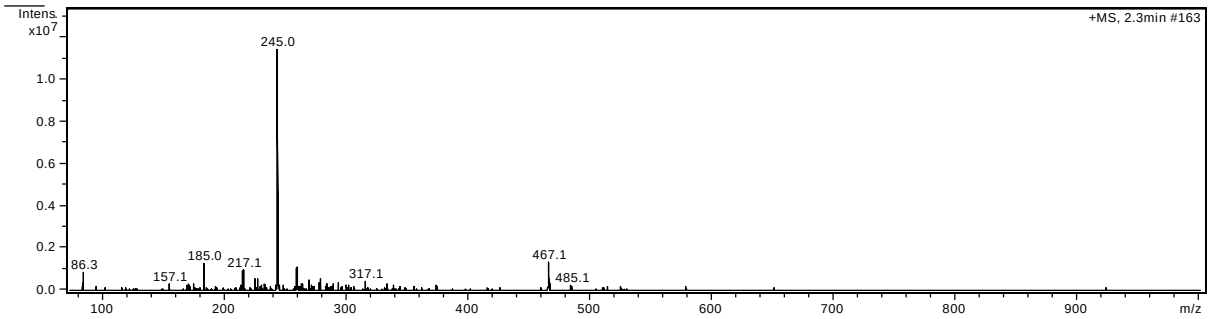

o)Sa1_D_1e + Cellulase from *Aspergillus niger* (Sigma) peak 2

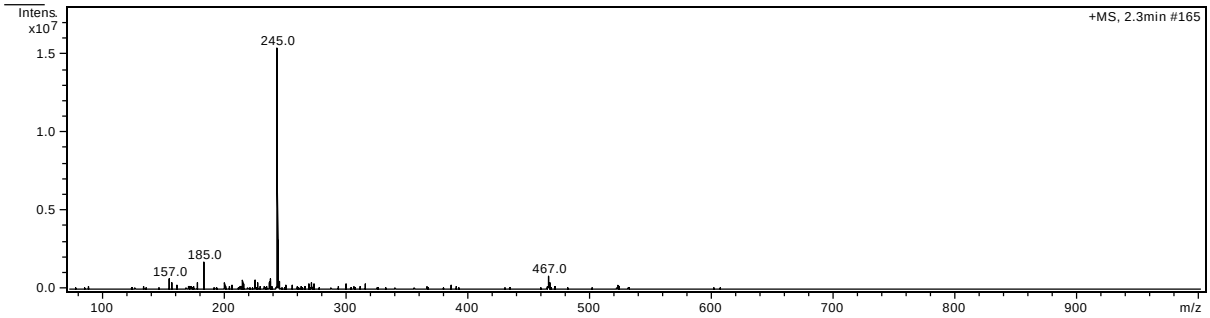

p)Sa1_D_1e + Cellulase from *Aspergillus niger* (Sigma) peak 3

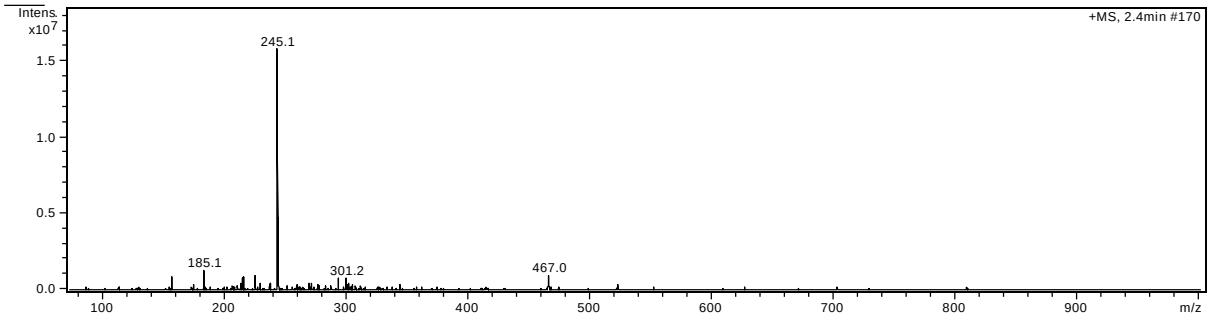

q)Sa1_D_1e + Cellulase from *Aspergillus niger* (Sigma) peak 4

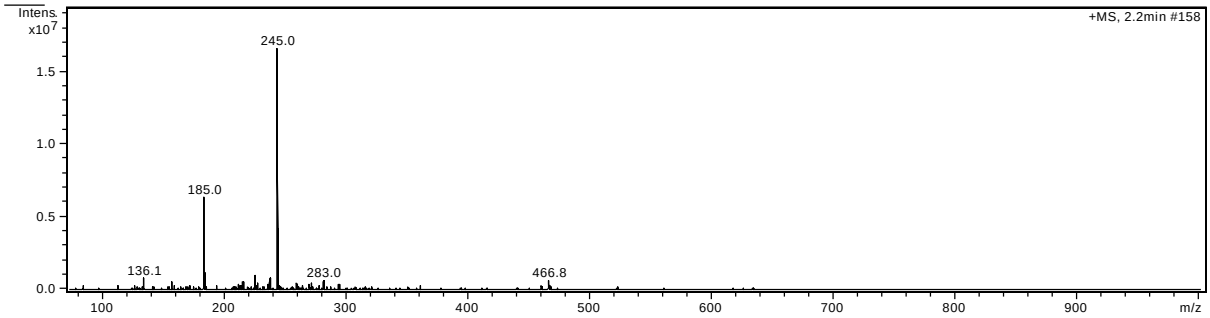

r)Sa1_D_1e + Cellulase from *Aspergillus niger* (Sigma) peak 5

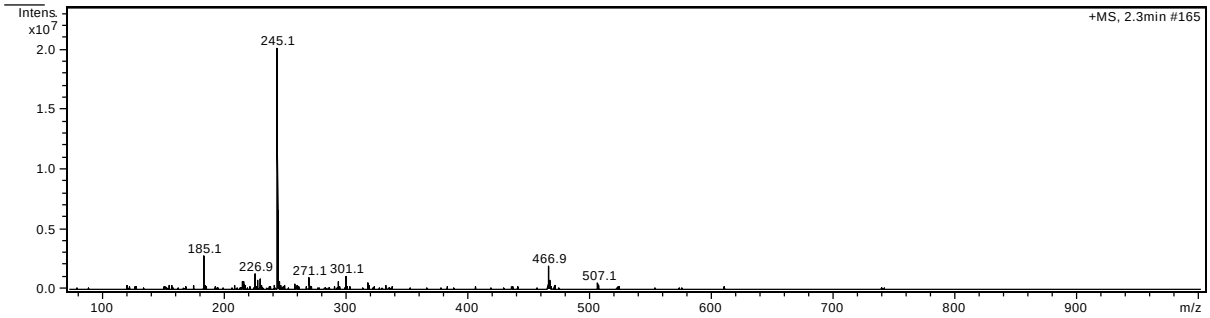

TLC

a)TLC plate I and II- Sa1_D_1e

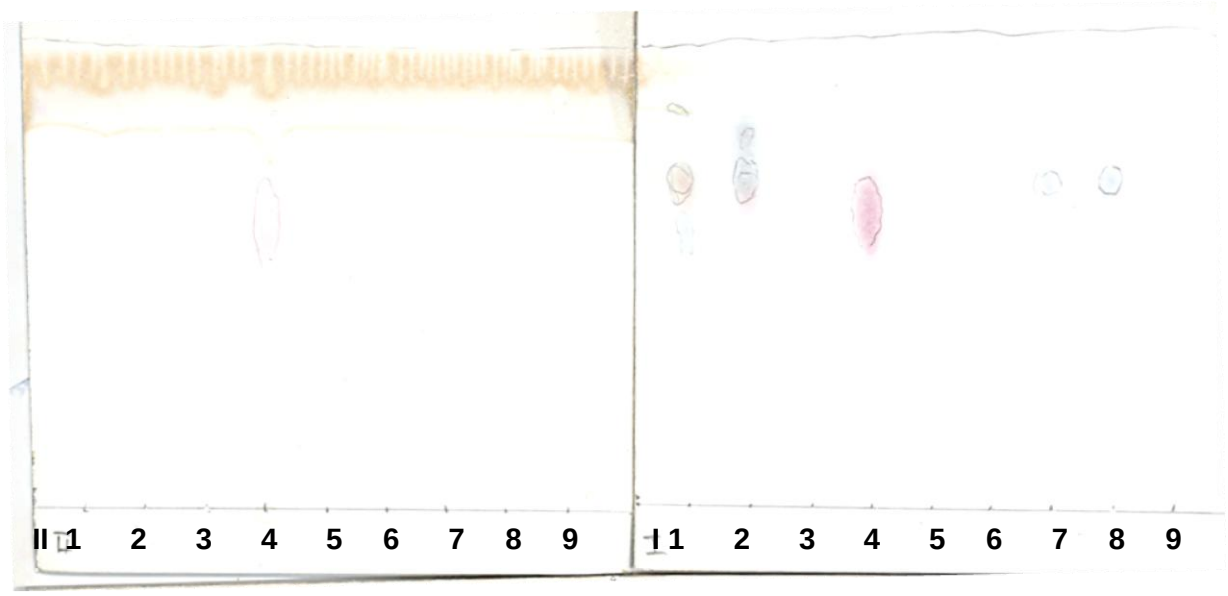

Plate I			
No.	**Sample Name**	**Rf-value**	**Color**
1	STD I	0.857	green
1	STD I	0.714	green
1	STD I	0.675	red
2	STD I	0.545	blue-grey
2	STDII	0.805	blue-grey
2	STDII	0.740	blue-grey
2	STDII	0.675	red
3	Blank SA		
4	Sa1_D_1e+A-amyla-Nov 1:20	0.649	red
5	Sa1_D_1e+A-amyla-Sig		
6	Sa1_D_1e+A-amyla-U		
7	Sa1_D_1e+Cellu-Sig	0.714	blue-grey
8	Sa1_D_1e+Cellu-Flk	0.727	blue-grey
9	Sa1_D_1e+Cellu-U		
Plate II			
1	Sa1_D_1e+Enz-mix-U		
2	Sa1_D_1e+B-Gluc-U		
3	Sa1_D_1e+Mann-Nov		
4	Sa1_D_1e+Pulp-Nov	0.623	red
5	Sa1_D_1e+Pect-Sig		
6	Sa1_D_1e+Lyso-Sig		

b)TLC plate III and IV

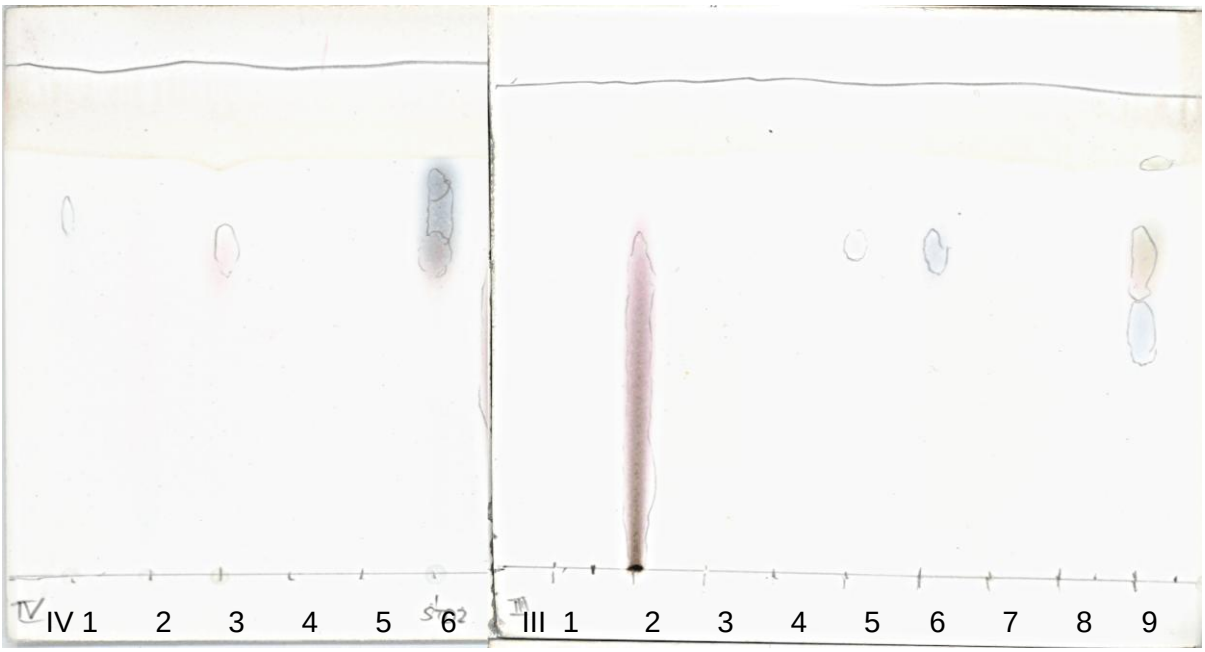

Plate III			
No.	**Sample Name**	**Rf-value**	**Color**
1	Ec1_D_1e-EPS		
2	Ec1_D_1e+A-amyla-Nov		
3	Ec1_D_1e+A-amyla-Sig		
4	Ec1_D_1e+A-amyla-U		
5	Ec1_D_1e+Cellu-Sig	0.662	blue-grey
6	Ec1_D_1e+Cellu-Flk	0.662	blue-grey
7	Ec1_D_1e+Cellu-U		
8	EC1_D_1e+Enz-mix-U		
9	STD I	0.844	green
9	STD I	0.688	green
9	STD I	0.623	red
9	STD I	0.506	blue-grey
Plate IV			
1	Ec1_D_1e B-Gluc-U	0.709	light grey
2	Ec1_D_1e+Mann-Nov		
3	Ec1_D_1e+Pulp-Nov	0.646	red
4	Ec1_D_1e+Pect-Sig		
5	Ec1_D_1e+Lyso-Sig		
6	STD II	0.772	blue-grey
6	STD II	0.709	blue-grey
6	STD II	0.633	red

* no clear spot due to high sugar concentrations

c)TLC plate V

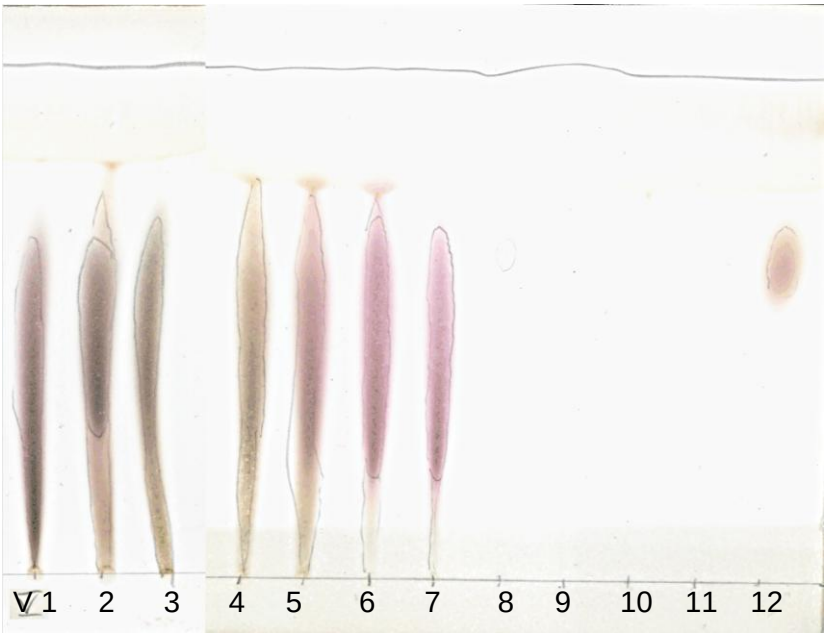

Plate V No.	Sample Name	Rf-value	Color
1	Sa1_D_1e-Ek1		
2	Sa1_D_1e-Ek2		
3	Sa1_D_1e-Ek3		
4	Sa1_D_1e-Ek4		
5	Sa1_D_1e-Ek5	0.633	
6	Sa1_D_1e-Ek6		
7	Sa1_D_1e-Ek7		
8	Sa1_D_1e-Ek8		light grey
9	Sa1_D_1e-Ek9	0.620	
10	Sa1_D_1e-Ek10		
11	Sa1_D_1e-Ek EPS		
12	Fructose	0.620	red

* no clear spot due to high sugar concentrations

d)TLC plate VII and VI

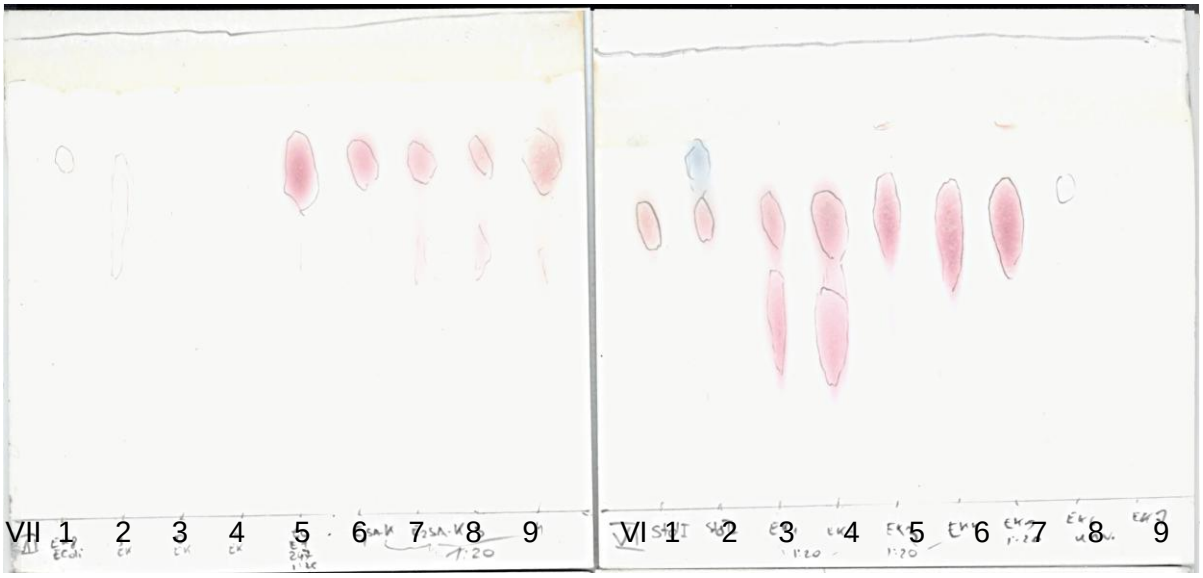

Plate VI			
No.	**Sample Name**	**Rf-value**	**Color**
1	STD I	0.813	green
1	STD I	0.675	green
1	STD I	0.625	red
2	STD II	0.775	light grey
2	STD II	0.713	light grey
2	STD II	0.625	red
3	Ec1_D_1e-Ek1	0.638	red
3	Ec1_D_1e-Ek1	0.413	red
4	Ec1_D_1e-Ek2	0.625	red
4	Ec1_D_1e-Ek2	0.400	red
5	Ec1_D_1e-Ek3	0.713	red
6	Ec1_D_1e-Ek4	0.613	red
7	Ec1_D_1e-Ek5	0.613	red
8	Ec1_D_1e-Ek6	0.688	light grey
9	Ec1_D_1e-Ek7		
Plate VII			
1	Ec1_D_1e-Ek8	0.708	light grey
2	Ec1_D_1e-Ek9	0.640	red
3	Ec1_D_1e-Ek10		
4	Ec1_D_1e-Ek11		
5	Sa1_D_1e-A-amyla-Nov 1:20*	0.685	light grey
6	Sa1_D_1e-Ek1 1:20*	0.697	red
7	Sa1_D_1e-Ek2 1:20*	0.697	red
8	Sa1_D_1e-Ek3 1:20*	0.697	red
9	Sa1_D_1e-Ek4 1:20*	0.685	red

* no clear spot due to high sugar concentrations

e)TLC plate VIII and IX

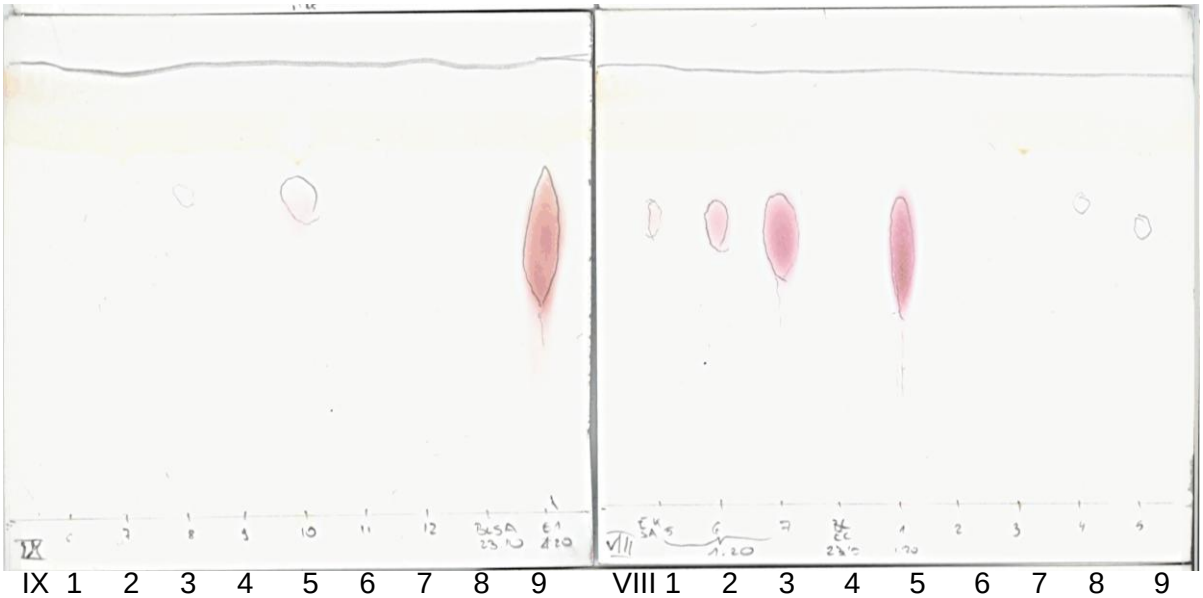

Plate VIII			
No.	**Sample Name**	**Rf-value**	**Color**
1	Sa1_D_1e-Ek5 1:20*	0.646	red
2	Sa1_D_1e-Ek6 1:20*	0.633	red
3	Sa1_D_1e-Ek7 1:20*	0.608	red
4	Sa2_D_1e-EPS		
5	Sa2_D_1e+A-amyla-Nov	0.532	red
6	Sa2_D_1e+A-amyla-Sig		
7	Sa2_D_1e+A-amyla-U		
8	Sa2_D_1e+Cellu-Sig	0.677	grey
9	Sa2_D_1e+Cellu-Flk	0.620	grey
Plate IX			
1	Sa2_D_1e+Cellu-U		
2	Sa2_D_1e+Enz-mix-U		
3	Sa2_D_1e B-Gluc-U	0.710	light grey
4	Sa2_D_1e+Mann-Nov		
5	Sa2_D_1e+Pulp-Nov	0.679	red
6	Sa2_D_1e+Pect-Sig		
7	Sa2_D_1e+Lyso-Sig		
8	Ec2_D_1e-EPS		
9	Ec2_D_1e+A-amyla-Nov	0.605	red

* no clear spot due to high sugar concentrations

f)TLC plate X

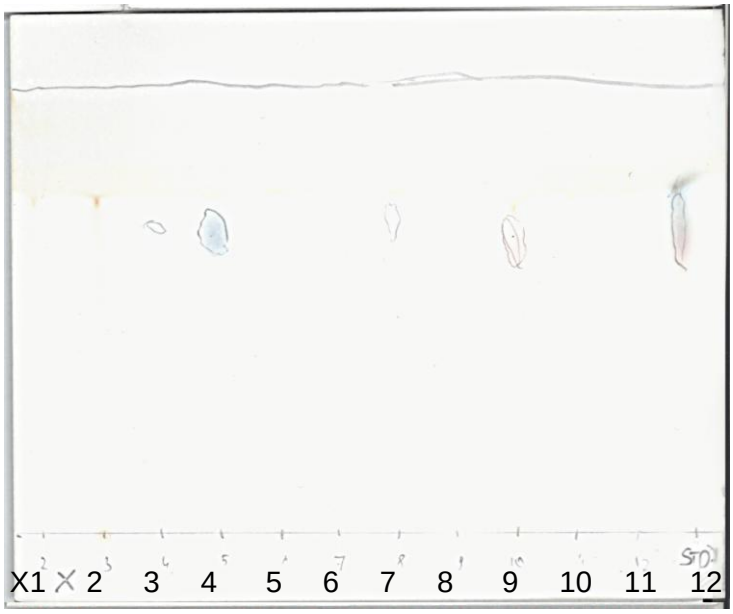

Plate X			
No.	**Sample**	**Rf-value**	**Color**
1	Ec2_D_1e+A-amyla-Sig		
2	Ec2_D_1e+A-amyla-U		
3	Ec2_D_1e+Cellu-Sig	0.684	grey
4	Ec2_D_1e+Cellu-Flk	0.671	grey
5	Ec2_D_1e+Cellu-U		
6	Ec2_D_1e+Enz-mix-U		
7	Ec2_D_1e B-Gluc-U	0.697	grey
8	Ec2_D_1e+Mann-Nov		
9	Ec2_D_1e+Pulp-Nov	0.658	red
10	Ec2_D_1e+Pect-Sig		
11	Ec2_D_1e+Lyso-Sig		
12	STD II	0.776	light grey. red
12	STD II	0.711	light grey
12	STD II	0.632	red

Staining-size exclusion chromatography

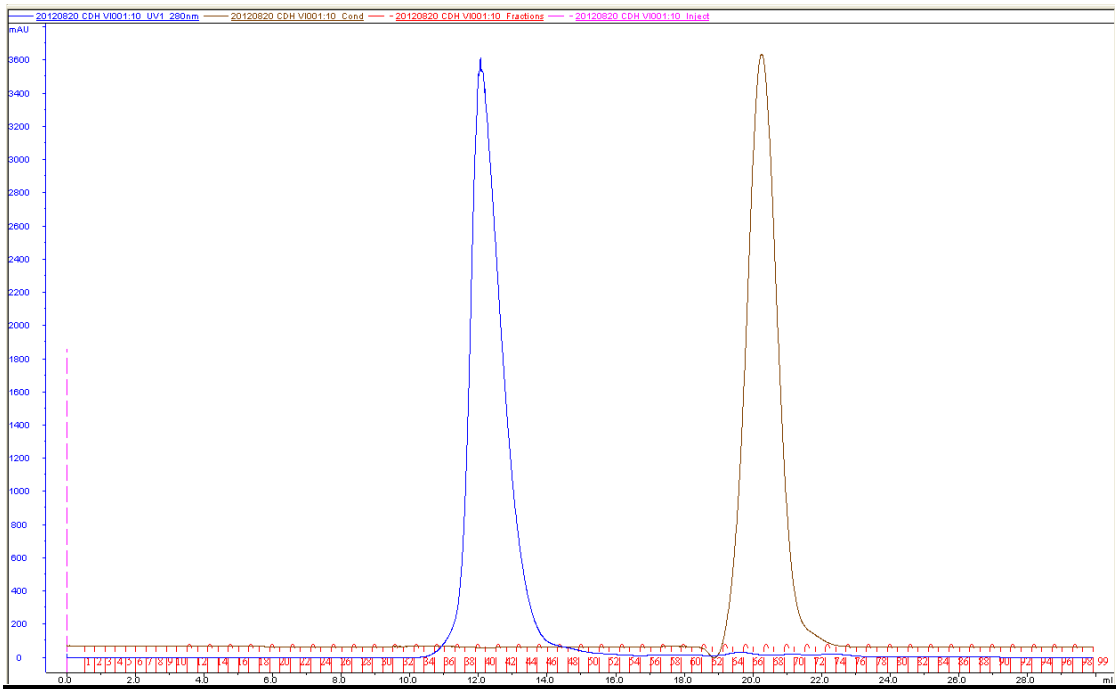

LCV assay

a)LCV of the Sa1_D_1e

Sample	Adsorption					Hydrogen Peroxide					addition 15 %
	1	2.	3.	Average	Standard deviation	1.	2.	3.	Average	Standard deviation	
Lactose	0.455	0.469	-	0.462	0.01	4.126	4.274		4.200	0.10	4.94
EPS Bl	-0.004	-0.004	-0.004	-0.004	0.00	-0.705	-0.705	-0.705	-0.705	0.00	-0.83
A-amyla-Nov	0.477	0.439	0.677	0.531	0.13	4.358	3.958	6.463	4.926	1.35	5.80
A-amyla-Sig	0.304	0.208	0.231	0.248	0.05	2.537	1.526	1.768	1.944	0.53	2.29
A-amyla-U	0.047	0.022	0.023	0.031	0.01	-0.168	-0.432	-0.421	-0.340	0.15	-0.40
Cellu-Sig	0.392	0.427	0.443	0.421	0.03	3.463	3.832	4.000	3.765	0.27	4.43
Cellu-Flk	0.192	0.177	0.182	0.184	0.01	1.358	1.200	1.253	1.270	0.08	1.49
Cellu-U	0.021	0.022	0.022	0.022	0.00	-0.442	-0.432	-0.432	-0.435	0.01	-0.51
Enz-mix-U	-0.012	-0.013	-0.013	-0.013	0.00	-0.789	-0.800	-0.800	-0.796	0.01	-0.94
B-Gluc-U	0.017	0.003	0.019	0.013	0.01	-0.484	-0.632	-0.463	-0.526	0.09	-0.62
Mann-Nov	0.075	0.047	0.067	0.063	0.01	0.126	-0.168	0.042	0.000	0.15	0.00
Pulp-Nov	0.07	0.108	0.107	0.095	0.02	0.074	0.474	0.463	0.337	0.23	0.40
Pect-Sig	-0.004	-0.001	0	-0.002	0.00	-0.705	-0.674	-0.663	-0.681	0.02	-0.80
Lyso-Sig	-0.003	-0.008	-0.002	-0.004	0.00	-0.695	-0.747	-0.684	-0.709	0.03	-0.83

b)LCV of the Ec1_D_1e

Sample	Adsorption					Hydrogen Peroxide					addition 15 %
	1.	2.	3.	Average	Standard deviation	1.	2.	3.	Average	Standard deviation	
EPS Bl	0.001	0.004	0.003	0.003	0.002	-0.653	-0.621	-0.632	-0.635	0.02	-0.75
Lactose	0.429	0.472	0.430	0.444	0.025	3.853	4.305	3.863	4.007	0.26	4.71
A-amyla-Nov	0.531	0.564	0.559	0.551	0.018	4.926	5.274	5.221	5.140	0.19	6.05
A-amyla-Sig	0.129	0.138	0.169	0.145	0.021	0.695	0.789	1.116	0.867	0.22	1.02
A-amyla-U	0.017	0.011	0.012	0.013	0.003	-0.484	-0.547	-0.537	-0.523	0.03	-0.62
Cellu-Sig	0.147	0.148	0.143	0.146	0.003	0.884	0.895	0.842	0.874	0.03	1.03
Cellu-Flk	0.333	0.387	0.398	0.373	0.035	2.842	3.411	3.526	3.260	0.37	3.83
Cellu-U	0.018	0.022	0.024	0.021	0.003	-0.474	-0.432	-0.411	-0.439	0.03	-0.52
Enz-mix-U	0.001	-0.001	-0.001	0.000	0.001	-0.653	-0.674	-0.674	-0.667	0.01	-0.78
B-Gluc-U	0.067	0.064	0.069	0.067	0.003	0.042	0.011	0.063	0.039	0.03	0.05
Mann-Nov	0.277	0.377	0.303	0.319	0.052	2.253	3.305	2.526	2.695	0.55	3.17
Pulp-Nov	0.274	0.217	0.217	0.236	0.033	2.221	1.621	1.621	1.821	0.35	2.14
Pect-Sig	0.014	0.006	0.008	0.009	0.004	-0.516	-0.600	-0.579	-0.565	0.04	-0.66
Lyso-Sig	0.000	0.001	0.003	0.001	0.002	-0.663	-0.653	-0.632	-0.649	0.02	-0.76

c)LCV of the Sa1_D_1e-Ek

Sample	Adsorption					Hydrogen Peroxide					addition 15 %
	1.	2.	3.	Average	Standard deviation	1.	2.	3.	Average	Standard deviation	
EPS Blank	0.034	0.037	0.039	0.037	0.003	-0.305	-0.274	-0.253	-0.28	0.03	-0.33
Lactose	0.571	0.425	0.533	0.510	0.076	5.347	3.811	4.947	4.70	0.80	5.53
Ek1	0.199	0.205	0.332	0.245	0.075	1.432	1.495	2.832	1.92	0.79	2.26
Ek2	0.109	0.14	0.126	0.125	0.016	0.484	0.811	0.663	0.65	0.16	0.77
Ek3	0.175	0.175	0.171	0.174	0.002	1.179	1.179	1.137	1.16	0.02	1.37
Ek4	0.181	0.199	0.149	0.176	0.025	1.242	1.432	0.905	1.19	0.27	1.40
Ek5	0.408	0.435	0.413	0.419	0.014	3.632	3.916	3.684	3.74	0.15	4.40
Ek6	0.396	0.408	0.683	0.496	0.162	3.505	3.632	6.526	4.55	1.71	5.36
Ek7	0.119	0.121	0.131	0.124	0.006	0.589	0.611	0.716	0.64	0.07	0.75
Ek8	0.101	0.1	0.098	0.100	0.002	0.400	0.389	0.368	0.39	0.02	0.45
Ek9	0.002	0.014	0.013	0.010	0.007	-0.642	-0.516	-0.526	-0.56	0.07	-0.66
Ek10	0.11	0.096	0.096	0.101	0.008	0.495	0.347	0.347	0.40	0.09	0.47

d)LCV of the Ec1_D_1e-Ek

Sample	Adsorption					Hydrogen Peroxide					addition 15 %
	1.	2.	3.	Average	Standard deviation	1.	2.	3.	Average	Standard deviation	
EPS Blank	0.054	0.106	0.068	0.076	0.027	-0.095	0.453	0.053	0.14	0.28	0.16
Lactose	0.182	0.142	0.16	0.161	0.020	1.253	0.832	1.021	1.04	0.21	1.22
Ek1	0.46	0.402	0.424	0.429	0.029	4.179	3.568	3.800	3.85	0.31	4.53
Ek2	0.345	0.537	0.354	0.412	0.108	2.968	4.989	3.063	3.67	1.14	4.32
Ek3	0.293	0.312	0.296	0.300	0.010	2.421	2.621	2.453	2.50	0.11	2.94
Ek4	0.632	0.604	0.486	0.574	0.077	5.989	5.695	4.453	5.38	0.82	6.33
Ek5	0.361	0.739	0.593	0.564	0.191	3.137	7.116	5.579	5.28	2.01	6.21
Ek6	0.131	0.131	0.137	0.133	0.003	0.716	0.716	0.779	0.74	0.04	0.87
Ek7	0.12	0.131	0.08	0.110	0.027	0.600	0.716	0.179	0.50	0.28	0.59
Ek8	0.4	0.41	0.48	0.430	0.044	3.547	3.653	4.389	3.86	0.46	4.54
Ek9	1.472	1.658	1.402	1.511	0.132	14.832	16.789	14.095	15.24	1.39	17.93
Ek10	0.264	0.316	0.293	0.291	0.026	2.116	2.663	2.421	2.40	0.27	2.82

e)LCV-testing-light sensitive

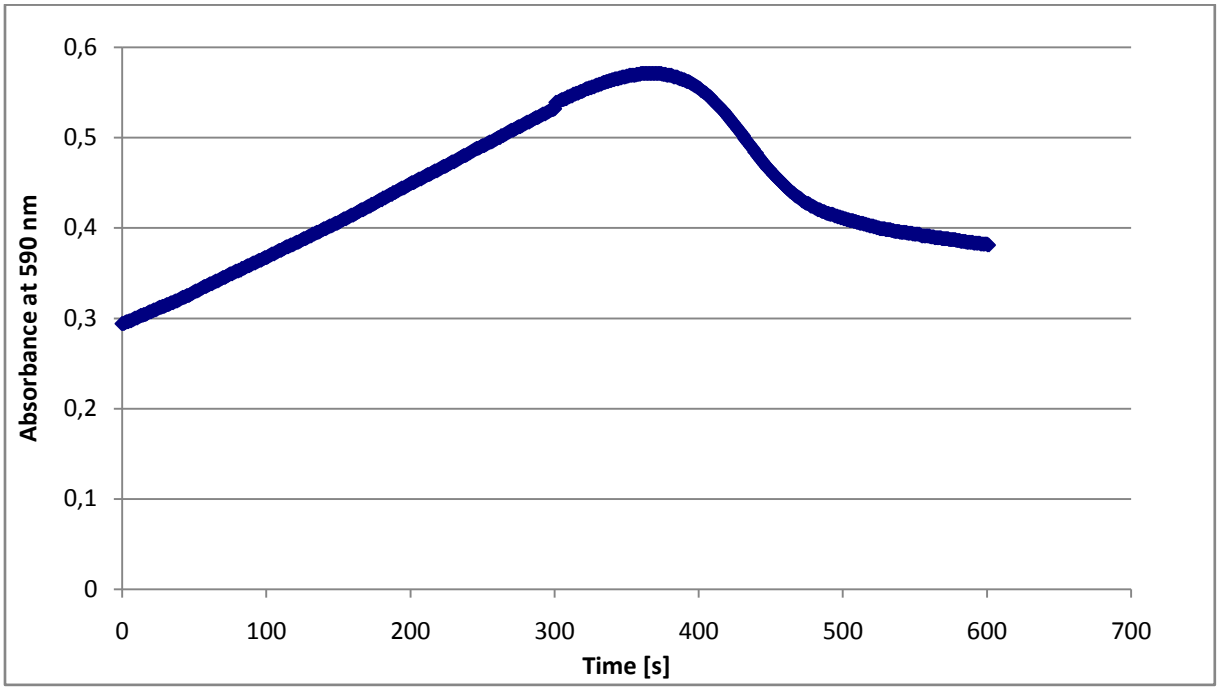

f)LIP+EDTA

No.	measured OD	calculated OD	Dilution factor	H_2O_2 concentration [µM]
1	0.095	0.095	1	0.95
2	0.995	0.995	1	9.52
3	1.247	2.494	2	23.81
4	0.945	3.780	4	35.71
5	0.505	5.050	10	47.62
6	0.650	6.500	10	71.43
7	0.822	8.220	10	95.24
8	0.626	6.260	10	190.48
9	0.533	5.330	10	238.10
10	0.483	4.830	10	285.71
11	0.397	3.970	10	333.33
12	0.340	3.400	10	380.95

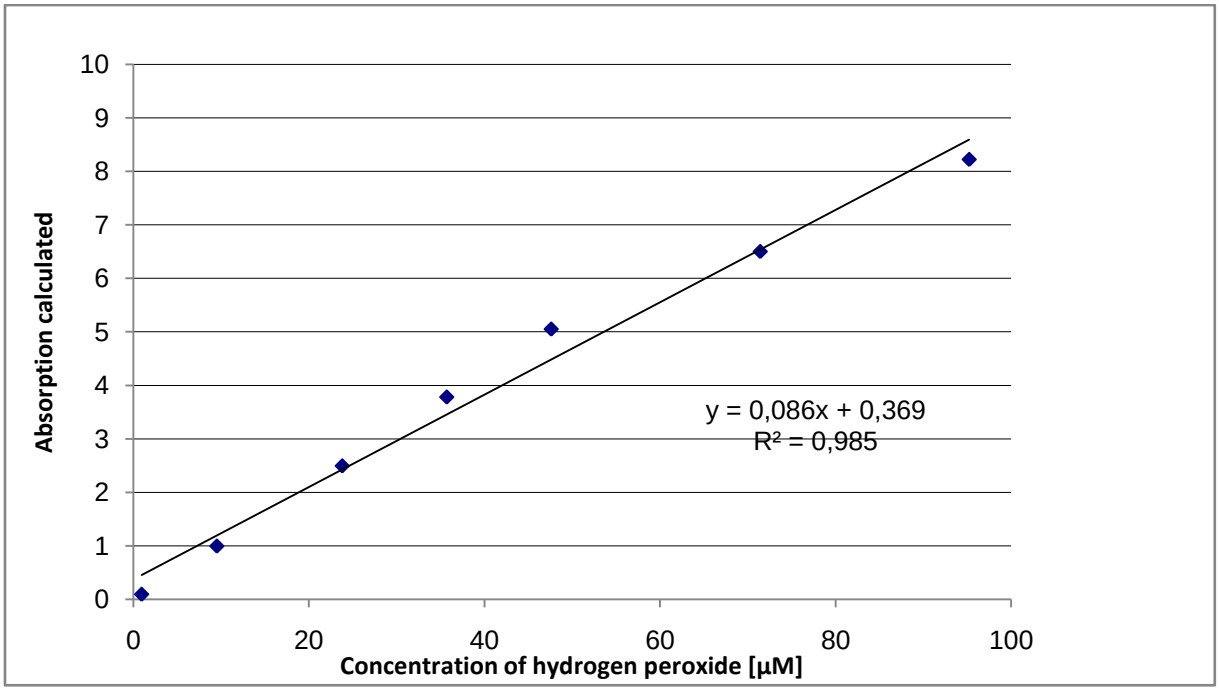

Amplex Red Assay

a)Sa1_D_1e

Sample	Maximum value	Concentration of hydrogen peroxide [µM]
Sa1_D_1e	603	0.00
Sa1_D_1e+A-amyla-Nov	33594	19.86
Sa1_D_1e+A-amyla-Sig	33268	19.66
Sa1_D_1e+A-amyla-U	3148	0.63
Sa1_D_1e+Cellu-Sig	18581	10.38
Sa1_D_1e+Cellu-Flk	8840	4.23
Sa1_D_1e+Cellu-U	900	0.00
Sa1_D_1e+Enz-mix-U	2233	0.05
Sa1_D_1e+B-gluc-U	2212	0.04
Sa1_D_1e+Mann-Nov	2853	0.45
Sa1_D_1e+Pulp-Nov	1497	0.00
Sa1_D_1e+Pect-Sig	622	0.00
Sa1_D_1e+Lyso-Sig	629	0.00

b)Ec1_D_1e

Sample	Maximum value	Concentration of hydrogen peroxide [µM]
Ec1_D_1e	987	0.00
Ec1_D_1e+A-amyla-Nov	23246	13.33
Ec1_D_1e+A-amyla-Sig	1400	0.00
Ec1_D_1e+A-amyla-U	2364	0.14
Ec1_D_1e+Cellu-Sig	9465	4.62
Ec1_D_1e+Cellu-Flk	15762	8.60
Ec1_D_1e+Cellu-U	1821	0.00
Ec1_D_1e+Enz-mix-U	5071	1.85
Ec1_D_1e+B-gluc-U	1235	0.00
Ec1_D_1e+Mann-Nov	2820	0.43
Ec1_D_1e+Pulp-Nov	1775	0.00
Ec1_D_1e+Pect-Sig	1344	0.00
Ec1_D_1e+Lyso-Sig	929	0.00

c)Sa1_D_1e-Ek and Ec1_D_1e-Ek

Sample	Maximum value	Enzymes combined	Concentration of hydrogen peroxide [µM]
Sa1_D_1e-Ek1	16605	A-amyla-Nov + A-amyla-Sig	9.13
Sa1_D_1e-Ek2	15694	A-amyla-Nov + Cellu-Sig + Enz-mix-U	8.56
Sa1_D_1e-Ek3	16632	A-amyla-Nov + Cellu-Flk	9.15
Sa1_D_1e-Ek4	6996	A-amyla-Nov + Enz-mix-U	3.06
Sa1_D_1e-Ek5	8850	A-amyla-Nov + B-Gluc-U	4.23
Sa1_D_1e-Ek6	8223	A-amyla-Nov + Pulp-Nov	3.84
Sa1_D_1e-Ek7	4480	A-amyla-Nov + Lyso-Sig	1.47
Sa1_D_1e-Ek8	2747	A-amyla-Sig + Cellu-Sig	0.38
Sa1_D_1e-Ek9	1322	A-amyla-Sig + Enz-mix-U	0.00
Sa1_D_1e-Ek10	1169	A-amyla-Sig + B-Gluc-U	0.00
Sa1_D_1e-Ek-EPS	928	-	0.00
Ec1_D_1e-Ek1	8775	A-amyla-Nov + Cellu-Flk	4.19
Ec1_D_1e-Ek2	22939	A-amyla-Nov + Cellu-Flk + Mann-Nov	13.13
Ec1_D_1e-Ek3	20572	A-amyla-Nov + Enz-mix-U	11.64
Ec1_D_1e-Ek4	20860	A-amyla-Nov + Mann-Nov	11.82
Ec1_D_1e-Ek5	7956	A-amyla-Nov + Pulp-Nov	3.67
Ec1_D_1e-Ek6	5450	Cellu-Flk + Cellu-Sig	2.09
Ec1_D_1e-Ek7	7703	Cellu-Flk + Mann-Nov	3.51
Ec1_D_1e-Ek8	7117	Cellu-Flk + Pulp-Nov	3.14
Ec1_D_1e-Ek9	1105	Mann-Nov +Pulp-Nov	0.00
Ec1_D_1e-Ek10	3695	Mann-Nov + A-amyla-Sig	0.98
Ec1_D_1e-Ek-EPS	610	-	0.00

d)Ec2_D_1e and Sa2_D_1e

Sample	Maximum	Concentration of H_2O_2 [µM]
Ec2_D_1e+A-amyla-Nov	6688	2.87
Ec2_D_1e+A-amyla-Sig	770	0.00
Ec2_D_1e+A-amyla-U	1049	0.00
Ec2_D_1e+Cellu-Sig	3538	0.88
Ec2_D_1e+Cellu-Flk	4469	1.47
Ec2_D_1e+Cellu-U	548	0.00
Ec2_D_1e+Enz-mix-U	828	0.00
Ec2_D_1e+B-gluc-U	1077	0.00
Ec2_D_1e+Mann-Nov	1106	0.00
Ec2_D_1e+Pulp-Nov	1440	0.00
Ec2_D_1e+Pect-Sig	437	0.00
Ec2_D_1e+Lyso-Sig	446	0.00
Ec2_D_1e	443	0.00
Sa2_D_1e+A-amyla-Nov	7800	3.57
Sa2_D_1e+A-amyla-Sig	802	0.00
Sa2_D_1e+A-amyla-U	953	0.00
Sa2_D_1e+Cellu-Sig	4791	1.67
Sa2_D_1e+Cellu-Flk	4013	1.18
Sa2_D_1e+Cellu-U	612	0.00
Sa2_D_1e+Enz-mix-U	974	0.00
Sa2_D_1e+B-gluc-U	997	0.00
Sa2_D_1e+Mann-Nov	1095	0.00
Sa2_D_1e+Pulp-Nov	1281	0.00
Sa2_D_1e+Pect-Sig	435	0.00
Sa2_D_1e+Lyso-Sig	464	0.00
Sa2_D_1e	489	0.00

Antibiofilm Assay

a)CV staining of *S. aureus*

Sample	1.	2.	3.	Average	Average-SC	Standard deviation	inhibition [%]	Standard deviation (%)
Positive Control	1.3328	1.1985	1.2385	1.2566	1.0885	0.07		8.7
Sterile Control (SC)	0.199	0.1169	0.1883	0.16806667	0.0000	0.04		0.8
Cellobiose Control	1.0594	1.0652	1.3649	1.16316667	0.9951	0.17	8.6	20.3
CDH Control	0.8597	0.5535	0.7014	0.70486667	0.5368	0.15	50.7	10.8
0.5 mM Cellobiose	0.7302	0.3649	0.4778	0.5243	0.3562	0.19	67.3	9.8
1 mM Cellobiose	0.2589	0.3124	0.1857	0.25233333	0.0843	0.06	92.3	1.6
2 mM Cellobiose	0.3886	0.2246	0.1867	0.26663333	0.0986	0.11	90.9	2.9
4 mM Cellobiose	0.1049	0.1979	0.2048	0.1692	0.0011	0.06	99.9	0.9
5 mM Cellobiose	0.2308	0.1792	0.3737	0.26123333	0.0932	0.10	91.4	2.6
6 mM Cellobiose	0.1954	0.1802	0.246	0.2072	0.0391	0.03	96.4	0.7
125 µM H_2O_2	0.9781	0.969	1.2612	1.06943333	0.9014	0.17	17.2	17.8
250 µM H_2O_2	0.7727	0.327	0.5685	0.55606667	0.3880	0.22	64.4	12.4
500µM H_2O_2	0.2337	0.8818	0.1101	0.40853333	0.2405	0.41	77.9	16.9
1000µM H_2O_2	0.1663	0.1257	0.1631	0.1517	-0.0164	0.02	101.5	0.3
1500µM H_2O_2	0.1617	0.143	0.1607	0.15513333	-0.0129	0.01	101.2	0.2
2000 µM H_2O_2	0.1069	0.0927	0.1068	0.10213333	-0.0659	0.01	106.1	0.1

b)CV staining of *S. aureus*

Sample	1.	2.	3.	Average	Average-SC	Standard deviation	inhibition [%]	Standard deviation (%)
Positive Control	1.5278	1.4427	1.2621	1.4109	1.3422	0.14		9.6
Sterile Control (SC)	0.0603	0.06	0.0856	0.0686	0.0000	0.01		21.4
Cellobiose Control	1.06	0.6641	0.955	0.8930	0.8244	0.21	38.58	23.0
CDH Control	1.5278	1.4427	1.2621	1.4109	1.3422	0.14	0.00	
0.5 mM Cellobiose	1.1334	1.1517	1.2518	1.1790	1.1103	0.06	17.28	5.4
1 mM Cellobiose	0.7851	1.3841	1.2982	1.1558	1.0872	0.32	19.00	28.0
2 mM Cellobiose	1.1319	1.081	1.2247	1.1459	1.0772	0.07	19.74	6.4
4 mM Cellobiose	0.7011	0.4703	1.2473	0.8062	0.7376	0.40	45.05	49.5
5 mM Cellobiose	1.2681	1.0711	0.7408	1.0267	0.9580	0.27	28.62	26.0
6 mM Cellobiose	0.7326	0.4906	0.4274	0.5502	0.4816	0.16	64.12	29.3
125 µM H_2O_2	0.8965	0.9202	0.9719	0.9295	0.8609	0.04	35.86	4.1
250 µM H_2O_2	0.8479	1.0101	1.1515	1.0032	0.9345	0.15	30.37	15.1
500 µM H_2O_2	0.466	0.3569	0.3949	0.4059	0.3373	0.06	74.87	13.6
1000 µM H_2O_2	0.079	0.0725	0.0882	0.0799	0.0113	0.01	99.16	9.9
1500 µM H_2O_2	0.0835	0.0971	0.0774	0.0860	0.0174	0.01	98.71	11.7
2000 µM H_2O_2	0.0918	0.0961	0.1247	0.1042	0.0356	0.02	97.35	17.2